Theses   Electronic Theses and Dissertations

4-2021

ELECTRODEPOSITION STUDY OF ALLOYS FOR SOLAR ENERGY, CORROSION RESISTANCE, AND BATTERY APPLICATIONS

Thaier Tawfeek Alawadh

United Arab Emirates University

College of Engineering

Department of Chemical and Petroleum Engineering

ELECTRODEPOSITION STUDY OF ALLOYS FOR SOLAR ENERGY, CORROSION RESISTANCE, AND BATTERY APPLICATIONS

Thaier Tawfeek Alawadh

This thesis is submitted in partial fulfilment of the requirements for the degree of Master of Science in Chemical Engineering

Under the Supervision of Dr. Salem Alzahmi

April 2021

Declaration of Original Work

I, Thaier Tawfeek Alawadh, the undersigned, a graduate student at the United Arab Emirates University (UAEU), and the author of this thesis entitled "Electrodeposition Study of Alloys for Solar Energy, Corrosion Resistance, and Battery Applications", hereby, solemnly declare that this thesis is my own original research work that has been done and prepared by me under the supervision of Dr. Salem Alzahmi, in College of Engineering at UAEU. This work has not previously been presented published or formed the basis for the award of any academic degree, diploma or a similar title at this or any other university. Any materials borrowed from other sources (whether published or unpublished) and relied upon or included in my thesis have been properly cited and acknowledged in accordance with appropriate academic conventions. I further declare that there is no potential conflict of interest with respect to the research, data collection, authorship, presentation and/or publication of this thesis.

Student's Signature: Date: 19/4/2021

Approval of the Master Thesis

The following Examining Committee Members have approved this Master Thesis:

1) Advisor (Committee Chair): Salem Alzahmi

   Title: Assistant Professor

   Department of Chemical and Petroleum Engineering

   College of Engineering

   Signature _____ Date 10 May 2021

2) Advisor (Internal Examiner): Abdulrahman Alraeesi

   Title: Assistant Professor

   Department of Chemical and Petroleum Engineering

   College of Engineering

   Signature _____ Date May 10, 2021

3) Member (External Examiner): Ricardo P. Nogueira

   Title: Professor

   Department of Chemical Engineering

   Institution: Khalifa University, UAE

   Signature on behalf of Prof. Ricardo _____ Date May 10, 2021

This Master Thesis is accepted by:

Dean of the College of Engineering: Professor James Klausner

Signature _James F. Klausner_   Date ___10/11/2021___

Dean of the College of the Graduate Studies: Professor Ali Al-Marzouqi

Signature ___Ali Hassan___   Date ____10/11/2021____

Copy _____ of _____

Abstract

Copper-Zinc-Tin sulphide (CZTS) compound is one of the alloys, which has significantly caught the attention of a considerable number of researchers since the beginning of the century. Consequently, academic laboratories started investigating the alloy in-depth with its various combination due to its valuable applications with high potential usage. The CZTS alloy has a high tendency to replace the current copper indium gallium selenide (CIGS) thin-film solar cell system due to scarcity of CIGS components, and toxic manufacturing-procedures comparing to CZTS. Nevertheless, CZTS is a new studied compound with exceptionally low photovoltaic empirical efficiency and an inadequate understanding of its chemical reaction behaviour. But, CZTS has high theoretical potential applications due to its superb theoretical photovoltaic properties such as bandgap. Additionally, there are multiple and great properties for copper, copper-zinc, copper-tin, tin-zinc, copper-tin-zinc combination alloys as well which will favour them to be used in different applications. For example, among many advantages of brass and bronze are corrosion resistance, strength, more ductile, high wear-resistance, and better appearance. Plus, a thin film of copper over carbon alloy has great application as a thin-film battery electrode due to its ability to store energy. In this study, the behaviour of the copper, zinc, tin, and their combination solutions electrodeposited over carbon substrate has been studied with a purpose to have a better understanding of the element behaviour during electrodeposition process which would get us a better understanding of the resulted compositions. The study has been done using the electrodeposition method because of its high cost-effectiveness, easiness in manufacturing, and rapid results comparing to all other methods. As a start, equimolar solutions have been stabilized under similar environmental conditions which will make the behaviour of the elements as a major factor in the yielded composition. Also, the electrical conductivity of the engineered stable solutions has been examined with varying pH. Then, each solution has been examined using cyclic voltammetry (CV) experiments. Finally, the samples result from constant deposition have been inspected with SEM, EDS, and XRD devices to determine the quality of the electrodeposited elements, their presence, and amount. In this study, it was found that the most stable equimolar solution mix had.03 M of Cu, Zn, and Sn and 0.125 M

of Sodium Citrate as complexing agent. The SEM mostly showed rough surfaces for all samples with electrodeposited particles with various style patterns over carbon. The EDS and XRD showed a good mass of the elements electrodeposited in a single step such as in sample C4 which contains 0.03 M Copper (II) Sulphate, 0.03 M Zinc Sulphate, 0.03 M Tin (II) sulphate, and 0.125 M Sodium Citrate. As a result, it was confirmed that 0.9 mg of CZT was electrodeposited over carbon where 24.99% zinc, 25.06% copper, and 42.75% tin weight percentage yielded of the sample.

Keywords: CZTS, electrodeposition, thin-film cells, photovoltaic, solar energy, alloys, corrosion resistant, brass, bronze, battery.

Title and Abstract (in Arabic)

<div dir="rtl">

دراسة الترسيب الكهربائي لبعض السبائك بهدف استخدامها كخلايا شمسية ولمقاومة للصدأ و صناعة البطاريات

الملخص

مركب (CZTS) هو أحد السبائك التي لفتت انتباه عدد كبير من الباحثين منذ بداية القرن. وبناءً على ذلك، بدأت المختبرات الأكاديمية بفحص السبيكة بعمق بمجموعتها المتنوعة نظرًا لتطبيقاتها القيمة ذات الاستخدامات المهمة المحتملة. يسعى الباحثين بسبيكة CZTS إلى استبدال نظام الخلايا الشمسية ذات الأغشية الرقيقة النحاسية سيلينيد غاليوم الإنديوم (CIGS) بسبب ندرة مكونات CIGS وإجراءات التصنيع السامة بمقارنة CZTS. ومع ذلك، فإن CZTS هو مركب تم دراسته حديثاً بكفاءة تجريبية كهروضوئية منخفضة للغاية وفهم غير كافٍ لسلوك تفاعله الكيميائي. لكن، CZTS لها تطبيقات نظرية عالية ومهمة محتملة بسبب خصائصها الكهروضوئية الرائعة. بالإضافة إلى ذلك، هناك خصائص متعددة ورائعة للسبائك المركبة Cu، CuZn، CuSn، SnZn، CuZnSn والتي سيتم استخدامها في تطبيقات مختلفة. على سبيل المثال، يتمتع النحاس والبرونز بالعديد من المزايا مثل مقاومة التآكل، والقوة، والمزيد من المرونة، والمظهر الجذاب. بالإضافة إلى ذلك، فإن طبقة رقيقة من النحاس فوق سبيكة الكربون لها تطبيق رائع كقطب بطارية ذو غشاء رقيق نظرًا لقدرتها على تخزين الطاقة. في هذه الدراسة، تمت دراسة سلوك النحاس والزنك والقصدير والمحاليل المركبة الخاصة بهم المطلية بالكهرباء فوق ركيزة الكربون بغرض الحصول على فهم أفضل لسلوك العنصر أثناء عملية الترسيب الكهربائي مما يجعلنا نفهم بشكل أفضل ما ينتج من التفاعلات. تمت الدراسة باستخدام طريقة الترسيب الكهربائي لما لها من فعالية عالية من حيث التكلفة، وسهولة في التصنيع، ونتائج سريعة مقارنة بجميع الطرق الأخرى. كبداية، تم تثبيت الظروف البيئية للمحاليل مما سيجعل سلوك العناصر حال التفاعل عاملًا رئيسيًا في الناتج. أيضًا، تم فحص التوصيل الكهربائي للمحاليل المستقرة المصممة هندسيًا بدرجات حموضة متفاوتة. بعد ذلك، تم فحص كل محلول باستخدام تجارب قياس الجهد الدوري (CV). أخيرًا، تم فحص العينات الناتجة من الترسيب المستمر باستخدام أجهزة SEM و EDS و XRD لتحديد جودة العناصر المترسبة كهربائياً ووجودها وكميتها. في هذه الدراسة، وجد أن خليط المحلول الأكثر استقرارًا يحتوي على 0.03 مولار من النحاس، والزنك، والقصدير و 0.125 مولار من سترات الصوديوم كعامل معقد. أظهر SEM

</div>

في الغالب أسطحًا خشنة لجميع العينات ذات الجسيمات المطلية بالكهرباء ذات أنماط مختلفة على الكربون. أظهر EDS و XRD سمكًا جيدًا للعناصر التي تم ترسيبها كهربائيًا في خطوة واحدة كما في العينة التي تتكون من محلول فيه 0.03 م نحاس (II) كبريتات، 0.03 مولار كبريتات الزنك، 0.03 مولار كبريتات القصدير (II)، و 0.125 مولار سيترات الصوديوم. النتيجة للترسيب الكهربائي كان 1.5 مجم من CZT تم طلاؤها على الكربون حيث 24.99٪ زنك و25.06٪ نحاس و42.75٪ قصدير.

مفاهيم البحث الرئيسية: الترسيب الكهربائي، نحاس، سبائك معدنية، الطاقة الشمسية، مقاومة الصدأ، البرونز، القصدير، خلايا الشمسية الرقيقة، صناعة البطاريات.

Acknowledgements

I would like to start by thanking God for giving me the strength and the power to finish such research with successful results. Also, I would like to thank my beloved parents for all the training, discipline, and trust. More importantly, I would like to thank Dr. Salem Alzahmi for allowing me to join his team and work under his gaudiness. Without his commitment, encouragement and support, this work would not be possible. Also, I would like to thank Prof. Ghaleb Al Breiki and Ms. Amna Al Baloushi for allowing me to be one of the graduate students at the UAEU and their valuable assistance throughout my studies.

I am incredibly grateful for all the support and guidance from the College of Engineering Department and my committee members. I would like to thank Dr. Abdulrahman Alraeesi for all his academic advice and examining the work. Also, my external examiner, Prof. Ricardo Nogueira, for his valuable time and effort. Furthermore, special thanks are extended to our Chemical and Petroleum Engineering Department Chair, Prof. Sulaiman Al-Zuhair, and our coordinator, Prof. Prof. Basim Abu-jdayil, for their assistance throughout my studies and research at United Arab Emirates University.

In addition, I am very thankful for all the kind help in SEM and XRD which I got from Dr. Hussain El Sayed, Dr. Venkatesha Narayanaswamy and my friend Eng. Ahmed Elsayed. Also, sincere thanks are due to Mr. Ahmed Taha for providing sufficient library research services.

Also, I would like to thank the United Arab Emirates and its leaders for their generous and kind hospitality. Finally, special thanks go to my beloved Kingdom of Saudi Arabia, King Salman Al Saud, and crown prince Mohammed bin Salman Al Saud, for all their encouragements and their investment in the mind of our youth. With these encouragements, Saudi Vision 2030, and our strong leaders, not only we will be able to lead the nations into a greater future, but we will also take a major part in making our world better.

Dedication

To my dear parents and family for their love, support, and encouragement

Table of Contents

List of Tables

List of Figures

List of Abbreviations

CdTe	Cadmium Telluride
CZTS	Copper Zinc Tin Sulphide/ Cu_2ZnSnS_4
CE	Counter Electrode
CIGS	Copper Indium Gallium Selenide Cu-In-Ga-Se_2
CIGS	Copper Indium Gallium Selenide
CdTe	Cadmium Telluride
EDTA	Ethylenediaminetetraacetic Acid
EC	Electrical Conductivity
EDS	Energy-Dispersive X-ray Spectroscopy
FEG	Field Emission Gun
HER	Hydrogen Evolution Rate
ITO	Indium Tin Oxide
MMR	Material Removal Reaction
NHE	Normal Hydrogen Electrode
NACE	National Association of Corrosion Engineers
OCV	Open Circuit Voltage
PV	Photovoltaic
PET	Polyethylene Terephthalate
RE	Reference Electrode
SEM	Scanning Electrode Microscopy
SHE	Standard Hydrogen Electrode
TF	Thin Film
TMF	Thin Metal Film
XRD	X-Ray Diffraction
XRF	X-Ray Florescence

Chapter 1: Introduction

1.1 An Overview

This thesis is proposed to deal with electrodeposition in a single step of CZT alloy and many of the combinations of its components generating a variety of alloys. CZTS alloy has the potential to be when of the greatest thin-film solar cell due to many factors which going to be discussed later in this thesis. Nevertheless, it is new studied material where has many obstacles one of which is manufacturing cost and time. It is often fabricated in layers or steps which makes it easy to control the process, but it is costly and time-consuming. This thesis will show that CZT can be electrodeposited in a single step. To manufacture CZTS, sulphur could be added using many other methods such as vapour deposition or annealing which is not the focus of this study. Furthermore, this study will go over many other alloys of CZTS which have very useful applications. Such as, copper over the carbon substrate which has applications as a thin-film battery electrode. Moreover, brass, and bronze alloys will be in a single step electrodeposited which has been proven for ages for their good corrosion resistance. This study should help advance the understanding of the chemical behaviour and the interaction between the CZTS elements in the electrodeposited solutions.

Many metals are famous when it comes to corrosion resistance such as stainless steel, aluminium, and copper. Nevertheless, copper by itself oxidizes with time to form a green substance over copper which slows the oxidization process after forming on the surface. To protect copper further, zinc is added with small amounts of other elements, brass. Also, tin could be added to copper to form a bronze alloy which will protect it from oxidizing as well [1]. Bronze is known to resist corrosion even when

submerged under liquids such as salt water, fresh water, most acids, and organic chemicals. Usually, under such a harsh environment, the corrosion process speeds up for regular metals such as copper. Thus, bronze is one of the most widely used copper alloys in the industry. For example, in making bushings, and valves [1].

Brass has great appeal and mechanical properties which is hardly attained with other materials such as low friction, low melting point, a good conductor of heat, and easy to cast. Brass often contains zinc ranges from 5-45% of the copper alloy. Furthermore, brass with a high content of zinc will increase ductility and strength. Also, has a wide range of colour from red to yellow depending on the amount of zinc added to the copper alloy which makes it known for its decorative purposes. Moreover, it is widely known to be used in a variety of applications in construction, electrical, manufacturing. For example, in making gears and engine bearings [1].

Comparing the bronze to brass, usually, bronze reddish brown and not as bright as brass. Moreover, brass is more malleable than pure copper and not as hard as steel but with great corrosion-resistant where if exposure to ammonia may result to stress cracking. On the other hand, bronze is a better conductor of electricity and heat than regular steel with often a higher melting point than brass. Furthermore, bronze used for its famous properties such as corrosion resistance, brittle, and resists fatigue. Thus, bronze has many uses such as in electrical connectors, sculpture, ship fittings, springs, and mirrors. On the other hand, brass can be seen in making parts used around explosives, Musical instruments, plumbing, decoration, and low-friction applications. Lastly, Bronze is an older alloy, dating back to about 3500 B.C.E. where Brass dates to around 500 B.C.E [2].

Copper by itself adding it to carbon substrate can be used as a thin-film battery electrode. Thin-film batteries are unique due to their low profile, flexibility, disposable, and small footprint. They are ideal to be used in wearable electronics, electric vehicle batteries, and biosensors. Thus, electrodeposition of a thin layer of copper over a surface to work as a battery electrode is unique due to its low-cost than other techniques such as chemical vapour deposition (CVD), and plasma vapour deposition (PVD). Also, electrodeposition effective in coating even in difficult surfaces where the mass and composition of films could be controlled by controlling some of the electrodeposition parameters [3]. When it comes to CZTS as semiconductor material provides a significant stock of prospective to be used in the energy systems like photovoltaic (PV) solar cells. Cu_2ZnSnS_4, which is denoted as 'CZTS,' nearly associated with a class of materials used in advanced making for photovoltaic (PV) applications from late 1969 [4].

That is analogous to the global utilization of the power of about 15 terawatts (TW) as the population on earth is continually growing by massive amounts. The necessity and demand for energy will increase tremendously by the end of 2026. By then, it is estimated to increase by two times than current electricity consumption. The requirement of energy by humankind, the mandate is commonly fulfilled through coal, oil, and many non-renewable resources, which are inadequate. Also, burning fossil fuels produces environmental pollution and releases some harmful gases, such as carbon dioxide, oxides of nitrogen, CO, Sulphur dioxide, etc. Solar energy is expected to play a vital role in the future of renewable energy development in the world through attaining a clean energy transporter [4].

Consequently, the necessity of the present time demand to discover and make the most renewable, ecologically energy resources from the environment would cause the modification of the conservative energy resources that can never deplete from the environment and can be used again. Among the various renewable energy sources that discovered up till now, solar energy is among the best plentiful, safe, and productive renewable energy resources for humankind.

With the growing utilization of conservative energy and the slowly but surely severe ecological dilemma, solar cells recently generated high global demand. In the recent decade, the thin film, TF, research technique's advancement stimulated the era of solar cells technology of second-generation of these solar cells of the second generation created on materials of TF. The wish for small scale material, the TF solar cell technique, can efficiently decrease materials' budget. Furthermore, TF materials can be installed on different surfaces of substrates like steel, glass, and the polymers which has multiple applications and benefiting the advancement of solar energy. CZTS is regarded as the ideal material for absorption for the future generation solar cells of TF due to critical constituent atoms in the earth's crust as non-toxic and ecologically appropriate. Thus, CZTS has great potential where its thin layer can be integrated to flexible and transparent substrate with good potential efficiency.

The continuing upsurge in the world's energy demand and the lack of the existing conventional energy sources, much more focus is shifted on the usage of other renewable energy resources like wind energy and solar energy [2]. A solar cell is designed in a way to uses the photovoltaic effect to transform the light energy into electrical energy. Extensively used solar cells nowadays are of silicon type that crystallized, which has an efficiency of around 15 to 20% [5]. The foremost

disadvantages of the type mentioned above of silicon photovoltaic (PV) cells are that they breakdown with extreme heat. In other hand, the usage of polycrystalline silicon for photovoltaic is not so costly and readily available and also provides more muscular cells; however, the conversion efficiency is about 10 to 14% [5, 6]. Thin-film solar cells have increased responsiveness in the current time because thin films can be attained by this method at much less construction cost. However, they undergo the disadvantage of low conversion efficiency [7].

Amongst the thin films considered for use in photovoltaic solar cells, amorphous silicon, cadmium telluride (CdTe) and copper indium dieseline (CuInSe$_2$) are of great significance [7, 8]. But Cd is toxic, and the production of CuInSe$_2$ includes the release of enormously toxic hydrogen selenide. As a way out to these complications, the study on Copper, Zinc, Tin, and Sulphur (CZTS) thin films for photovoltaic applications has gained much attention. Copper (Cu) Zinc (Zn) tin (Sn) sulfide (S), which is commonly known as CZTS that proved one of the best choices with a bandgap of about 1.4 to 1.5electron Volts and co-efficient of absorption is 104 cm to 1. The development of the thin film of Copper Zinc Tin Sulphide does not include releasing any toxic gas and the raw materials included are ample on earth [8].

1.2 Statement of the Problem

In the present research work, the primary purpose behind this is to enhance the process of electrodepositing of mixture of alloys, Cu, Zn, Tin, brass, bronze, and CZT over carbon substrate by trying to understand their chemical behaviour of the solution's reaction. Not only electrodeposition is very cost-effective which add to its value and the need of understanding its process behaviour, the elements themselves can be found easily with low toxicity. Nevertheless, such a method is easy to be used

but complex to study due to many factors or parameters controlling it. For example, the temperature of the solution, its pH, the voltage supplied, complexing agents, agitation, and concentration of elements. Thus, in this study, many parameters such as concentration, pH, no agitation, and temperature have been fixed to allow the study of the chemical reaction yield behaviour of the elements alone.

This study could be the foundation of creating chemical reaction rate formula which can have way better control on the yielded product. Another big obstacle in electrodeposition, it is true that you can electrodeposit such elements but to have a stable solution with no precipitation sometimes is not an easy task especially when multiple elements are present in the solution. To go over such obstacles, you could electrodeposit each element by themselves. Nevertheless, it will require more time and will increase the manufacturing cost. Thus, in this study, it has been tried to electrodeposit all metals in a single step.

Another problem that the study faced, picking appropriate complexing agents to the stable solution. Also, the amount of such complexing agent while keeping an eye on the stability of the solution. Although, there are many complexing agents that could be used but finding one that will fit all the solutions with no problem was not easy. Then, different concentrations of that complexing agent have been used while testing the solution's electrical conductivity and keeping an eye on the stability as well. After successfully finding a stable equimolar concentration of the solutions with no agitation, added heat, or changing pH, trying to optimize the electrical conductivity of the solution as another goal. Dropping the pH could yield better electrical conductivity but it could have a negative effect with the stability of the solutions. In

addition, such effect in the study was not clear or immediate which required sometimes days or week to ensure that there are no precipitations in the solution.

After finding the right mix and prepare the stable solutions, the behaviour of the solutions was able to be studied using cyclic voltammetry experiments to determine the right voltages. Then, successfully all targeted elements were electrodeposited in a single step. Then, the yielded products of the reactions were able to be analysed using XRD, EDS, and SEM machines which gave us a broad understanding of the behaviour of the chemical reaction mostly eliminating all other factors which could typicality affect the electrodeposited metals.

Finally, CZTS can work as a thin-film solar cell but unfortunately, it has low empirical theoretical efficiency till now and the cost of manufacturing is high. Thus, electrodeposition of at least the CZT layer in a single step with an understanding of yielded reaction behaviour would help to solve the global energy problem in the future. Furthermore, electrodeposition of different alloy competition of CZT in a single step such as copper, brass, and bronze would reduce their cost of manufacturing especially when it is done with the focus on the interaction and behaviour of the elements themselves. This would yield more controlled alloys which could work as thin-film electrodes and it would be great alloys with anti-corrosion resistance.

1.3 Applications and Potentials

1.3.1 Importance of Batteries

The importance of batteries has been increased over the past few years due to the rapid growth in renewable energy farms, electrical cars, and cell-phones. Solar and

wind renewable energy got lots of attraction due to the unaffordable prices of fossil fuel and the need for green energy to less impact the environment. The issue of most renewable energy that it is not a steady energy supply throughout the whole hours of the day, and it is affected by many factors. Thus, the need of storing such energy has rapidly increased which will solve such a problem. Therefore, it has been seen many researchers investing their time and effort in advancing such a field with better efficiency batteries and lower their cost of manufacturing.

Electric cars on the other hand rely on such technology heavily. This type of car mostly has an electric engine with a massive number of batteries. The race of developing better cars depends on many factors which include the capacity of the batteries, efficiency, charge cycle, size, heating factor, safety, availability of the elements, and manufacturing cost. Thus, the batteries are a large area to study with very high potential and applications in the future.

Traditional batteries like acid batteries are good with many life applications like the one found in traditional cars with a combustion engine. Nevertheless, due to many factors such as safety and storage density, thin-film batteries have the lead advantage. In 1998, The Machine Design published an article talking about thin-film batteries providing more power which claiming that size and weight of the batteries are less than the conventional types at that time. The design consists of a thin metal film (TMF) wraps two layers of active paste and lead foil around a central core which going to create high power delivery and fast charging time. It claims that such a design produces a low resistance current path, minimizes the voltage drop with applications such as portable power tools [9]. In addition, many trials have been done to make batteries more flexible. For example, it was reported in the Journal of Power

Sources in 1998 that a group made a thin-film lithium battery polymer that exhibits excellent charge-discharge characteristics as an active material of a positive electrode of a secondary battery [10].

To be able to construct a battery where the electrodes are made of thin-film metals would decrease the size of the battery and would open the door in making low size and flexible batteries. Also, managing the coated substrates, that lead to bendable batteries with endless shapes. In addition, it was estimated that some thin-film battery designs eliminate the risk of battery fire [11]. This shed some light on the importance of such technology and how researchers since then trying to be finding ways to enhance it.

Copper has been used extensively in the use of thin-film batteries due to its electrical and mechanical properties. Copper can be plated over many substrates to work as a cathode in lithium thin-film batteries because it has a superb ability to collect current. In addition, copper is a malleable metal and easy to work with comparing to all other metals. Plating it to flexible thin substrates would not only reduce the weight of the overall battery but would reduce the rigidity of the overall battery which means more shapes could be achieved and applications [12].

1.3.2 Corrosion Resistance

Metals have great useful properties and can be found in various applications. Nevertheless, many metals tend to rust with time where some have more resistance to oxidation. Thus, it is important to pick the right metals for the application. Also, with the advances in science alloys could be engineered to enhance the properties. In addition, nowadays scientists got the machines to measure the resistance and can simulate most environments in the lab before using the metals in a bigger scale

project. In an article published by Saudi Aramco company in 2019, it was estimated that corrosion loss is about $2.5 trillion problem globally. Also, the National Association of Corrosion Engineers (NACE), estimated that corrosion cost the oil and gas production industry about $1.37 billion annually [13]. All this increases the search for solutions of better metals that can resist corrosion.

Copper is a metal with great resistance to corrosion which was estimated to last for up to 1000 years in some applications and environments. Copper corrodes at a rate of approximately 0.4mm every 200 years [14]. Thus, copper is plated over many metals to enhance its corrosion resistance ability. However, even copper in harsh environments such as saline water might exhibit pitting corrosion which could affect the surface and efficiency [15]. This adds to the importance of corrosion protection and the value of picking the right metals for the application. Also, it pushes scientists to do more research in such fields trying to produce cheaper and easier ways to coat copper over other weaker metals or even better alloys mix which going to enhance the overall corrosion resistance. This can be done by picking a cheap manufacturing method as electrodeposition and studying the parameters that could affect the process such as chemical reaction behaviour.

1.3.3 Solar Energy

Solar is a harmless alternative used to replace current fossil fuels used for the generation of electricity that pollute. Electricity generation from fossil fuels leads to pollution of air causing acid rain, destruction of forest areas, and the decline in agricultural production. With time, there is an increase in energy demand, and the world is facing a shortage of energy resources. There is a continuous depletion in energy resources. Solar energy is the form of light energy coming from the sun.

Plants capture most of this energy for photosynthesis, but this form of energy can also be used in non-renewable resources. Many techniques can be used to convert solar energy directly or indirectly into electricity. The primary transformation technology is the photovoltaic solar system. This cell works as an electrical instrument that transforms the energy coming through light from the sun into electrical energy directly through the effect of PV [16].

Solar energy is expected to play an essential starring role in the world's future energy development that provides the benefits of solar-to-hydrogen through obtaining a clean energy transporter. Hydrogen is a viable energy carrier, accomplished for replacing fossil fuels and reducing carbon dioxide (CO_2) emission to protect the domain from global warming. Solar energy is pollution-free and richly exists which consumes sunlight to give electricity for multiple usages. With the frightening decrease of significant energy resources such as coal, petroleum, and gas, along with the environmental lack caused by binding these energy sources. It has become a compulsion to exploit renewable energy resources that would power the upcoming energy needs sufficiently deprived of humiliating the environment through greenhouse gas discharge [16].

With time, the energy necessity is rising beyond the parameters as the growth rate exceeds a profound, thoughtful significance because there is a population pressure increasing every year [8]. Electricity is the chief elastic and appropriate energy. On the other hand, electricity is not only a crucial phase of energy. Electricity can be produced by many different forms of energy resources just as biomass, petroleum, wind energy, hydrothermal, geothermal energy, sunlight, tides in deep-sea or tidal energy, biomass, atomic emission, energy cells, natural gasses from dead matter [17].

The non-stoichiometry of alloy semiconductors draws a parallel associated with the electrical characteristics of these semiconductors.

The request for small scale material, the TF solar cell technique, can efficiently decrease materials' budget. Furthermore, TF contents can adaptably be installed on the surface of substrates like steel must be stainless, glass, and the polymer of plastic, particularly appropriate for the construction of solar incorporation. CZTS regarded as the ideal material for absorption for the future generation solar cells of TF owing to critical constituent elements in the earth crust's as non-toxic and ecologically appropriate [18]. Thin-film solar cells have increased responsiveness in the current time because thin films can be attained electrodeposited at much less construction cost. However, they undergo the disadvantage of low conversion efficiency [19].

1.3.3.1 CZTS Solar Cells- Properties and Device Efficiencies

Cu-Zn-Sn-S is one of the I2–II–IV–VI4 quaternary compounds with semiconductor property, which is achieved by replacing the Se with S, a scarce element. Every constituent of thin films of CZTS is ample in the upper layer of earth's crust (Copper: 49.9 ppm, Zinc: 74.9 ppm, Tin: 3.0 ppm, Sulphur: 261 ppm) and they are very less toxic [20]. Earth profuse Copper-zinc-tin-chalcogenide (in this communally denoted by CZTS) has fascinated growing consideration for photovoltaic applications. Manifold vacuum and non-vacuum established techniques for fabrication of thin film have been testified for the development of CZTS thin films [21].

CZTS quaternary compounds with semiconductor properties have arisen a capable applicant for materials that absorb solar energy. Every component of CZTS is cost-effective, with less toxicity, and plentiful for the earth. The elements in the

upper layer of earth's crust used in CIGS, CZTS, CIS, and CdTe, which are applicable for light absorption [22].

1.3.3.2 Chemical and Physical Properties of CZTS

CZTS is composed of four elements, Zinc, Copper, Sulphur, and Tin. CZTS is a quaternary type of complex semiconductor that refers to a stannite structure, and its chief constituent is the combination of two forms containing zinc and iron. There are other structures of CZTS other than stannite such as an orthorhombic superstructure and a hitherto unknown structure as well. Usually, stannite grants steel grey colour with small shining metallic colours like olive green, in the vast particle form. It primarily takes place as hydrothermal deposits in some regions, such as the UK, Cornwall and Bolivia [23]. In 1960, a scientist had anticipated a stannite structure containing iron in place of zinc (Copper iron tin sulphide) semiconductor of quaternary structures of ultra-crystal written in the journal 'Nature' [24]. Until 1974, it is not the first time that two scientists Schafer and Nitchey had made-up CZTS up to that era [23].

Another chemist offered that only one phase of Copper Zinc Gallium Sulphide existed there, which is present in this system's complex and two transitional stages of quaternary type. And the iso-thermal segment of the two methods used was created by using the X-ray diffraction technique at 670 K for analysis [25]. The quaternary group of CZTS I_2-II-IV-VI$_4$ is acquired over and done. Group III element, which is indium, is swapped by Group II element Zinc and Group IV element Tin in Copper indium selenide in the progression [26].

The non-stoichiometry of alloy semiconductors draws a parallel associated with the electrical characteristics of these semiconductors. To achieve high proficiency

Copper Zinc Tin Sulphide solar cells, now there is a practical instruction that the Copper: (Zinc + Tin) and Zinc: Tin atomic ratios ought to be from the range of 0.74 to 1.0 and 1.0 to 1.252, correspondingly. The Copper: (Zinc + Tin) and Zinc: Tin ratios are 0.59 and 1.10, individually, for the originator thin films, and 0.70 and 1.20 for the sulfurized thin films of Copper Zinc Tin Sulphide. The Copper: (Zinc + tin) and Zinc: Tin ratios of the thin films of the CZTS are a little higher than those of the originator thin film. That is endorsed to the emission of tin all through the addition of sulphur [28]. The progressive association of the two systems of Copper Indium Selenide and CZTS is illustrated in is given in Figure 1.
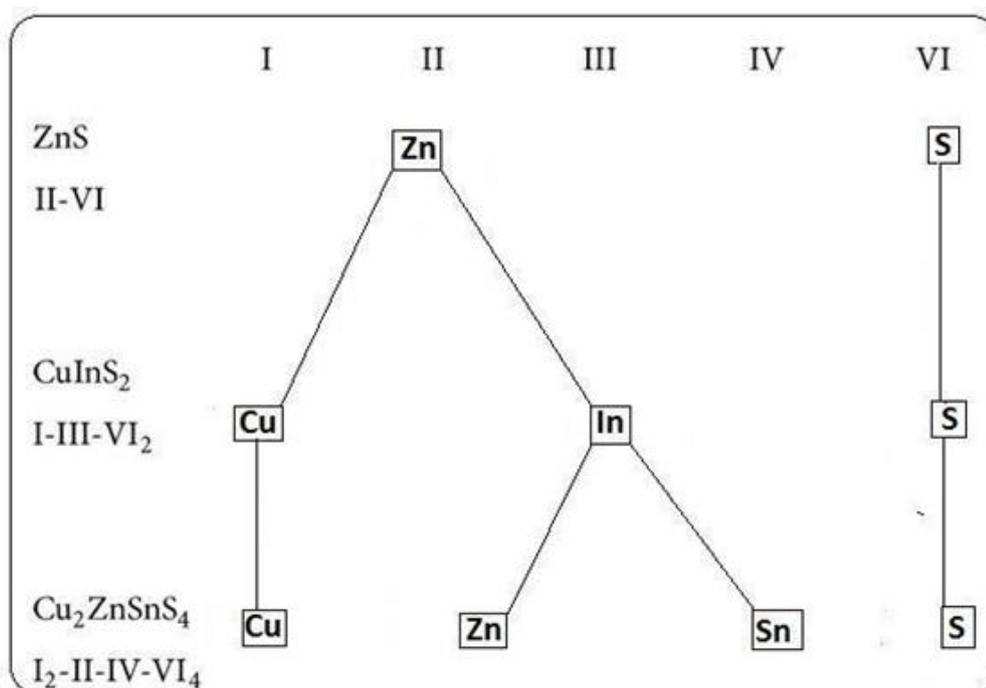
Figure 1: The progression graph of quaternary CZTS

(Source [27])

1.3.3.3 CZTS Thin-Film Preparation by Electrochemical Deposition

One of the most attractive techniques, in this case, is electrodeposition, which is used for the little cost development of various semiconductor thin films on a small scale in research work as well as on broad-scale applications in industries. The specific deposition procedures smeared for thin films of CZTS (atom beam sputtering, photochemical deposition, thermal evaporation, electron beam evaporation, hybrid sputtering, pulsed laser deposition, and screen printing,) involve complex apparatus which is very costly [19].

In the field of electrochemical deposition, the path gives the idea of great attention because it is straightforward to perform; it is without a vacuum. This is a cheap technique that can be operated at standard temperature and utilizing the solvents of less toxicity and chemical agents, which have remarkably high output and the consumption of large materials. Electrochemical deposition which has the benefit of being a technologically proven procedure for massive field area semiconductor electrochemical deposition of higher homogeneity in the arrangement. Also, up till now, the relevant literature shows its composition, which is non-uniform, and the occurrence of other phases inhibiting the acquisition of electrochemical deposition of thin films of CZTS is of excellent value [29]. Now at the present work, the primary purpose of boosting the electrodeposition procedure for the flexible substrate in command for getting the best quality of thin films of CZTS.

To decrease the positive ions in the water solution, carbon-based solution, or heated liquid in the negative electrode by providing potential difference and the external power circuit, the electrochemical deposition coating process is used. In the middle of 1970s, the public initiated the electrochemical deposition of materials with

semiconductor nature [30]. In the late of the year 2008, the University of Bath in Britain successfully electrodeposited Cu, Sn and Zn to achieve the Cu-Zn-Sn-S solar cells with a transformation efficiency of about 0.8 percent [31].

1.3.3.4 Advantages and Disadvantages of CZTS Films

For the development of solar cells of thin films, silicon is one of the most dominant elements. Solar cells that are based on silicon are not expensive. Many depositing techniques have manufactured the CZTS based solar cells as drop coating, an electrochemical, sputtering method, spray pyrolysis, thermal evaporation, and photochemical deposition. Electro depositing is a commonly used technique because it is easy to use, inexpensive and non-toxic. It enhances the CZTS thin filming due to its advantage in the industrial process.

To elaborate the CZTS films, three processes of electrochemical deposition are used: the first one is the single-step deposition in this process all components Zn, S, Cu and Sn are established in one electrolytic bath, the second process is stacked sequentially depositing: in this process, each component have deposited in a sequence that forms layers and gives a stacked film, the third one is called co-deposition in which all needed ions such as Zn, Sn and Cu can be settled as a compound to synthesize a mixed film.

Furthermore, co-deposition is a process that a matrix metal is deposited by one of the deposition techniques such as electrolytic co-deposition, spray co-deposition, vapor co-deposition, introduction, rinsing, electrodeposition, diffusion layer, electro-deposition alloys, vapor deposition, sputtering, thermal spraying, electropolishing, and electrochemical machining. Where the co-deposition methods used for manufacturing metal matrix alloys are electrolytic co-deposition, spray

co-deposition, and vapor co-deposition [32]. The stacked deposition and co-deposition for CZTS are required an extra step that is a normal way to obtain thin films by using Sulphur. In the electrodeposition technique, the first one is the cleanest and easy method, and it also gives satisfactory results because it is a Sulphur free route.

1.3.3.5 Band Gap and Theoretical Efficiency of CZTS

Band gap is known as the energy change between the upper part of the valence band and the lower part of the conduction band. Knowing the and gap of a material is good indicator to the wavelength of light needed for absorption to transfer electrons or power. CZTS has a bandgap of 1.53 eV that makes it good for its optimum electrochemical properties. Great research has been done in CZTS technology to improve CZTS solar cells performance which means achieving the theoretical efficiency. Nevertheless, the empirical efficiency of CZTS solar cells is still far from the theoretical. This is due to many factors such as the limitations which have been observed for some made CZTS solar cells of kieserite which have a short lifetime and high resistance [17].

There are many approaches to overcome these problems to achieve high-performance devices. To enhance the performance of solar cells, the optimism theoretical bandgap must be achieved. One way to increasing the bandgap is by changing the Se constituent for the modulation of electric field in the layer of absorber which may improve the transport of photo-generated carriers [33]. If the right bandgap is not achieved which means the efficiency not improved significantly, CZTS still has a lot of potentials if the manufacturing cost is low with applications exceeds regular PV rigid cells. As it was mentioned, CZTS can be electrodeposited

over the transparent glass and over flexible polymers which mean generating energy anywhere even if that energy empirically small. Also, CZTS elements that easy to be found, as well as collaborated with them are less toxic than another thin-film solar cells. Lastly, getting done in cheap ways as electrodeposition in a single or two steps would drop the cost of manufacturing significantly which would make it visible to compete in the market.

1.3.3.6 Cyclic Voltammetry and CV Studies of CZTS

As it is noticed, the CV can provide a vast number of characteristics and analysis tools such the system electric-chemical behaviour. Quantities at varied scan amounts used to also conclude the diffusion coefficient of the metal ion along with the transfer coefficient α. With the help of such device, the redox potential and other readings can be determined in the most fit solution environments. Figure 2 depicts the deposition potentials were found to move on the road to the right with the rise in pH.
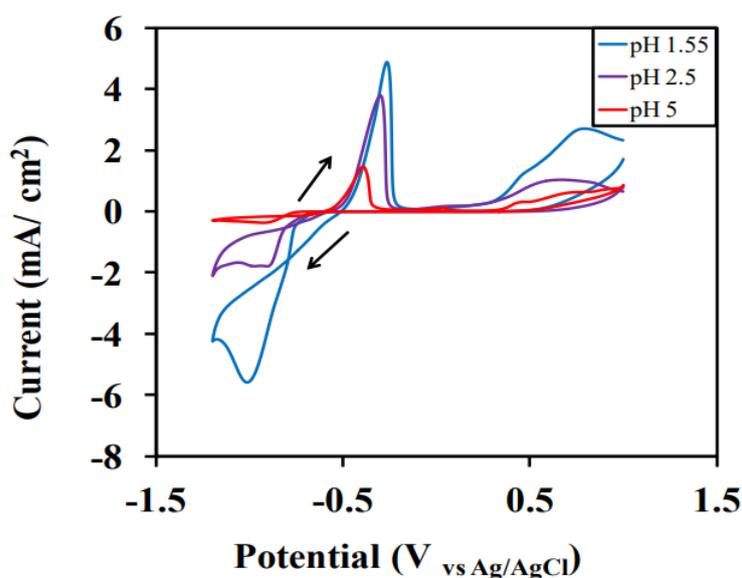
Figure 2: Example of cyclic voltammetry graph of CZTS at different pH
(Source: [39])

The voltammogram in Figure 3 shows a single peak anodic (I) and one cathodic (II). The reduction peak that starts at -1 V and reaches its maximum at a potential of -1,315 V matches the reduction of Zn^{2+} to Zn^0. Peak I which reaches its maximum peak around -800 mV corresponds to the oxidation of Zn to Zn^{2+}. Therefore, reduction of zinc on the gold electrode was conducted in a single Step:

$$\text{Peak II } Zn^{2+} + 2e^-\ldots\ldots Zn^0$$

$$\text{Peak III } Cu^{2+} + 1e^- \ldots\ldots C^u$$
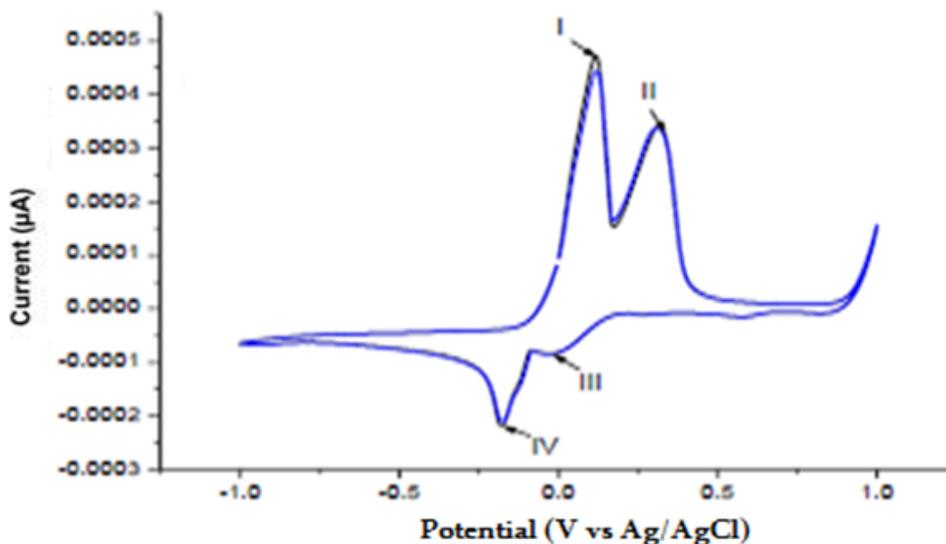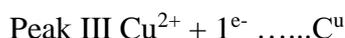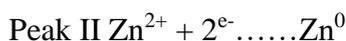
Figure 3: Example showing CZTS full cyclic voltammetry
(Source: [21])

The voltammogram displays anodic and cathodic structures, each having two peaks. In cathode, the initial peak (III) starts to show from 200 mV with its peak at -7 MV. It matches the reduction of Cu^{2+} to Cu^+. The next peak (IV) starts at -80 mV and obtains its peak at -200 mV. It matches the reduction of Cu^+ to Cu^0. Anodic peaks I and II match respectively to the oxidation of Cu^0 and Cu^+.

$$\text{Peak IV} \qquad Cu^+ + 1e^- \ldots\ldots Cu^0$$

In electrochemical experiment study, analysing the electrical cell properties is essential. One of the experiments which helps in characterize the electrical properties is cyclic voltammetry (CV). Cyclic voltammetry allows the study of redox properties and interfacial structures. Also, it can provide qualitative information about catalysts and the reaction such as the catalytic activity of the catalysts, the electrochemical response, and the interaction of a catalyst with an electrolyte [34].

Most commonly, it can provide the reaction potential under different conditions like what is in Figure 4 where even the scan rate, sweep, plays a role in the analysis. The graphs readings give redox peaks which are a representation of the reduction and oxidation process which predict the capacitive behaviour. After analysis, the material potential for the oxidation and reduction process can be found.   Also, CV graphs reading gives essential information about the system behaviour such as irreversible, reversible, or quasi-reversible [35].
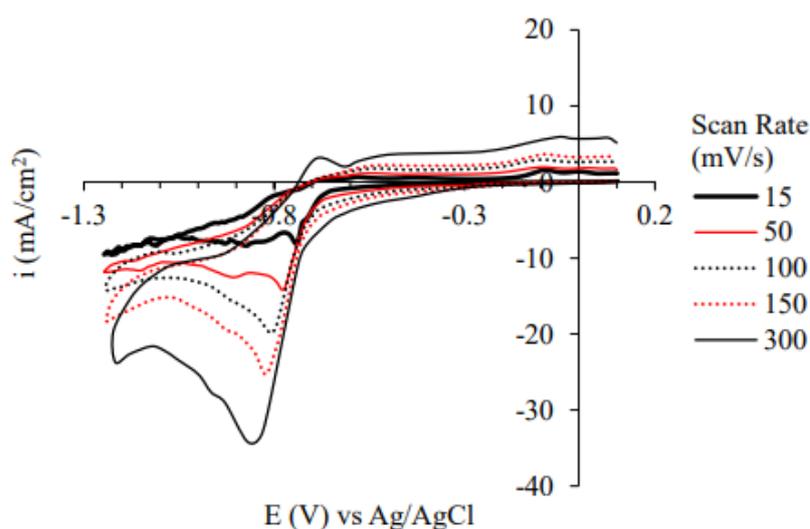
Figure 4: Plots of CuSnIn full cyclic voltammetry of different sweep rates
(Source: [54])

1.4 Electrodeposition

1.4.1 Electrodeposition Basics and Parameters

Growth at the edges of the electrodes is prevented by ensuring that the deposition current density is lower than some critical value. A confounding factor in an electrical deposition from water solutions is that water has inherent analogous abilities to most ions. Results in the progression of H_2 (Hydrogen) gas from the operational electrode in the electrolyte solution. In acidic and basic solutions, the hydrogen evolution reactions (HER) revealed here:

$$H^+ \text{ (aqueous)} + e^- \rightarrow \tfrac{1}{2}H_2 \text{ (gas)}$$

$$H_2O + e^- \rightarrow \tfrac{1}{2}H_2 \text{ (gas)} + OH^- \text{(aqueous)}$$
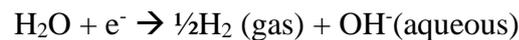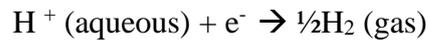
The average decrease in the impending HER is described as 0 Volt in comparison with the Normal Hydrogen Electrode (NHE), but the possible practical variations in pH, conferring to the following equation [36]:

$$E_{H_2} = E_{H_2}^0 - \frac{RT}{F} \ln \frac{1}{a_{H^+}}$$

Like the HER, there might be some other procedures limiting the variety of possibilities for a particular system. For instance, water oxidation that takes place, which has similar actions to the hydrogen evolution rate but provides current from the anode, and an additional prospect, is the oxidation process to happen in the substrate's material. Table 1 list commonly used substrates., which would be creating a loss of electrical power at the base that should be fled away [37].

Table 1: The hydrogen potentials of some pertinent metals. (Source: [26])

Substrate material	η_{H_2} [V]
Cu	0.45
Mo	0.57
Pt	0.09
Zn	0.83
Sn	0.75

1.4.2 Faraday's Law of Electrolysis

Faraday's law has application in an electrochemical deposition. In this case, the chemical change caused by the quantity of electricity is designated as Faraday. This is still used in electrochemistry and analytical chemistry. This law can be express as:

$$Q = m/z$$

$$Q = It = z*Fn$$

Where Q in ampere seconds or coulombs represents the charge that passed, I represent the amount of current which passed, t is the time of current that passed, and 'z' is the change in oxidation state. F represents faraday's constant, and n is the quantity of a reduced or oxidized substance. Thus, in any electrodeposition study, one of the major things which would affect the quality and the quantity of the deposited materials would be the electrolyte. As result, the major part which should be investigated before deploying the experiment is the solution itself. For example, electrical conductivity of the solution not only should be measured but could be engineered based on many factors such as the concentration of the elements and complexing agents.

After understanding the behaviour, more quantity of electrodeposited materials would be done in less time which by itself would decrease the manufacturing labour cost. More importantly, would result to better control of the electrodeposited mass. Below in Figure 5 and example of faradays law graphed where the frequency and rate of removal of material measured. Various substances released by electrical quantity have an inverse relationship with the equivalents of chemical weights like what it seen in Figure 5.
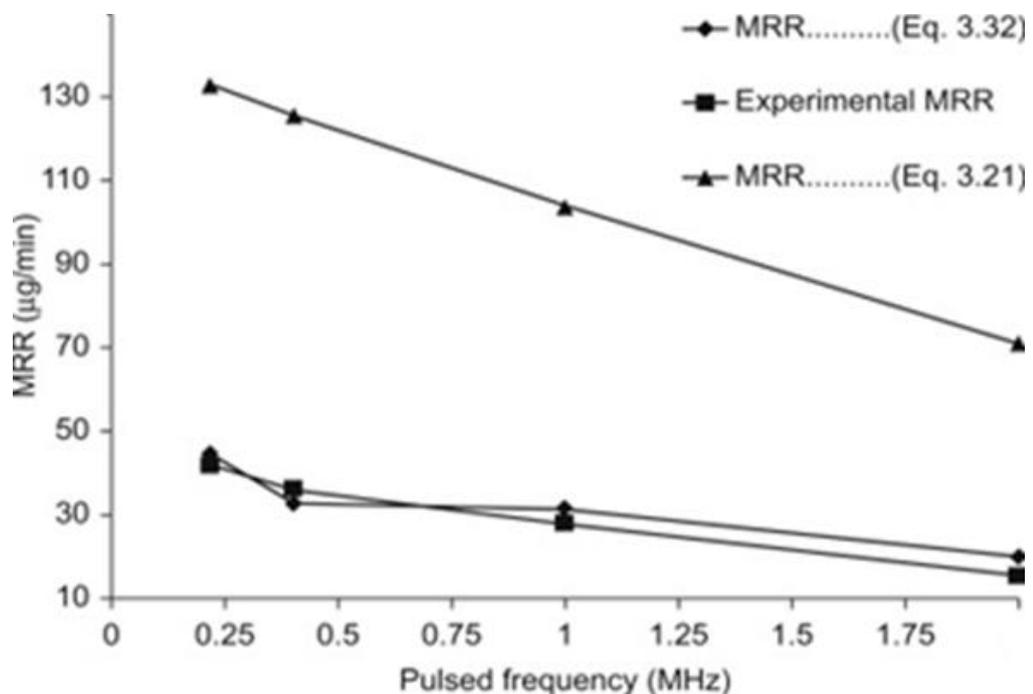
Figure 5: Faradays law of electrolysis graph shows the material removal rate vs.
potential frequency rate. (Source: [37])

Electrodeposition is a method used to produce metallic coatings using an electric current on a conductive material dipped in a solution having a salt of the metal for deposition. The relevant literature reported that the following factors affect the rate of electrodeposition.

1.4.3 Effects of pH on the Electrodeposition Rate

Acidic electrodeposition solutions consist of a pH below 7. Acidic solution is used in Tin electrodeposition. Basic electrodeposition solutions consist of a pH above 7. Cyanide alkaline solution can be applied in Zinc electrodeposition. A basic solution result in hydroxide ions [17]. The value of pH must maintain for reliable results. Any drastic change in pH can cause a disturbance in the equilibrium between different processes taking place. When the cathode is not suitable, hydrogen evolution takes place. Another experiment has shown different outcomes regarding the pH of the solution effect on the morphology or the structure of the electrochemically deposited CZTS thin films.

The experiment has used a sodium thiocyanate electrolyte at three solutions of 2.5 M of NaSCN at pH values of 1.55, 2.5, and 5 respectively [38]. Based on the cyclic voltammetry plots for CZTS precursors, it was noticed that the deposition potentials have moved in the right direction as the pH of the solution increased. For the SEM analysis of this experiment, it was found that the CZTS films produced at a pH value of 2.5 consist of a densely packed structure compared to the samples produced at solutions that have either a pH of 1.55 or 5 [39]. This might contradict with the fact founded in the previous study mentioned [40]. This current study shows that the packed structure might not be a result of the pH effect, it is a result of the stoichiometric composition of the CZTS produced at a pH of 2.5. Where the other deposits have been prepared at non- stoichiometric compositions with higher sulphur contents.

1.4.4 Effect of Temperature of the Electrodeposition Rate

High-temperatures can cause an increase in the size of a metal structure. As a result, the conductivity of the solution increases. It also decreases the solution viscosity. Elevated temperature also decreases the adsorption of hydrogen ions on the deposition layer, which reduces the tendency towards cracks and damage. But an increase in temperature above 55°C causes the contrary effect. Concentration decreases with risen temperature since mass of diffusion layer reduces and ionic diffusion increases. Elevated temperature increases energy used and heat supplied for bath evaporation.

In another study, the resulted CZTS electrodeposited thin films have shown a non-uniform distribution of the electrodeposited particles with more definite boundaries. The crystallization of the films has started at the temperature of 350°C, and it kept increasing in size with larger and flatter grains and surfaces with increasing the temperature [41]. Large grains formed from the accumulation of small CZTS nanoparticles creates more compacted films that lack for cracks and voids, but this does not eliminate that it could be rough [42]. It was also found that the band gap of the films increases with the annealing temperature. Therefore, to obtain solar cells with high efficiencies, treatments with elevated temperatures are required, as the efficiency of polycrystalline solar cell increases with an increase in grain size of the adsorbed layer [42]. Based on the mentioned studies it could be concluded that CZTS thin films are strongly dependent on temperatures.

1.4.5 Effect of Time Factor on the Electrodeposition Rate

In one of the electrodeposition studies, it was found that time allocated to the electrodeposition process is long, more uranium is deposited to the Pt cathode. Electrodeposition time of sixty minutes results in deposition of uranium

about 74.96% of the initial uranium [16]. Electrodeposition time is directly proportional to the mass and thickness according to the law of Faraday:

$$I*t = Q$$

In an experiment related to electrodeposition and time, Tang have summarized the time effect on the CZTS electrodeposited thin film mass and morphology. Since the accurate stoichiometry is difficult to achieve, the study has shown the study has focused on an off-stoichiometry CZTS synthesized thin films by one-step electrodeposition. Experimentally, the electrolyte consisted of 2.5 mM $CuSO_4 \cdot 5H_2O$, 1.25 mM $ZnSO_4 \cdot 7H_2O$, 2.5 mM$SnSO_4$, 5 mM $Na_2S_2O_3 \cdot 5H_2O$, 25 mM triSodium Citrate di-hydrate ($C_6H_5Na_3O_7 \cdot 2H_2O$), and 5 mM L-(+)-tartaric acid ($C_4H_6O_6$). Each of the working electrode and the reference electrodes was indium-tin oxide (ITO) covered glass and saturated calomel electrode (SCE), respectively [43].

To study the time effect on the CZTS thin film electrodeposition, SEM pictures have been compared at various times of annealing. The longer the deposition time was conducted the smoother surfaces have been produced, while the CZTS thin films that have been produced within the lower time periods had cracks nor holes. Annealing has shown an effect on the morphology of the thin film, as it changed the films from less flat surfaces into more compacted flat surfaces, which is what is preferred in the solar cell applications. Time has also an effect on the mass of the electrodeposited films. As the mass increases slowly with the time elapse. In the later stage of the electrodeposition, it was observed that the mass of the film increased in a slower rate [43]. Tables 2 and 3 show the increase in the grain size as the time increases, which promotes by its turn the mass and smoothness, respectively.

Table 2: Compare deposition grain size, band gap, carrier size property of 550°C
annealed CZTS thin films. (Source: [43])

Deposition time (min)	Grain size (nm)	Band gap (eV)	Carrier type
90	21.76	1.50	p
100	22.58	1.43	p
110	20.31	1.49	p
120	28.52	1.52	p

Table 3: Compare carrier concentration, and carrier mobility property of 550°C
annealed CZTS thin films. (Source: [43])

Deposition time (min)	Carrier concentration (cm^{-3})	Carrier mobility (cm^2/Vs)
90	1.85×10^{20}	1.68
100	4.71×10^{19}	7.13
110	2.09×10^{18}	28.20
120	5.64×10^{17}	17.57

1.4.6 Effects of Molecular Composition on the Electrodeposition Rate

Cu_2ZnSnS_4 (CZTS) has been fabricated as the absorber layer on thin film solar cell technology. Controlling the concentration of each substance influences the final coating results and the efficiency. designed a three stage system to obtain CZTS absorber layer carried on SnO_2/F coated glass substrates, the concentration was as follows; zinc chloride (0.088 M), copper was deposited using a cyanide medium bath [NaCN (1.3 M), Na_2SO_4 (0.017 M), ZnCN (0.068 M), $Na_2SnO_3 \cdot 3H_2O$ (0.018 M), CuCN (0.78 M)], and tin chloride (0.088 M), the report mentioned that high zinc and low copper contents in the electrodeposited film showed good quality uniformity, also excess zinc obtained poor quality film with less adhesion. Zinc and tin concentration in electrodeposited film were kept almost equal for superior quality film [44]. In 2010, the Japanese Nagaoka University of Technology reported that absorber layers with

high efficiencies are recorded for cells with Cu-poor, Zn-rich chemical concentration, this is because Cu-poor contributes to the formation of Cu vacancies, while Zn-rich suppress the substitution of Cu at Zn [45].

1.4.7 Effect of Complexing Agents on the Electrodeposition Rate

Complexing agents used in electrochemical cell deposition for the purpose of reducing the standard potential values of the materials, therefore, it can be said that complexing agents effects the final coated film. To co-deposit CZTS on a single step mechanism, one must make sure to add the suitable complexing agent, TriSodium Citrate, tartaric acid, and sorbitol have been found to be suitable complexing agents for single step electrodeposition of CZTS on metal and on transparent conducting oxide substrates [38]. Shin, Park et al. mentioned the effect of complexing agents by comparing Cu electrolytes with and without the complexing agent. The solution with no complexing agents showed reduction peak at -0.1 V (vs. Ag/Agcl), on the other solution the reduction peak was observed at -0.8V. This was due to the bare Cu ion being unstable in the triSodium Citrate solution and forming complex with citrate ions [46].

1.4.8 Procedures for Manufacturing of Thin-Film (TF) Constituents

In broad-spectrum, the methods applied to formulate TF plunge into two classifications, which are by the name called "single-stage" moreover the second name as "two-stage." According to these names, the single-stage procedures are those who manufacture the whole crystal film in a single step [18]. The primary step is the grounding of a 'predecessor,' which is, in general, formed at room temperature. It comprehends any i) merely the metal type elements, and ii) all the un-reacted or non-crystalline element forms. While performing the second stage, in which the predecessor is heated, typically by aerobic way comprising sulphur. That is termed as

sulfurization or salinization. The development and crystallization of the preferred phase from the predecessor film have opted at heating.

The use of the first stage in an abundant variety of different means can be conceded, examples included from the CZTS collected works are pulsed, deposition, sputtering and electron beam evaporation [47], electrodeposition, nanoparticle, or suspension printing, as well as spray pyrolysis [48]. Thus, the advantages and disadvantages of the concerned method are:

- Advantages: i) lower cost compared to some of the methods out there such as vapor deposition, ii) control of homogeneity, and rate of deposition, iii) deposition is made on several shapes, iv) significant manufacturability, v) strong adhesion of the coating on, vi) it is used in decorations to coat metal surfaces with required metal coatings, and vii) stops rusting and prevents corrosion of metal surfaces.

- Disadvantages: i) electrodeposition can lead to the low standard appearance of the plated material case it is not uniform, ii) with some reactions the exact product or mass is hard to predict, and iii) requires sometimes controlled environment such as less noises.

1.5 Characterization of Electrodeposited Products Using XRD and SEM

1.5.1 Scanning Electron Microscope (SEM)

SEM is a type of electron microscope, which gives zoomed imaged by shedding a light over the surface of a sample. The light reflected electrons signal produces much information about the composition and the surface topography of the used material. All that done by examining the electron beams pattern, position of beams, and its

intensity. Typically, a small attachment to the SEM device call EDS which will be used in this study to find the quantity and the presence of electrodeposited elements.

At the institution of Nagaoka National College of Technology, CZTS thin film study was done by sulfurization of stacked metallic layers. Furthermore, SEM was used to study the properties based on the morphology of some contained samples. Figure 6 displays of the constant film with massive particles were shaped on or after the accumulation of minor nanoparticles Copper Zinc Tin Sulphide. SEM displays the thin film as a dense part in structural properties deprived of cavities and different crashes. However, with present some irregularity. For getting hold of high efficiency solar cells, very high-temperature action is crucial to upturn the crystal-like form and particle size of films of CZTS. The effectiveness of the complex structure of polycrystalline solar cells rises with a surge in the particle size of the absorbed [49]. Also, it was found using SEM in another study that the morphological studies of thin films' surfaces will be varied depending on distinct mass order in ancestors [50].

CZTS SEM image revealed that the lowering percentage of mass incrementing at the later stage of electrodeposition may be owed to less accessibility of the bath species. As a result, the mass of the TF could easily organize in an appropriate variety. The abridged atoms are likely to fill in the lowest point and trenches to form an even and uniform surface because of the complexing agents ' flattening effect [51]. Figure 6 shows an example of CZTS SEM image.
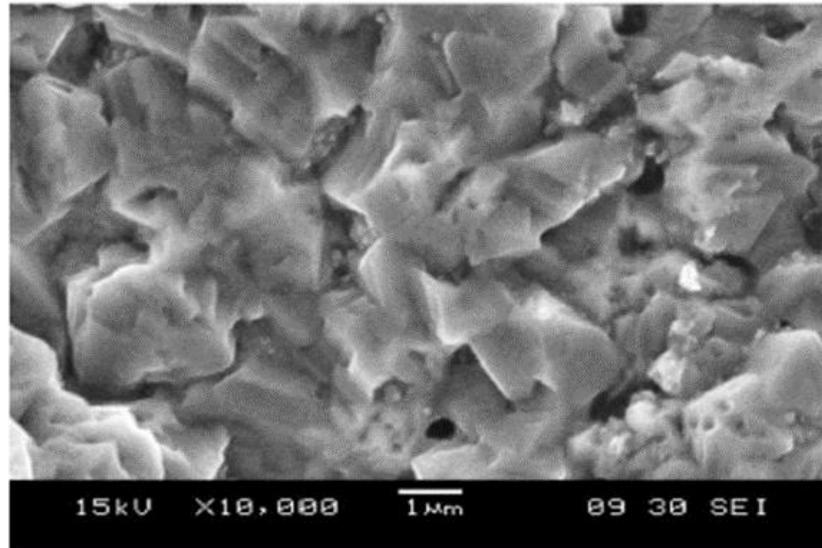
Figure 6: Example of an SEM image of a thin film of CZTS
(Source: [51])

As it can be seen, having such device was particularly useful in understanding the chemical reaction behaviour of the product. Researchers not only can determine the quantity, but they can microscopically look at the interactions analysing the behaviour which makes their predictions more accurate. Also, the composition of each plated elements will be present which should shed a light on chemical reaction behaviour of each element in the mixed solution. This could be a good start to knowing the behaviour of the reaction and in the future engineer the exact composition based on the requirement predicting each element behaviour while electrodeposition it.

1.5.2 X-Ray Diffraction (XRD)

XRD is used for identifying the atomic and molecular structure of a crystal from the pattern formed by the diffracted x-ray beams. Thus, can be done by measuring the beam angles, and intensities. This data can help to picture a 3d model of the sample

which tells more about the type of crystalline, chemical bonds, and much other information about the specimen.

In the below CZTS study, XRD showed the development of kieserite phase CZTS in the deposits. The crystal structures of the previously manufactured nanostructures of CZTS were studied through X-ray diffraction technique and x-ray diffraction measurements. Figure 7 displays the X-ray diffraction patterns of the previously manufactured CZTS nanoparticles set down by electrodeposition with 2-degree theta scanning from 20 degrees to 100 degrees. X-ray diffraction measurement displayed crests are ascribable for CZTS was (112), (220), (220), and (312), respectively [52].
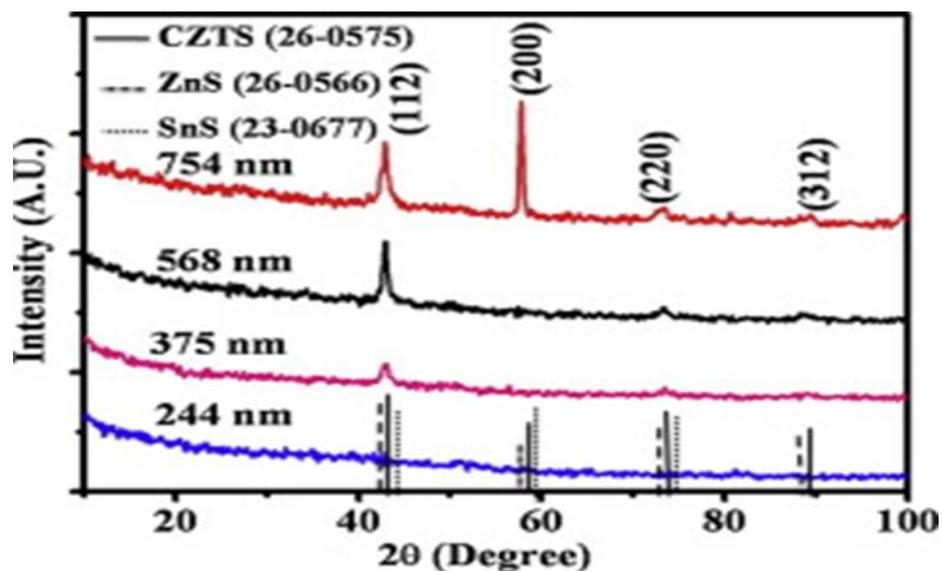
Figure 7: The XRD patterns of CZTS thin films and different alloys
(Source: [52])

Using an XRD device can give lots of information about the electrodeposited sample. Looking at the XRD sample peaks like the ones in Figure 7, the presence of elements can be identified. Also, the quality of the crystalline of each plated element. Furthermore, it helps to visualize the plated sample in a 3D model which would help to understand the reacted element behaviour. Also, XRD can be used as validation to

EDS results. Both devices should validate the presence of an element. Nevertheless, it all depends on how powerful or accurate the devices and their stored data that related to behaviour of the elements' patterns.

Chapter 2: Methodology and Research Design

2.1 Apparatuses and Experiment Set-Up

In the experiment, the pH of the solutions will be investigated which should help in the stability study of the solutions using a pH meter, Figure 8. Also, the Total Dissolved Solids (TDS) device, Figure 9, will be used to measure the number of solid particles in the solutions. Moreover, Electronic Data Sheet (EDS) device. Figure 8 shows the instrument that used to measure the conductivity of the solutions to try to enhance the engineered solution by studying its electrical properties.

Figure 8: APERA pH meter

The Potentiostat device, as shown in Figure 9, has been used for running the cyclic voltammetry analysis study and electrodeposit our alloys using the constant potential feature. Furthermore, Figure 10, shows an example of the step-up which has been used to get the cyclic voltammetry graphs or to electrodeposit the samples. Also, it

shows other equipment and solutions that have been used in the experiment. For example, Acetone to clean the beakers, distilled water, and electronic scales.

Figure 9: TDS and EC meter

Figure 10: Model Modu-Lab XM ECS- potentiostat - galvanostatic system

Furthermore, screen-printed carbon electrodes have been used in most of the experiments due to their cost-effectiveness and the enormous potential of carbon electrodes due to carbon useful properties. For few other times, silver and gold electrodes were used for testing and validation only such as the ones, as seen in Figure 11.
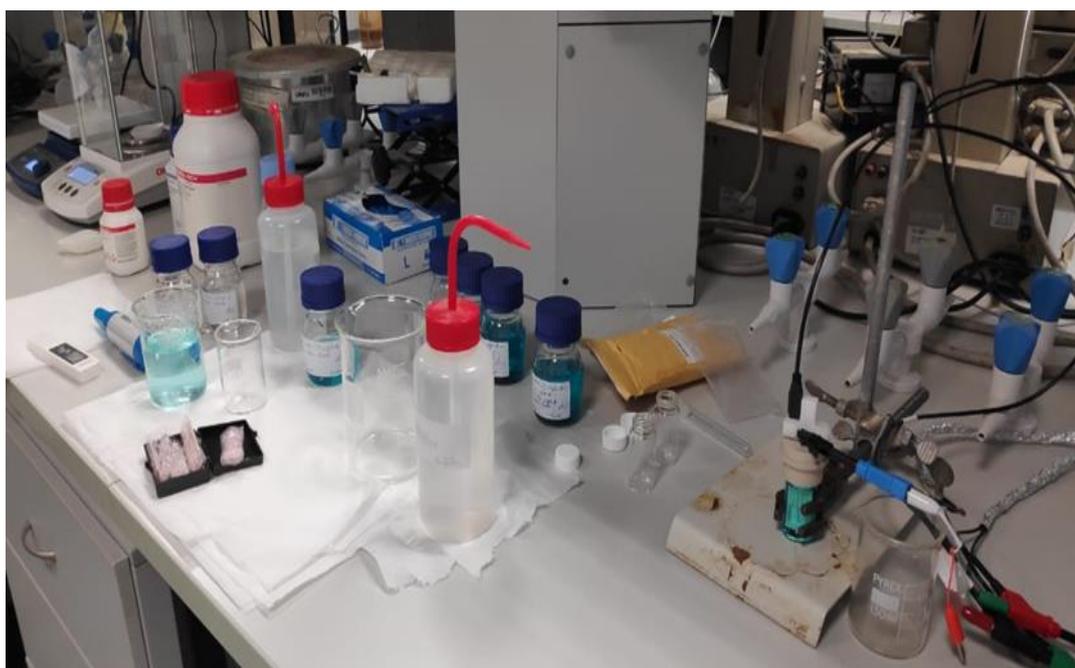
Figure 11: Experiment set up

Characteristic and details of the used carbon electrodes can be found in Figures 12 and 13. Nevertheless, for better measurement, an external Ag/AgCl reference electrode has been used even though the screen-printed electrodes have one already, as shown in Figure 14. Furthermore, a special jar, Figure 15, was used to mount the set-up which has an electrical board to connect all wires.

Figure 12: Sample of different electrodes used in the study

Figure 13: Screen printed carbon electrodes from Pine research company
(Source: [53])
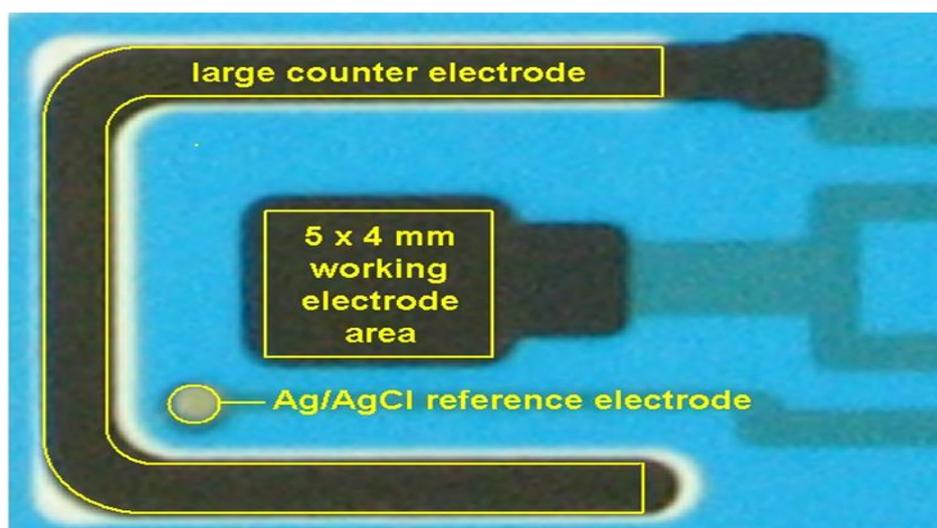
Figure 14: Screen printed carbon electrodes details
(Source: [53])
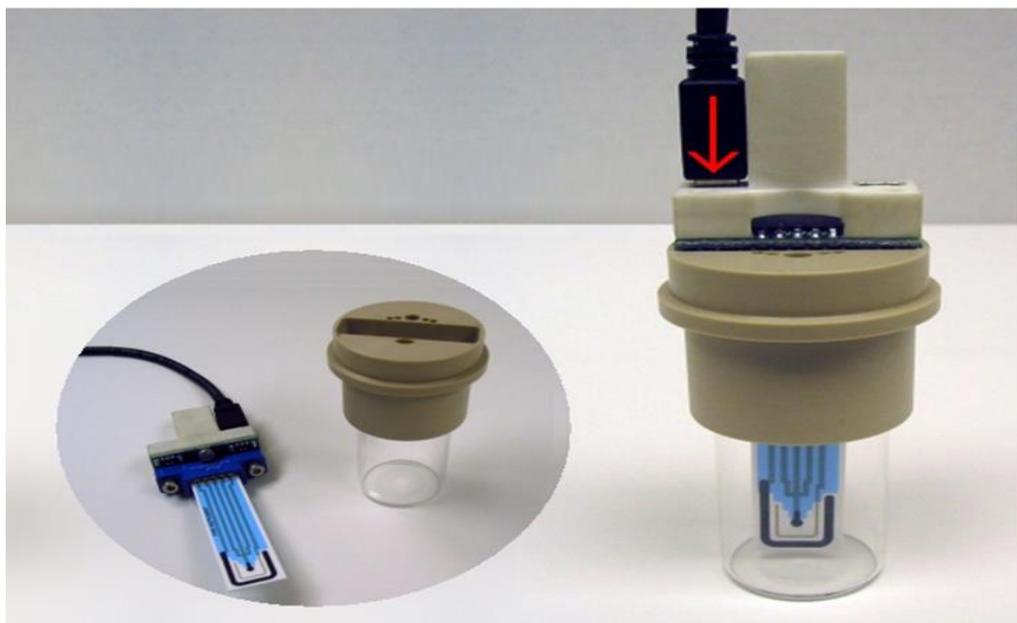
Figure 15: Electrode card mounted in jar cell
(Source: [53])

Moreover, a Scanning Electron Microscope (SEM) was used to analyse the surface morphology of the electrodeposited samples, as shown in Figure 16.

Figure 16: RRPEAGCL2 low-profile Ag/AgCl reference electrode (60 mm)
(Source: [53])

To do such, each sample needed to be plated with a thin layer of gold before using the SEM as part of the process and gold plating device used, as shown in Figure 17.
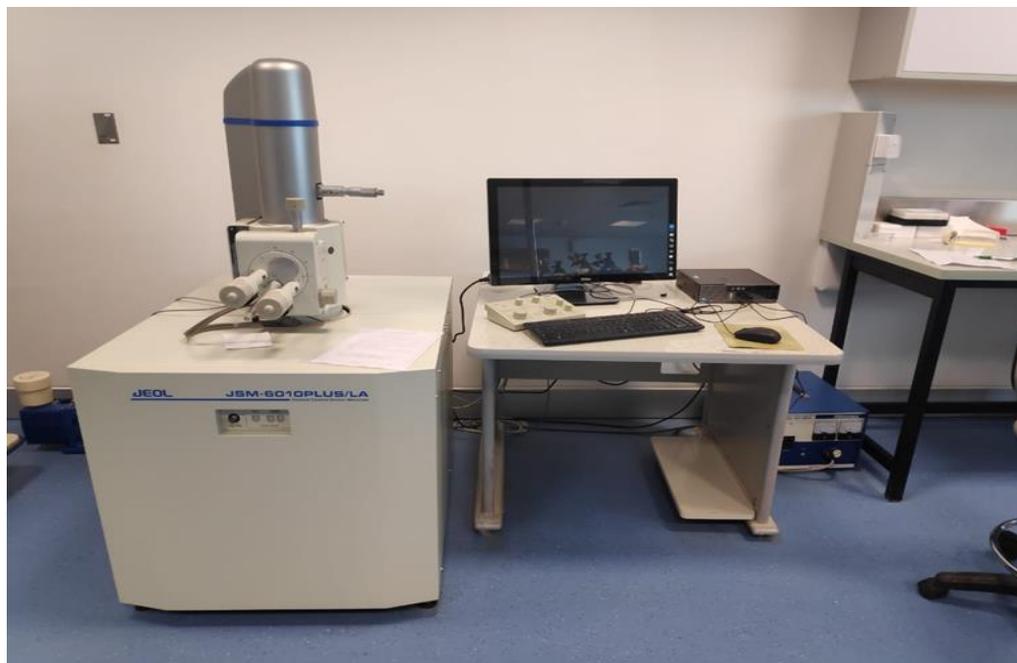
Figure 17: SEM JEOL (JSM-6010PLUS/LA)

Energy Dispersive Spectroscopy (EDS) device was used to identify the presence of elements and their mass quantity percentage in each sample, as shown in Figure 18.

Figure 18: Gold plating device to be used for SEM

Likewise, the X-ray powder diffraction (XRD) device, as shown in Figure 19, was used to validate the presence of elements and to compare such results with EDS obtained results.

Figure 19: X-ray diffractometer (XRD) and X'Pert PRO system

2.2 Engineering the Solutions

The CZTS solutions which will be used in electrodeposition is one of the major parts of this study. There were many options and parameter to study to get us stable solution that can electroplate and report the results safely. For the solution to be stable, it means that no precipitation visible which can be a flaw of the study process.

Thus, two sets of chemicals were valid options to make CZTS. The first consist of copper chloride, zinc chloride and tin chloride. The second set consist of: copper sulphate, zinc sulphate and tin sulphate.

Due to the presence of sulphur in the 2nd set, the second set was picked to study its behaviour. Parameters such as the temperature of the solution, pH, order of mixing, concentration, and which complexing agent to be used. It can be assumed that with increasing temperature better, well-mixed solutions are produced. Nevertheless, that would mean that thermal energy needed to form the final product which means the cost of manufacturing would be higher. Thus, it was decided to run the study under room temperature.

There were many complexing agents in the market which can be used in electrodeposition and the CZTS system as Sodium Citrate, ethylenediaminetetraacetic acid (EDTA), thiourea, tartaric acid, and many other complexing agents which can enhance the process with better yield. Moreover, complexing agents help in achieving higher electrical conductivity and smaller charge transfer resistance in the solution.   In this study, the two complexing agents which was tried were EDTA and Sodium Citrate. However, Sodium Citrate was more stable and has been researched intensively before due to its stability mixing it with other elements and non-poisonous nature.

Thus, it has been decided to focus on the study of Sodium Citrate as primary complexing agent in the systems. Adding Sodium Citrate to the bath shifted the reduction potential of the metals towards more negative potentials. When it comes to EDTA, it works as sequester metal ions prevent them from oxidizing onto pool

surfaces. Moreover, many trials have been done to EDTA but with no success to make all solutions stable, as shown in Figure 20.

Figure 20: Left jar contains solutions with EDTA; right jar is stable contains sodium citrate

When it comes to the concentration of the copper sulphate, zinc sulphate and tin sulphate with Sodium Citrate. To study other parameters and the behaviour of the reaction in depth, the concentration of the elements had to be equimolar to narrow the complexity of the research and focus on the chemical behaviour elements. Thus, for copper sulphate, zinc sulphate and tin sulphate elements different equimolar molarity had been tried trying to get a stable solution which its behaviour can be studied. When it comes to the Sodium Citrate as a complexing agent, it was found that at least 1 M of the solution is needed.

After experiments with different solutions and validating their stability, it was found that 0.03 M of copper sulphate, zinc sulphate, and tin sulphate with 0.125 M of Sodium Citrate gave the most stable solution between all trails. When it came to determining the right pH of the CZTS solution system, many experiments conducted

to get us a stable solution without the need of dropping the pH at first. After mixing 0.03 M copper sulphate, 0.03 M zinc sulphate and 0.03 M tin sulphate with 0.125 M Sodium Citrate in an ionized water, the solution gets a pH of about 4.4. Many researchers expressed the benefit of dropping the pH when it comes to plating solutions and the stability of the solution itself.

Nevertheless, that would mean cost of manufacturing would increase due to the danger factors while managing low pH solutions and extra elements need to be bought or considered. Sulfuric acid and hydrochloric acid were the options to drop the pH in the solutions. Sulfuric acid was the choice because sulphur is one of the elements which is already in the solutions. In contrast, if hydrochloric acid used, chloride is going to be added to the mix which could change the behaviour. Thus, the same solutions with the same concentration involved in testing the elements stability under lower pH.

In this study, HSC Chemistry software were used to initially determine the stability areas of the solutions. Unfortunately, the software used, or its version does not compensate for the use of Sodium Citrate complexing agent which could have a major effect in the stability. Yet, the graphs generated from the HSC software, as shown in Figure 21, hinted toward the right formula which was used in the study and guided towards it. Also, having multiple elements at once added to the complexity of the stability study.
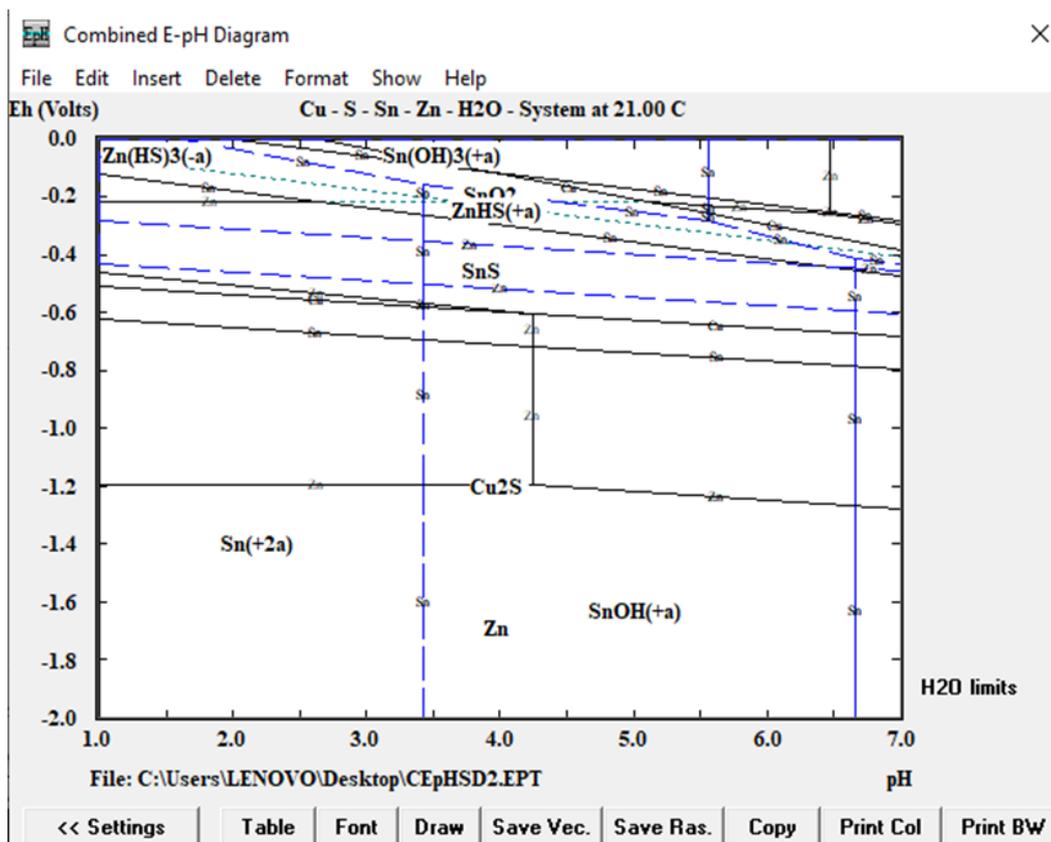
Figure 21: Pourbaix diagram (Eh vs pH) using HSC Chemistry software

After investigating many solutions with simple mix of the elements, a stable solution with 4.4 pH was found to be more suitable choice. Thus, many other solutions made with dropping the pH to 3, 2, and 1 with the use of sulfuric acid. At first, all of them were stable with no issues. After leaving the solutions for about a week, the solution which has a pH of 1 started to develop milky and cloudy white solution which means that it has suspensions. Thus, successfully narrowed down the most stable pH for the solutions with the specified chemical concentrations to be 4.4. Figure 22 shows different experiments investigating the right pH solution.
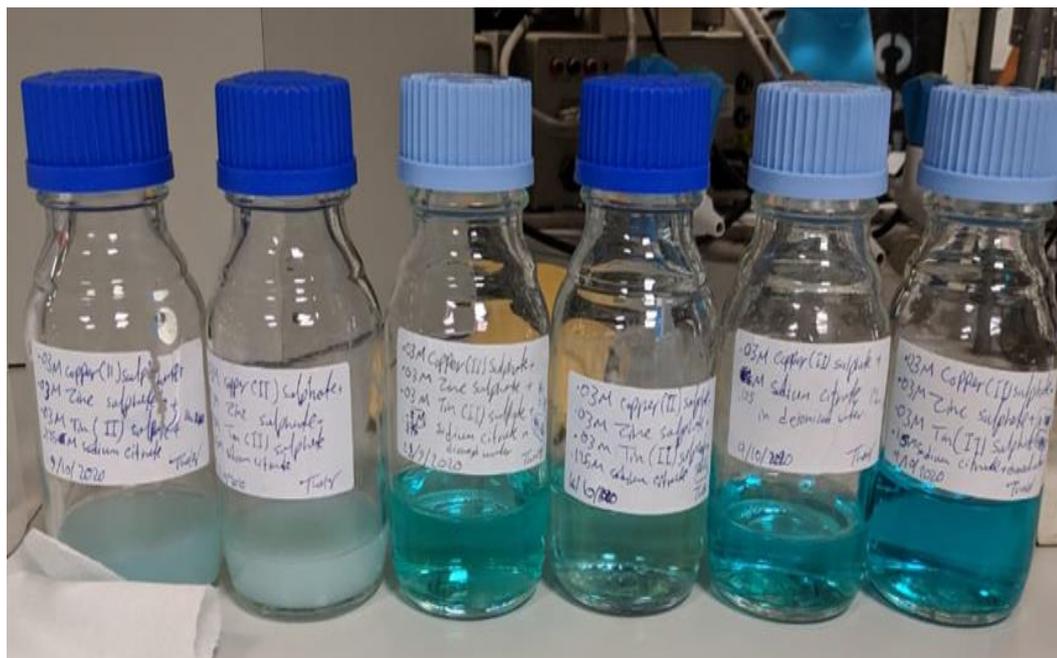
Figure 22: Similar concentrations of different CZTS solutions with with different pH
values to show different stabilities

To determine which stable solution should be studied, it was decided to check the
electrical conductivity (EC) of the solutions. Theoretically, when the EC increases in
a solution with the purpose of electrodeposition, it means better movement of
electrons which might yield better product. To increase the EC, Sodium Citrate had
to be added more or the pH had to be dropped. In case of Sodium Citrate, it was
shown that 1 M Sodium Citrate with 0.03 M copper sulphate, 0.03 M zinc sulphate,
and 0.03 M tin sulphate elements is stable. Furthermore, many solutions made with
Sodium Citrate ranging between 0.1 to 0.175 and it was found that0.125 M gave a
solution without any precipitations and remained stable with no changes for days.
After that, sulfuric acid added to 0.03 M copper sulphate, 0.03 M zinc sulphate and
0.03 M tin sulphate with 0.125 M Sodium Citrate solutions to check the electrical
conductivity, which is presented in Table 4.

Table 4: Different pH CZTS solutions and their electrical conductivity

pH of (0.03 M copper sulphate, 0.03 M zinc sulphate and 0.03 M tin sulphate with 0.125 M Sodium Citrate solution)	Electrical Conductivity (EC) – [uS/cm]	Stability
4.4	12,910	Stable
3	13,750	Stable
2	16,070	Stable
1	18,850	Unstable

It was found after a while that the solution with pH 1, is not stable. Thus, solutions with pH of 4.4, 3, and 2 where the only options for the study. It was decided that pH of 3 has good EC and would be enough for the study; thus, all other solutions were made with pH of 3. When it comes to the order of mixing; after investigation, below is the steps for the most founded stable way to prepare the solutions for the electrodeposition study after trying different orders of procedures:

- ❖ 0.03 M Copper (II) sulphate + 0.03 M Zinc Sulphate + 0.03 M Tin (II) sulphate + 0.125 M Sodium Citrate.
- ▪ Wash the new bottle with Acetone and deionized water.
- ▪ Add 50 ml of deionized water.
- ▪ Add 3.23 g of Sodium Citrate.
- ▪ Shake/mix the bottle for 30 seconds – 1 minute until the solution is well mixed with no clear precipitation.
- ▪ Add 0.75 g of Copper (II) Sulphate.
- ▪ Shake/mix the bottle for 30 seconds – 1 minute until the solution is well mixed with no clear precipitation with dark blue colour developed.
- ▪ Add 0.86 g Zinc Sulphate.

- Shake/mix the bottle for 30 seconds – 1 minute until the solution is well with well mixed dark blue solution.

- Add 0.64 g of Tin (II) sulphate.

- Shake/mix the bottle for 30 seconds – 1 minute.

- Add 50 ml of deionized water- Dark blue solution.

- Mix the solution and measure the pH=4.39, Temp= 21.1^{o}C, EC=1291 uS/cm, 6360 ppm -Dark blue solution with no visible precipitation.

- After 21 drops of Sulfuric acid: pH= 3.03=~ 3, EC= 1375 uS/cm.

❖ 0.03 M Copper (II) sulphate + 0.03 M Zinc Sulphate + 0.125 M Sodium Citrate.

- Wash the new bottle with deionized water and Acetone

- Add 50 ml of deionized water.

- Add 3.23 g of Sodium Citrate.

- Shake the bottle by hand for 30 seconds – 1 minute until well mixed with no clear precipitation.

- Add 0.75 g of Copper (II) Sulphate.

- Shake the bottle by hand for about 30 seconds- well mixed dark blue solution

- Add 0.86 g Zinc Sulphate.

- Shake the bottle by hand for 30 seconds. - well mixed dark blue solution

- Mix the solution and measure the pH=5.04, Temp= 27.78^{o}C- dark blue solution with no participation.

- Measure pH= 5.22, EC= 1332 uS/cm, 6661 ppm, Temp = 21.5^{o}C -no visible participation.

- After 29 drops of Sulfuric acid: pH= 3.03, EC= 1421 uS/cm.

- ❖ 0.03 M Copper (II) sulphate + 0.03 M Tin (II) sulphate + 0.125 M Sodium Citrate.

  - ▪ Wash the new bottle with deionized water and Acetone.

  - ▪ Add 50 ml of deionized water.

  - ▪ Add 3.23 g of Sodium Citrate.

  - ▪ Shake the bottle by hand for 30 seconds – 1 minute until well mixed with no clear precipitation.

  - ▪ Add 0.75 g of Copper (II) Sulphate.

  - ▪ Shake the bottle by hand for about 30 seconds- well mixed dark blue solution

  - ▪ Add 0.64 g of Tin (II) sulphate.

  - ▪ Shake the bottle by hand for about 30 seconds - well mixed dark blue solution

  - ▪ Measure pH= 4.97, EC= 1291 uS/cm, 6457 ppm, Temp = 21.5°C -no visible precipitation after mixing.

  - ▪ After 22 drops of Sulfuric acid: pH= 3.04, EC= 1375 uS/cm.

- ❖ 0.03 M Zinc Sulphate + 0.03 M Tin (II) sulphate + 0.125 M Sodium Citrate.

  - ▪ Wash the new bottle with deionized water.

  - ▪ Add 50 ml of deionized water.

  - ▪ Add 3.23 g of Sodium Citrate.

  - ▪ Shake the bottle by hand for 30 seconds – 1 minute until well mixed with no clear precipitation.

  - ▪ Add 0.86 g Zinc Sulphate.

  - ▪ Shake the bottle by hand for 30 seconds. - well mixed dark blue solution

  - ▪ Add 0.64 g of Tin (II) sulphate.

  - ▪ Shake the bottle by hand for about 30 seconds - well mixed dark blue solution.

- Measure pH= 5.30, EC= 1311 uS/cm, 6558 ppm, Temp = 21.8°C- no visible precipitation after mixing.

- After 30 drops of Sulfuric acid: pH=3.00, EC= 1421 uS/cm.

❖ 0.03 M Copper (II) sulphate Pentahydrate + 0.125 M Sodium Citrate.

- Wash the new bottle with deionized water and Acetone.

- Add 50 ml of deionized water.

- Add 3.23 g of Sodium Citrate

- Shake the bottle by hand for 30 seconds – 1 minute until well mixed with no clear precipitation.

- Add 0.75 g of Copper (II) Sulphate.

- Shake the bottle by hand for 30 seconds.

- Tap the bottle with deionized water till you get to 100 ml.

- Shake the bottle by hand for 30 seconds.

- Measure pH= 5.76, EC= 1272 uS/cm, 6360 ppm, Temp = 21.4°C -no visible participation.

- After 31 drops of Sulfuric acid: pH= 3.02, EC= 1398 uS/cm- no visible precipitation.

❖ 0.03 M Zinc Sulphate Heptahydrate + 0.125 M Sodium Citrate.

- Wash the new bottle with deionized water and Acetone.

- Add 50 ml of deionized water.

- Add 3.23 g of Sodium Citrate.

- Shake the bottle by hand for 30 seconds – 1 minute until well mixed with no clear precipitation.

- Add 0.86 g Zinc Sulphate.

- Shake the bottle by hand for 30 seconds.

- Tap the bottle with deionized water till you get to 100ml.

- Shake the bottle by hand for 30 seconds.

- Measure pH= 7.01, EC= 1253 uS/cm, 6265 ppm, Temp = 21°C -no visible precipitation after mixing.

- After 39 drops of Sulfuric acid: pH= 2.99, EC= 1398 uS/cm.

❖ 0.03 M Tin (II) sulphate + 0.125 M Sodium Citrate.

- Wash the new bottle with deionized water and Acetone.

- Add 50 ml of deionized water.

- Measure the pH= 6.7, Temp= 19.4°C.

- Add 3.23 g of Sodium Citrate.

- Shake the bottle by hand for 30 seconds – 1 minute until well mixed with no clear precipitation.

- Add 0.64 g of Tin (II) sulphate.

- Shake the bottle by hand for 30 seconds.

- Tap the bottle with deionized water till you get to 100 ml.

- Shake the bottle by hand for 30 seconds.

- Measure pH= 5.71, EC= 1234 uS/cm, 6173 ppm, Temp = 20.9°C -no visible participation.

- Thereafter, add 30 drops of Sulfuric acid: pH= 2.99, EC= 1353 uS/cm.

2.3 Cyclic Voltammetry (CV) Experiments and Analysis

Cyclic voltammetry is an electrochemical technique for measuring the current response of a redox active solution to a linearly cycled potential sweep between two or more set values. It is a useful method for quickly determining information about the thermodynamics of redox processes, the energy levels of the electrolyte and the

kinetics of electronic-transfer reactions. When it comes to this study, to determine the right voltage to be applied in the solutions, cyclic voltammetry (CV) experiments have been done multiple times over carbon substrate with an area of 0.2 cm^2. CV experiments help to understand the system by showing the redox peaks which consists of the reduction and oxidation peaks of the examined material. Also, it can predict the capacitive behaviour of the electrode resulting of the potential at which the material is oxidized and reduced to be found. Besides that, it can be used to look for presence of intermediates in oxidation-reduction reactions, determine the electron stoichiometry of a system, the diffusion coefficient of an analyte, and the reversibility of a reaction.

There are 3 major elements to any CV experiment: voltage, current density, and time. In this CV experiments and based on previous experiments in such metals, it was decided to run it with these factors: -0.209 to -0.214 voltage range with Ag/AgCl (silver chloride electrode), scan rate of 5 mV/s, and 5 cycles. Furthermore, the negative part of the system was only considered which shows the behaviour where the elements get electrodeposited. Also, it was repeated for five cycles to make sure of the outcome.

2.3.1 Copper Electrodeposition CV Analysis

Cyclic voltammetry graphs were generated for copper over the carbon substrate using different electrolyte. Five cycles in total were done with 5 mV/s scan rate using Ag/AgCl as a reference electrode for each electrolyte. Also, the area of the working electrode was 0.2 cm^2. During this experiment, no visible bubbling was found. This experiment run in a stagnant solution with no rotating in a room temperature. This should indicate the copper element general behaviour in the different solutions. CV

analysis for copper showed one major reduction peak which appears at -0.3589 V vs. Ag/AgCl. Furthermore, in the CV for copper-zinc there were one major reduction peak appears to be on -0.369 V vs. Ag/AgCl. In the CV of copper-tin, there were two major reduction peaks appears to be on -0.359 V vs. Ag/AgCl. Another one appears to be on -1.029 V vs. Ag/AgCl. When it comes to CZT CV, there were 3 major reduction peaks. The first one, appears to be on -0.3244 V vs. Ag/AgCl. Second one, appears to be on -0.97995 V vs. Ag/AgCl. Third one, appears to be on -1.5592 vs. Ag/AgCl. Figure 23 cyclic solutions of CV experiments.
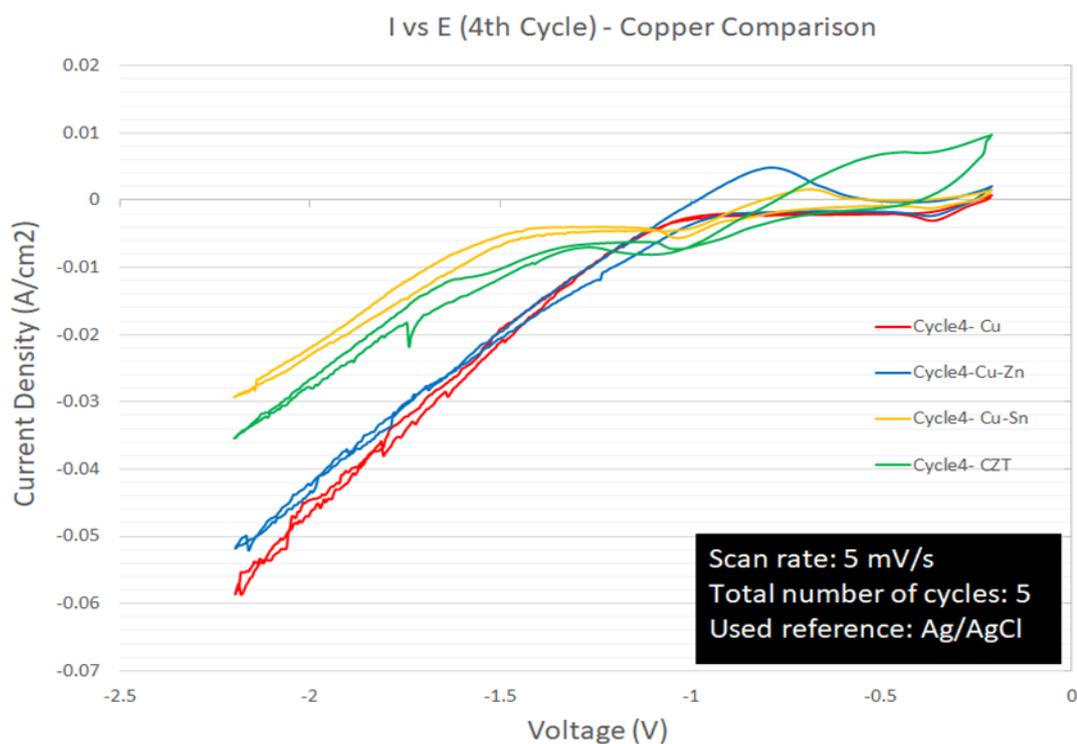
Figure 23: CV cycles solutions for Cu behaviour study

As a result, analysing all the four CV cycles data for the purpose of copper electrodeposition, it can be concluded that the potential voltage for copper shift a bit toward more negative side in each cycle but in the general copper start reduction process around -0.35 V vs. Ag/AgCl in the same conditions and concertation over

carbon substrate. Nevertheless, when it comes to CZT behaviour, there is a noticeable shift than other solutions where copper expected almost the same behaviour in all.

2.3.2 Tin Electrodeposition CV Analysis Experiment

Cyclic voltammetry graphs were generated for tin over the carbon substrate. Five cycles in total were done with 5 mV/s scan rate using Ag/AgCl as a reference electrode. Also, the area of the working electrode was 0.2 cm^2. During this experiment, no visible bubbling was found. This experiment runs in a stagnant solution with no rotating in a room temperature, which should indicate that the general Tin behaviour in the different solutions. Thus, Sn CV analysis showed two major reduction peaks as i) appears to be on -0.359 V vs. Ag/AgCl, and ii) appears to be on -1.029 V vs. Ag/AgCl. In the CV cycle of copper-tin, there were two major reduction peaks i) appears to be on -0.359 V vs. Ag/AgCl, and ii) appears to be on -1.029 V vs. Ag/AgCl. When it comes to the Zinc-Tin cycle, there is one peak showing on -1.0637807 V vs. Ag/AgCl. Moreover, CZT on CV cycle. Also, 3 major reduction peaks existed as i) appears to be on -0.3244 V vs. Ag/AgCl, ii) appears to be on -0.97995 V vs. Ag/AgCl, and iii) appears to be on -1.5592 V vs. Ag/AgCl, as shown in Figure 24.
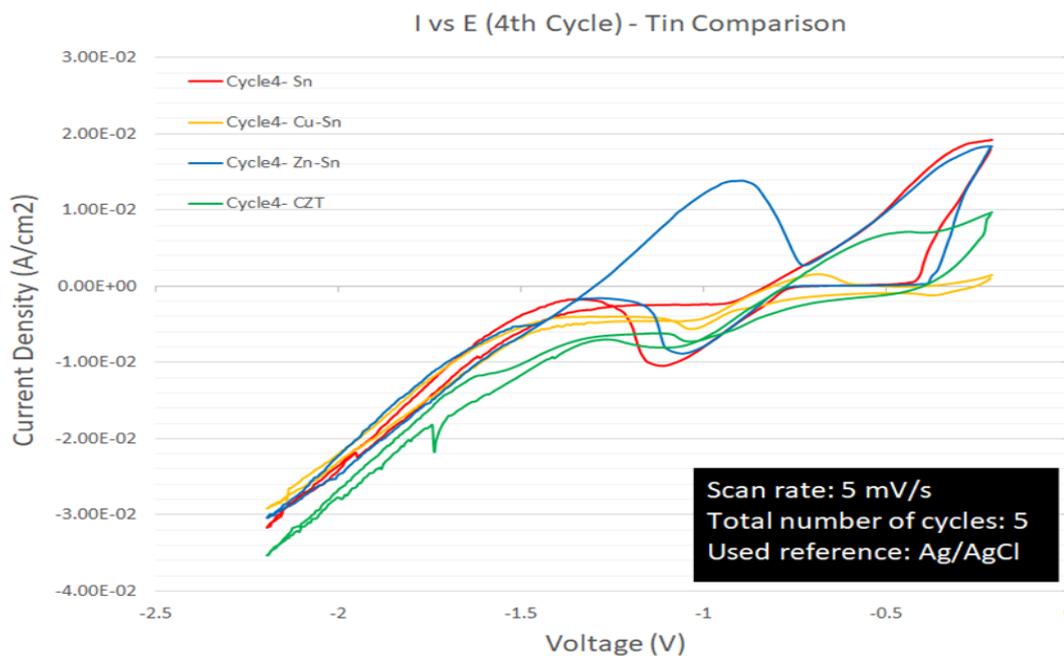
Figure 24: CV cycles solutions for Sn behavior study

As a result, analysing all the four CV cycles data for the purpose of tin electrodeposition, it can be concluded that the potential voltage for tin shift a bit toward more positive side in each cycle starting of tin solution alone and upward but in the general tin start reduction process around -1.1 V vs. Ag/AgCl in the same conditions and concertation over carbon substrate. Nevertheless, when it comes to CZT behaviour, there is a noticeable shift which different than all other solutions. Also, tin CV graphs exhibit similar behaviour to zinc-tin solution.

2.3.3 Zinc Electrodeposition CV Analysis

In this CV experiment, cyclic voltammetry graphs were generated for zinc over the carbon substrate. Five cycles in total were done with 5 mV/s scan rate using Ag/AgCl as a reference electrode. Also, the area of the working electrode was 0.2 cm^2. During this experiment, no visible bubbling was found. This experiment run in a stagnant solution with no rotating in a room temperature. This should indicate the zinc element general behaviour in the different solutions.

In the CV cycle of zinc solution, there were one weak reduction peak appears to be on -0.369 V vs. Ag/AgCl. Furthermore, in the CV cycle for copper-zinc there were one major reduction peak appears to be on -0.369 V vs. Ag/AgCl. Where when it comes to the CV cycle of Zinc-Tin, there is one peak showing on -1.0637807 V vs. Ag/AgCl. Moreover, CZT on CV cycle, there were 3 major reduction peaks. The first one, appears to be on -0.3244 V vs. Ag/AgCl. Second one, appears to be on -0.97995 V vs. Ag/AgCl. Third one, appears to be on -1.5592 vs. Ag/AgCl, as shown in Figure 25.
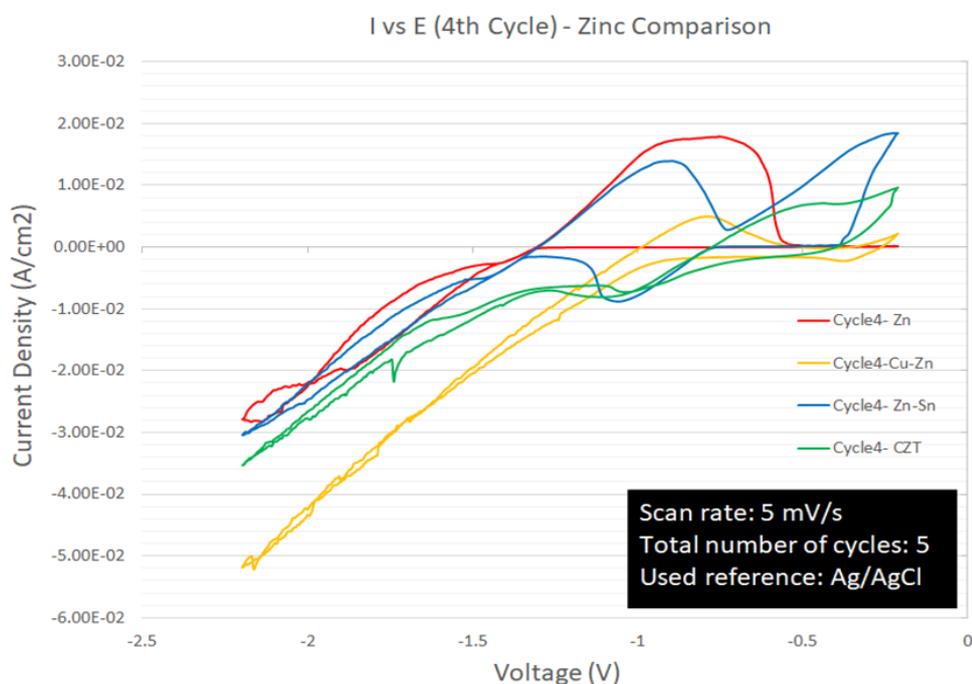
Figure 25: CV cycles solutions for Zn behavior study

As a result, analysing all the four CV cycles data for the purpose of zinc electrodeposition, it can be concluded that the potential voltage for zinc was all over showing that other elements suppress its electrodeposition. Nevertheless, from CZT solution, it can be confirmed that zinc starts its reduction process with higher

voltages than all other elements around -1.5 V vs. Ag/AgCl in this case with the same conditions and concertation over carbon substrate

2.3.4 CZT Electrodeposition CV Analysis

Comparing all 5 cycles together, it can be concluded that the reduction potential voltage for CZT after the 1 cycle begins to act the same in most other cycles except the 5th cycle where the 1st peak was not clear, and it could be due to some disturbance or error. In the fifth cycle of CZT, there were one major clear reduction peak. Ep1, appears to be on -0.9852 V vs. Ag/AgCl. Generally, analysing all cycles there were 3 major reduction peaks around -0.33 V, -0.99 V, and -1.53 V vs. Ag/AgCl, as shown in Figure 26.
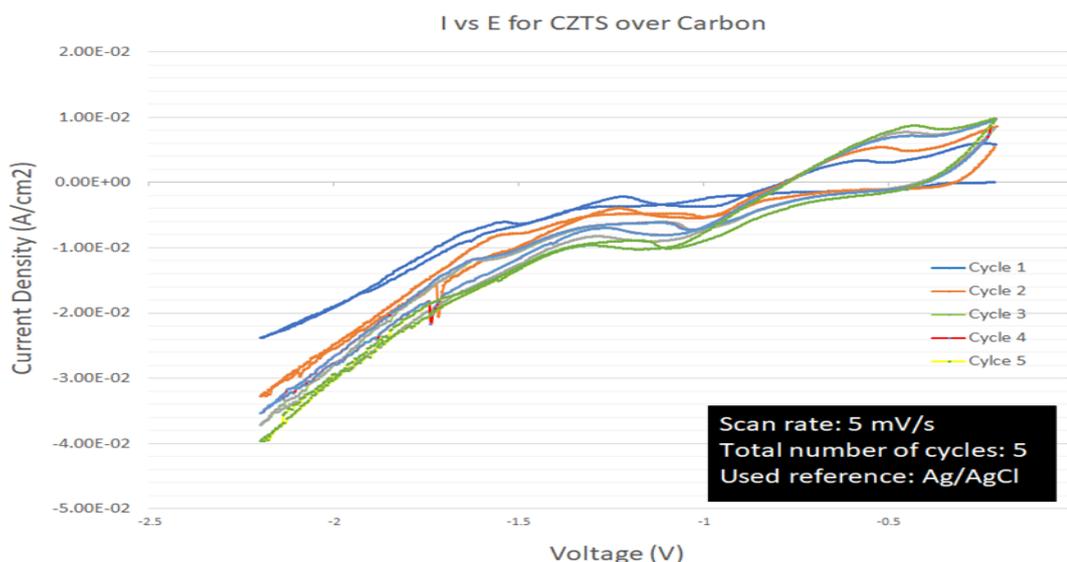
Figure 26: CV cycles for CZT over carbon substrate

After analysing the CV graphs, it was found that around -0.4 V vs. Ag/AgCl copper should be electrodeposited, -1.12 V vs. Ag/AgCl tin should be electrodeposited, and -1.56 V vs. Ag/AgCl zinc should be electrodeposited. All work done without any agitation even though it could enhance the electrodeposited process. It was decided

to do such, to make the electrodepositing as much cost effective as possible and to understand the system behaviour without any added complexity. Furthermore, for the same reasons it was decided to go with the room temperature conditions. Initially, few samples generated with varying the time randomly 10, 13, 15, 20 and 25 minutes to determine the optimum time of plating to study. Then, it was determined to electroplate all the samples in 25 minutes due the clear visible change and excellent mass of the samples. Also, it would make it easier to study the overall behaviour of the system.

Chapter 3: Results and Discussion

This Chapter discusses the research results that generated from a series of laboratory experiments, along with presenting result interpretation and discussion.

3.1 Series-A Samples: Cu Electrodeposition by Different Electrolytes

In the below solutions, it was expected to find copper in all plated because the constant voltage which has been specified, -0.4 V vs. Ag/AgCl, was for Cu region. Also, the time of electrodeposition for all samples was 25 minutes.

3.1.1 Sample- A1: EDS and SEM Analysis

Sample A1 consists of 0.03 M Cu(II) Sulphate ($CuSO_4$) with 0.125 M Sodium Citrate ($C_6H_5O_7Na_3$); its pH= 3 and plated mass was 0.8 mg.

It was found from the EDS analysis that around 96.40% of the mass of this sample was copper and about 3.6% was oxygen whereas 87.08% Cu atoms and 12.92% oxygen, as shown in Figure 27.
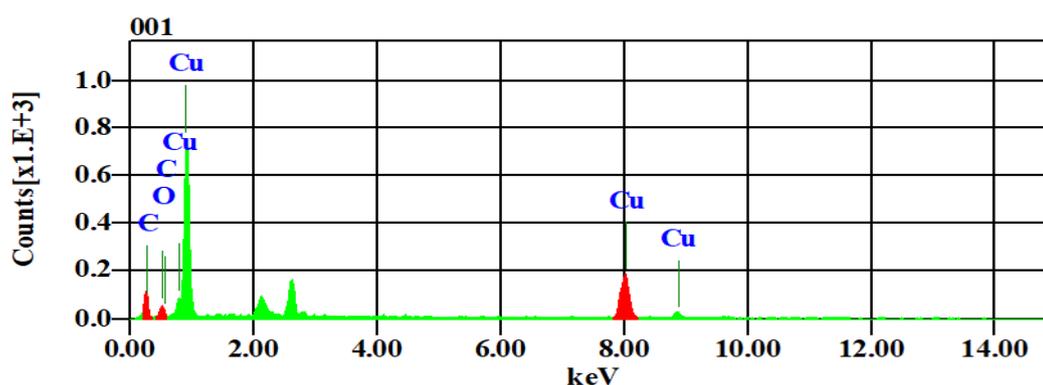
Figure 27: EDS of sample A1

In the SEM images, copper particles are plated in a fine spherical shape over the carbon with some small micro level gaps in between the particles. However, the surface looks uniform in the macro level where brown colour copper is visible over the substrate. Figure 27 revealed the synthesized copper particles are spherical, and their size is less than 3 µm.
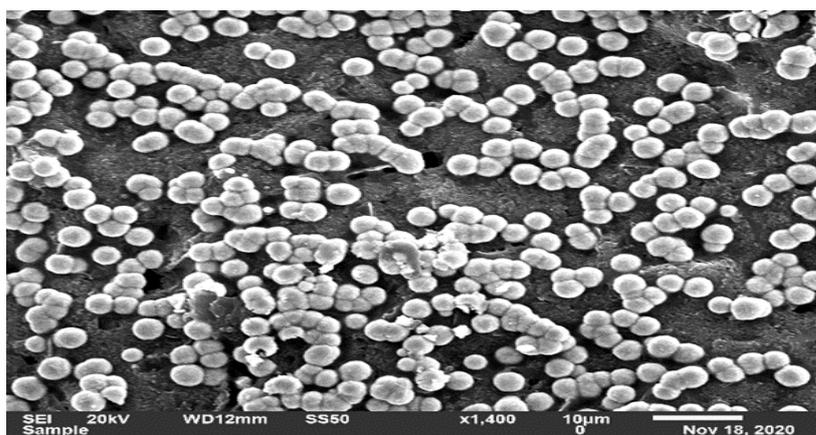
Figure 28: SEM image of sample A1

3.1.2 Sample- A2: EDS and SEM Analysis

Sample A2 consists of 0.03 M $CuSO_4$, 0.03 M Zinc Sulphate ($ZnSO_4$), and 0.125 M $C_6H_5O_7Na_3$; its pH= 3 and the plated mass was 0.2 mg.

It was found from the EDS analysis that 94.58% of the A2 mass was copper, while 5.42% was oxygen, i.e., 13.29% copper atoms and 6.48% oxygen. Also, EDS analysis also found small trace of Zn, which is negligible, as shown in Figure 29.
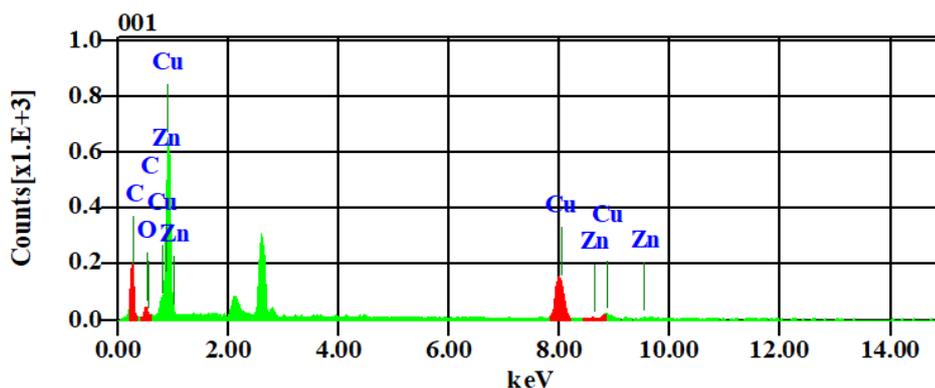
Figure 29: EDS of sample A2

From SEM images, particles are plated in the form of spheres with some grouping over the carbon with some small micro level gaps in between the particles. Furthermore, individual copper particles clump together and with the small traces of Zn in the SEM picture. Particles show agglomerated in Figure 29 with several individual crystals visible. Nevertheless, the surface looks uniform at the macro level where copper brown colour is visible over the carbon substrate, as shown in Figure 30.
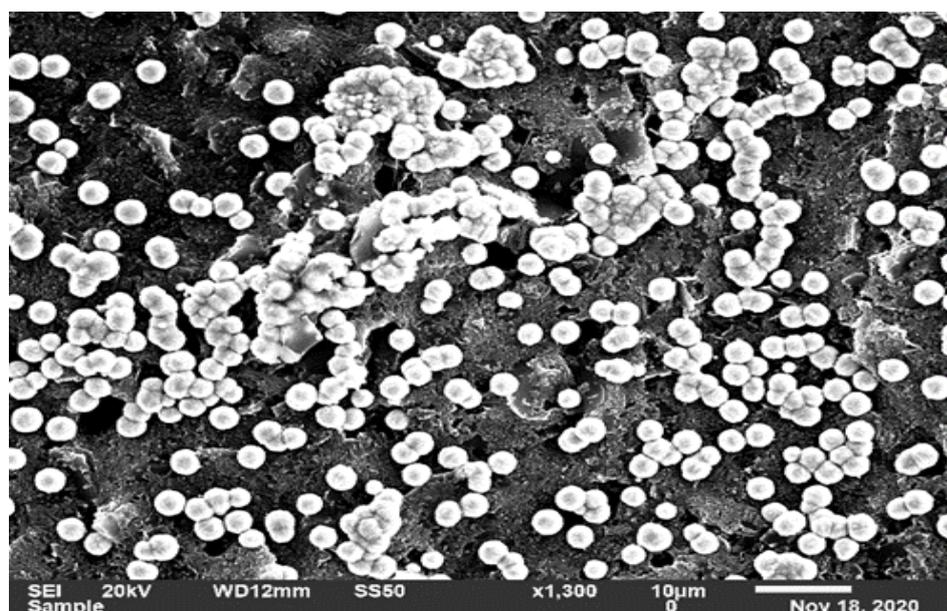
Figure 30: SEM image of sample A2

3.1.3 Sample- A3: EDS and SEM Analysis

Sample A3 consists of 0.03 M $CuSO_4$, 0.03 M Tin (II) sulphate ($SnSO_4$), and 0.125 M $C_6H_5O_7Na_3$; its pH= 3 and the plated mass was 0.2 mg.

It was found from the EDS analysis that around 91.04% of the mass of this sample was copper and about 8.93% was oxygen whereas 71.96% copper atoms and 28.03% oxygen. Also, the EDS graph shows small trace of tin to be negligible, as shown in Figure 31.
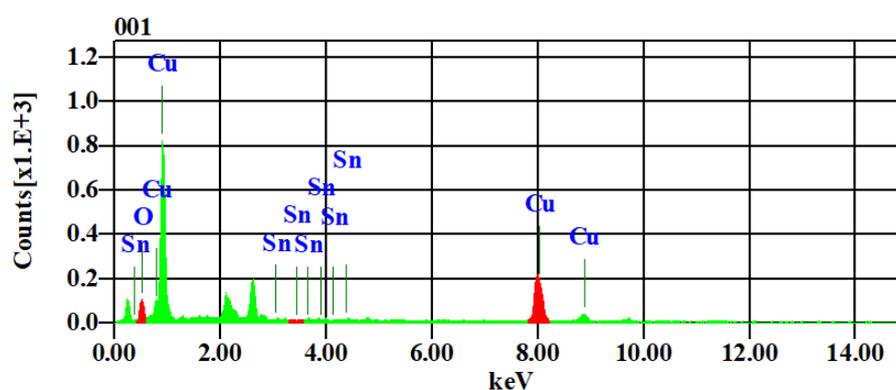
Figure 31: EDS of sample A3

The SEM picture, along with small traces of Tin, shows that the particles are agglomerated, with multiple individual particles and a very few particles of zinc are found. It looks that Cu particles where plated in spiral shape over carbon with some small micro level gaps in between the particles. Also, it was found that there were fine clusters of copper particles in some areas. Furthermore, Individual copper particles agglomerated together. Yet, the surface looks uniform in the macro level where copper brown colour was visible over the carbon substrate, as shown in Figure 32.
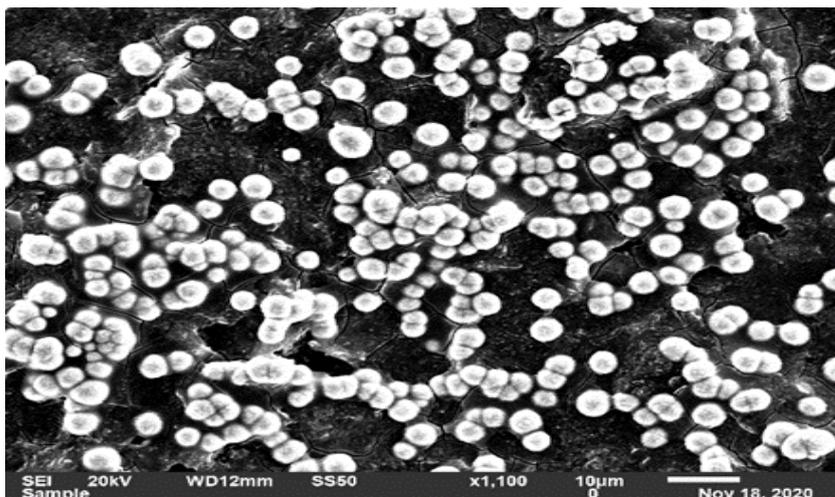
Figure 32: SEM image of sample A3

3.1.4 Sample- A4: EDS and SEM Analysis

Sample A4 consists of 0.03 M $CuSO_4$, 0.03 M $ZnSO_4$, 0.03 M $SnSO_4$, and 0.125 M $C_6H_5O_7Na_3$; its pH= 3 and the plated mass was 0.3 mg.

It was found from the EDS analysis that around 91.76% of the sample mass was Cu, 8.24% oxygen, and 73.70% Cu and 26.30% oxygen. Also, the EDS analysis also demonstrated no trace of tin or zinc in the plated sample.

The SEM image displays the agglomeration of individual copper particles are spherical, and their size is 0.5 to 3 µm. It looks that Cu particles were plated in spiral shape over carbon with some small micro level gaps in between the particles. Besides that, it was found that there were some clusters and grouping of Cu particles in the same areas. A closer look at the agglomerated lump reveals the presence of a variety of nanoparticle aggregates. Particles tend to be agglomerated and certain individual crystals are visible. Thus, the surface looks uniform in the macro level where copper brown colour was visible over the carbon substrate with some cracks, as shown in Figure 33.
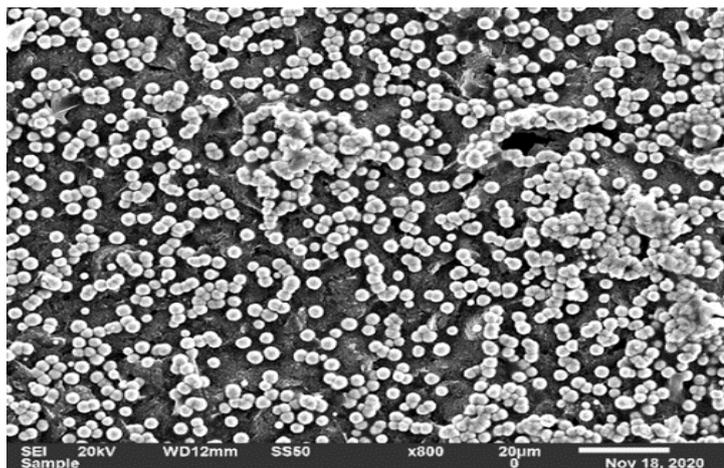
Figure 33: SEM image of sample A4

It was expected to find copper in all samples because of the constant voltage which has been used, -0.4 V vs. Ag/AgCl, pH 3. As stated in the table, sample A1 has the most mass weight with 0.8 mg and 96.4% of the sample was copper. Also, it shows other samples with a small trace of the other elements but was not significant to be reported. Furthermore, even when the solutions had other elements in them such as sample A4, 91% of the sample was copper. Yet, the overall weight of such sample was only 0.3 mg. Table 5 shows availability of Cu in the four solutions.

Table 5: Cu electrodeposition using different electrolyte composition and mass

Samples	Cu		Zn		Sn	
	Weight %	Atomic %	Weight %	Atomic %	Weight %	Atomic %
A1; plated mass (0.8 mg)	96.40	87.08	-	-		
A2; plated mass (0.2 mg)	94.58	13.29	Small trace	Small trace	-	-
A3; plated mass (0.2 mg)	91.04	71.96	-	-	Small trace	Small trace
A4; plated mass (0.3 mg)	91.76	73.70	No traces	No traces	No traces	No traces

From the SEM images, it can be concluded that the best solution to electrodeposit copper is the one where it has only copper in it due to the great outcome mass measured. Nevertheless, sample A2 and A3 which had small trace amounts of zinc and tin exhibit some sort of nucleation of big ball shape over the spherical copper shape particles. Finally, sample A4 had a good quantity of copper particles aligned but less mass than sample A1. This might be due to some of the charge get distributed to other elements in the solution without having them electrodeposited due to the low voltage than their threshold needed one for electrodeposition, as shown in Figure 34.
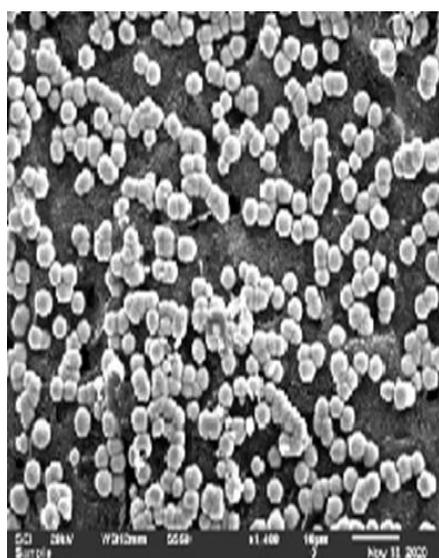
Cu solution electrodeposited product

(Sample A1)
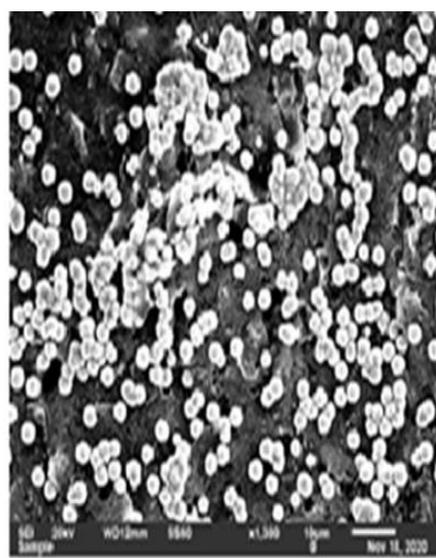
Cu-Zn solution electrodeposited product

(Sample A2)
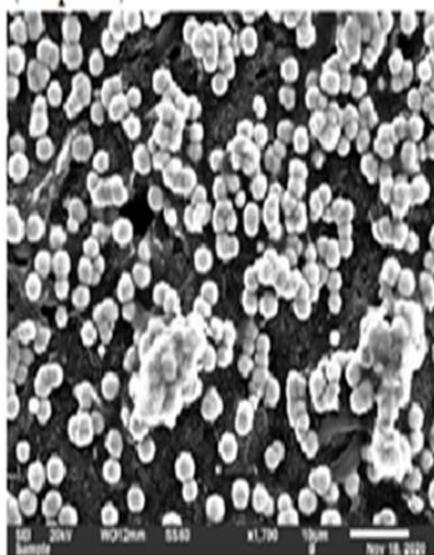
Cu-Sn solution electrodeposited product

(Sample A3)
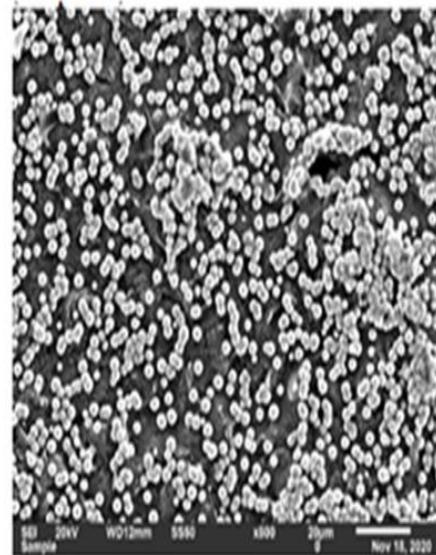
Cu-Zn-Sn solution electrodeposited product

(Sample A4)

Figure 34: Cu electrodeposition using different electrolyte SEM images

3.1.5 XRD Graphs of Series-A

The constant voltage of -0.4 V vs. Ag/AgCl is specific to the electrodeposition of Cu metal and XRD graphs are demonstrating the comparable results to the EDS device, as illustrated in Figure 35.
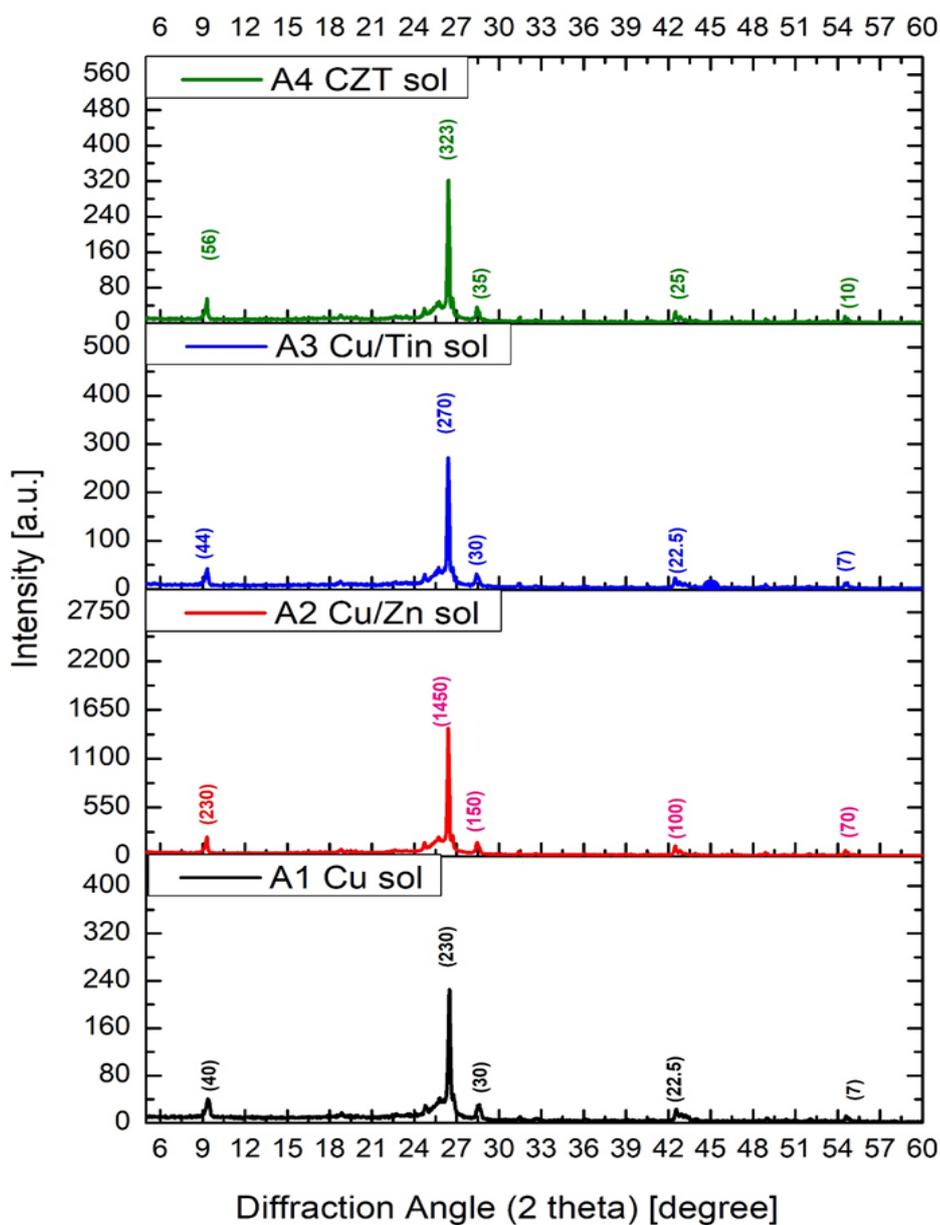
Figure 35: XRD results of the sample A set

In case of control sample A1, the perfect electrodeposition of Cu was done as the potential region is specific for the stated metal. The characteristic peaks of Cu are obtained at 2 theta values of 9, 26.5, 28.5, 43 and 55.

Considering A2, when along with Cu, Zn metal was also used in the solution to form an alloy but only Cu peaks are demonstrated in the XRD graph. The graph has shown no peak shifting towards either side and the characteristic peaks of Cu are obtained at 2 theta values of 9, 26.5, 28.5, 43 and 55. There are no additional peaks observed for Zn metal.

Considering A3, when along with Cu, Sn metal was also used in the solution to form an alloy but only Cu peaks are demonstrated in the XRD graph in Figure 35. The graph has shown no peak shifting towards either side and the characteristic peaks of Cu are obtained at 2 theta values of 9, 26.5, 28.5, 43 and 55. There are no additional peaks observed for Sn metal.

Considering A4, when along with Cu, Zn and Sn metals were also used in the solution to form an alloy but only Cu peaks are demonstrated in the XRD graph. The graph has shown no peak shifting towards either side and the characteristic peaks of Cu are obtained at 2 theta values of 9, 26.5, 28.5, 43 and 55. There are no additional peaks observed for Zn and Sn metal.

Hence, all the four samples fabricated in the plating potential of -0.4 V vs. Ag/AgCl exhibited that even with different metals' presence, the plating is only done for Cu metal at the stated potential. The metals of Zn and Sn do not disrupt the plating of Cu metal at the stated potential. All the results are confirmed by SEM, EDS and XRD. SEM demonstrated the spherical morphology retention. EDS exhibited the maximum

atomic percentage for Cu metal. XRD demonstrated some peak shifting and similar spectra for all the four samples. Only change of peak height is observed in XRD which only signifies the change in plated metal crystallinity, Table 6 summarize the results.

Table 6: Results of XRD analysis for sample A set

Peak	$1000*Sin^2\phi$	Reflection	Remarks
9.1°	6	0+0+0	000
24.9°	46	1^2+0+0	$1^2+0+0=1$
28.1°	58	1^2+0+0	$1^2+0+0=1$
43.26°	138	$1^2+1^2+1^2$	$1^2+1^2+1^2=3$

Table 6 also shows four characteristic peaks at 9.1°, 24.9°, 28.1° and 43.2° corresponding to the crystallographic directions of 000, 100, 100 and 111, respectively. These peaks were shifted towards lower angles in comparison with the position of the characteristic peaks of pure copper (suggesting that a certain amount of Zinc atoms had entered the copper crystal lattice and therefore had warped the unit cell, causing the observed shift of the diffraction peaks. These peaks were shifted more while Sn atoms had entered the copper lattices in comparison with copper and zinc and wrapped the unit cell more. The XRD Cu-Zn-Sn alloy shows that there is small traces of Tin and zin atoms are in the copper because major peak is near to the copper peak, but it is its angle of diffraction is little bit shifted.

3.2 Series-B Samples: Sn Electrodeposition using Different Electrolyte

In the below solutions, it was expected to find Sn and small traces of Cu in all electrodeposited carbon substrates, because the constant voltage which has been

specified, -1.12 V vs. Ag/AgCl, was for Sn region. Also, the time of electrodeposition for all samples was 25 minutes.

3.2.1 Sample-B1: EDS and SEM Analysis

Sample B-1 consists of 0.03 M $SnSO_4$, and 0.125 M $C_6H_5O_7Na_3$; its pH=3 and the plated mass was 0.4 mg.

It was found from the EDS analysis in Figure 37 that around 66.23% of the mass of this sample was tin and about 33.77% was oxygen whereas 20.91% tin atoms and 79.09% oxygen, as shown in Figure 36.
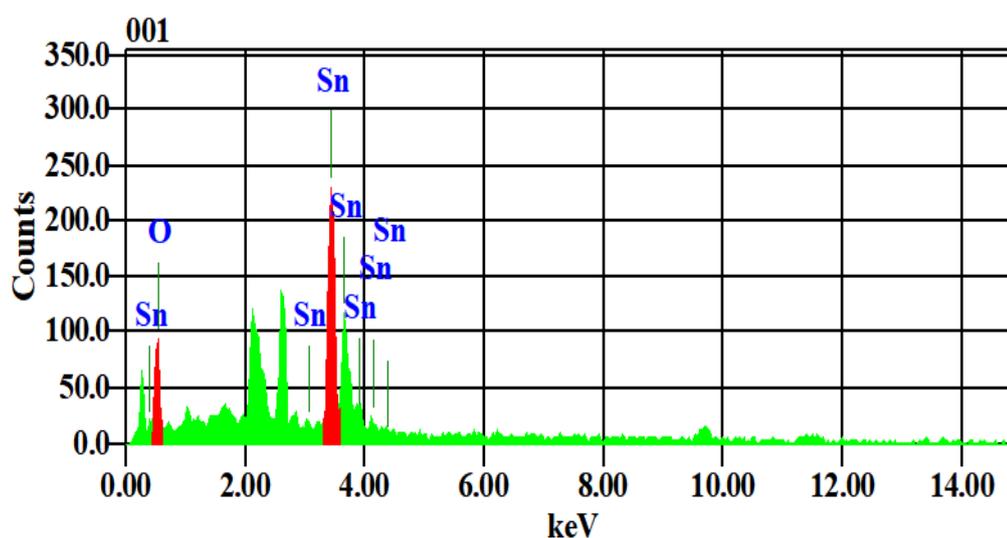
Figure 36: EDS results of sample B1

Looking at the SEM image, the scratches, and porous structure on the surface of Sn substrates formed during the electrodeposition process were not observed due to the forming of metal oxide film. It looks that Sn particles where electrodeposited in good film over carbon with some small micro level cracks in between. Also, the outside surface looks uniform in the macro level where tin silver colour was visible over the carbon substrate A sufficiently consistent plain field and a cracked-mud foundation

have been achieved. The forming of cracks can take place during the evaporation and cooling phase of the electrodes, as shown in Figure 37.
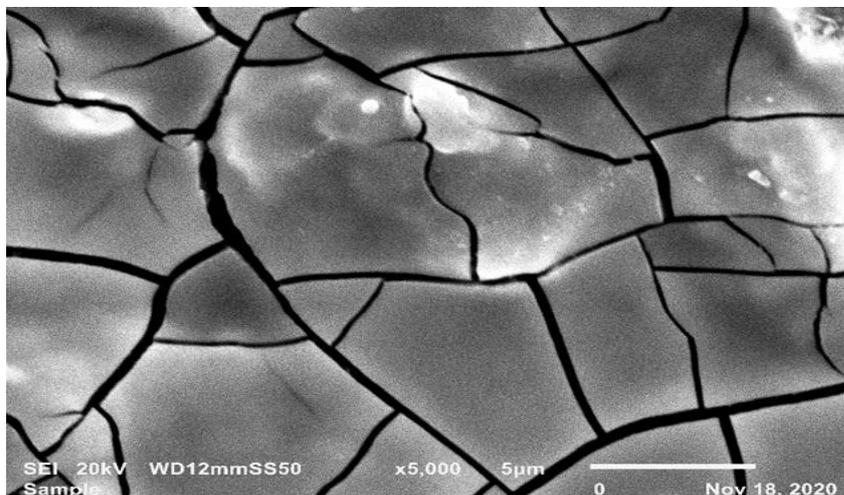
Figure 37: SEM image of sample B1

3.2.2 Sample-B2: EDS and SEM Analysis

Sample B2 consists of 0.03 M $CuSO_4$, 0.03 M $SnSO_4$, and 0.125 M $C_6H_5O_7Na_3$; its pH= 3 and the plated mass was 0.6 mg.

It was found from the EDS analysis that around 46.26% of the sample mass was Sn, 6.65% oxygen and 47.09% Cu. While the atomic percentages are 47.92% Cu, 26.89% oxygen, and 46.26% Sn. Also, the EDS analysis found no trace of tin or zinc in the plated sample, as shown in Figure 38.
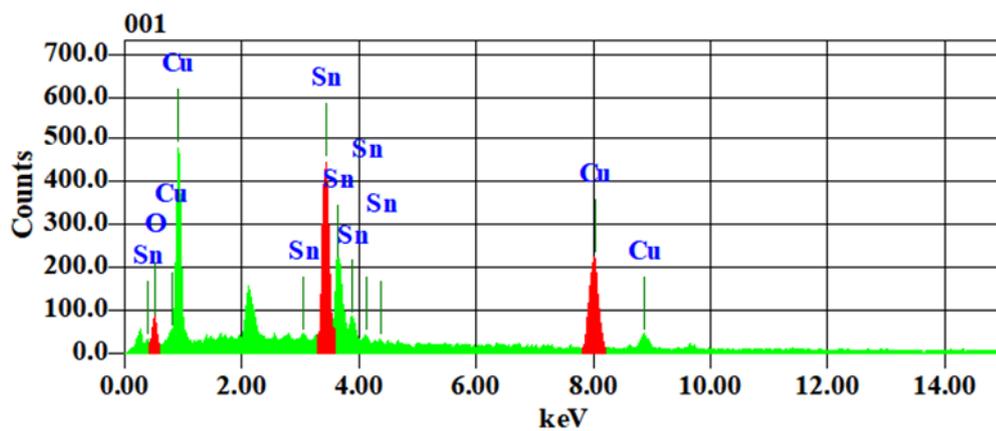
Figure 38: EDS results of sample B2

The film of the SEM image of a (Sn-Cu) alloy shows a porous structure and a vast surface that contributes to the sensitivity. It looks that copper particles are plated in flowery shape over carbon substrate with some small micro level gaps and cracks in between the particles. Yet, the surface looks uniform in the macro level where copper/tin dark silver brownish colour was visible over the carbon substrate with some cracks in the edges, as shown in Figure 39.
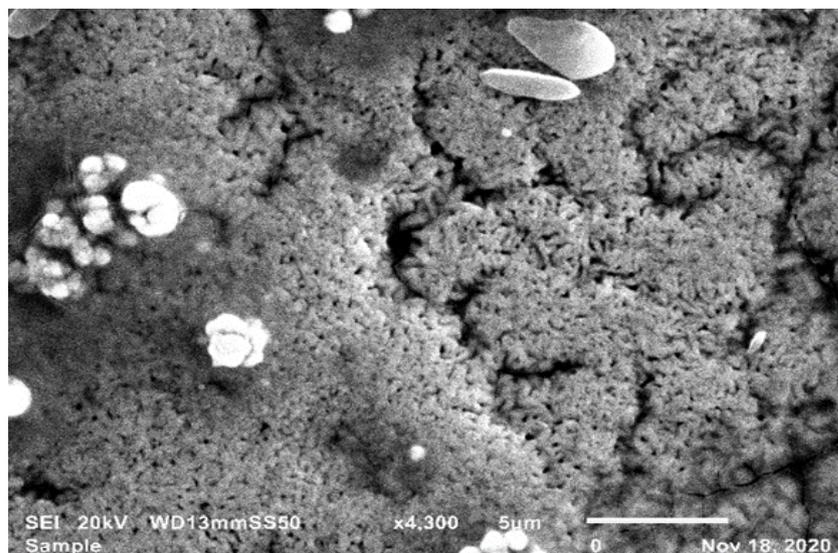
Figure 39: SEM image of sample B2

3.2.3 Sample- B3: EDS and SEM Analysis

Sample B3 consists of 0.03 M $ZnSO_4$, 0.03 M $SnSO_4$, and 0.125 M $C_6H_5O_7Na_3$; its pH= 3 and there was no plating.

The EDS analysis shows that Au electrodeposited over the substrate, which means that there is no plating has been done and the gold is from the sputtering process, which is the part of SEM only, as shown in Figure 40.
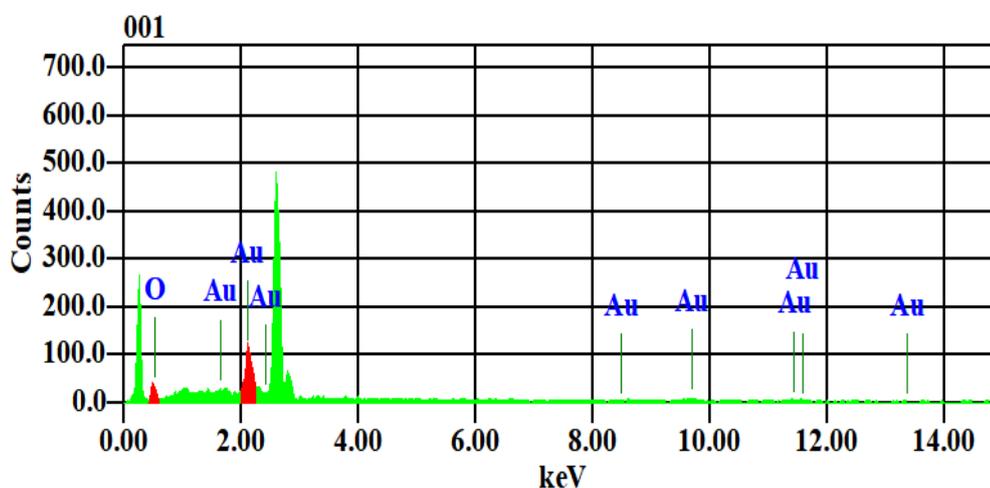
Figure 40: EDS results of sample B3

The SEM image shows that the surface morphology is of gold plated, because Zn suppresses the Sn electrodeposition in the solution. Hence, the presence of Zn in the solution seems to repress the electrodeposition of Sn. This confirms some of the odd behaviour exhibited while running the CV for such solution, as shown in Figure 41.
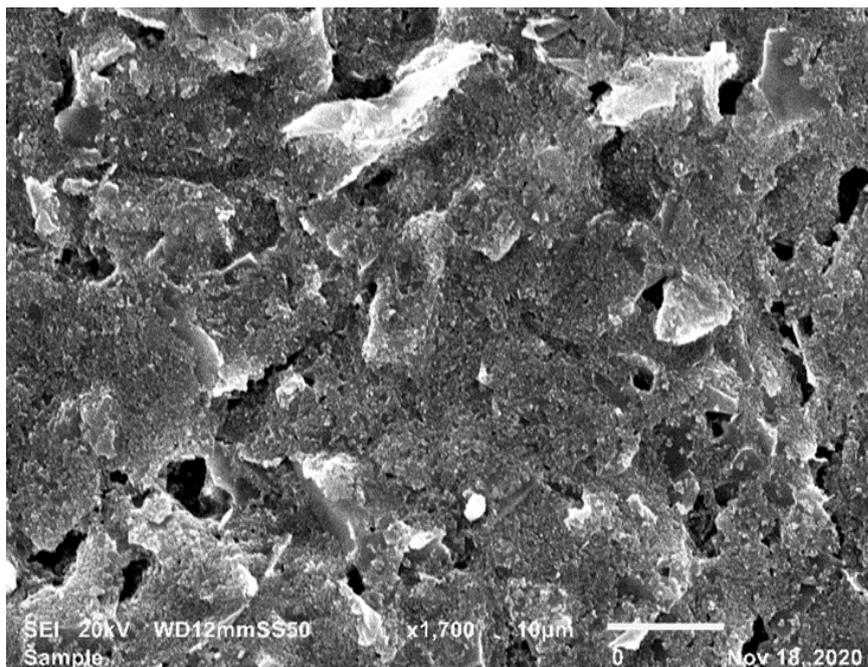
Figure 41: SEM image of sample B3

3.2.4 Sample-B4: EDS and SEM Analysis

Sample B4 consists of 0.03 M $CuSO_4$, 0.03 M $ZnSO_4$, 0.03 M $SnSO_4$, and 0.125 M $C_6H_5O_7Na_3$; its pH= 3 and the plated mass was 1.5 mg.

It was found from the EDS analysis that 52.80% of the mass of sample B4 was Sn, 3.37% was oxygen, and 36.37% Cu. While the atomic percentage was 44.5% Cu, 18.12% oxygen, and 34.58% Sn. Also, EDS analysis found small Zn traces in the plated sample, which is, as shown in Figure 42.
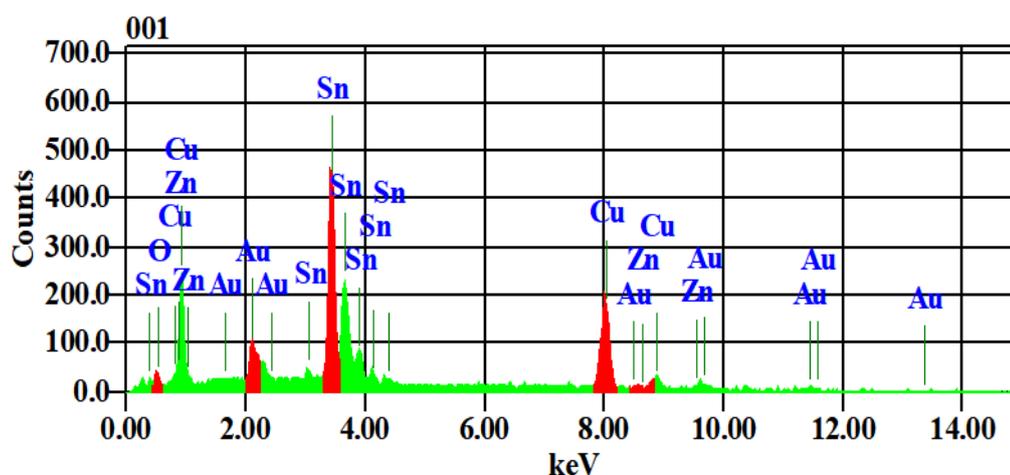
Figure 42: EDS results of sample B4

Regarding SEM analysis, the image of the SEM surface concerning Cu-Zn-Sn alloy gaining an electro-depository mass of 1μm. It looks that both Cu and Sn particles are electrodeposited in flowery shapes over carbon substrate. Also, the surface looks very uniform in the macro level where Cu-Sn link was taking dark silver brownish colour and visible over the carbon. Grains with size of 0.5-1 μm are apparent in pillar-shaped form. Figure 43 and Figure 44 displaying the alloy surface look.
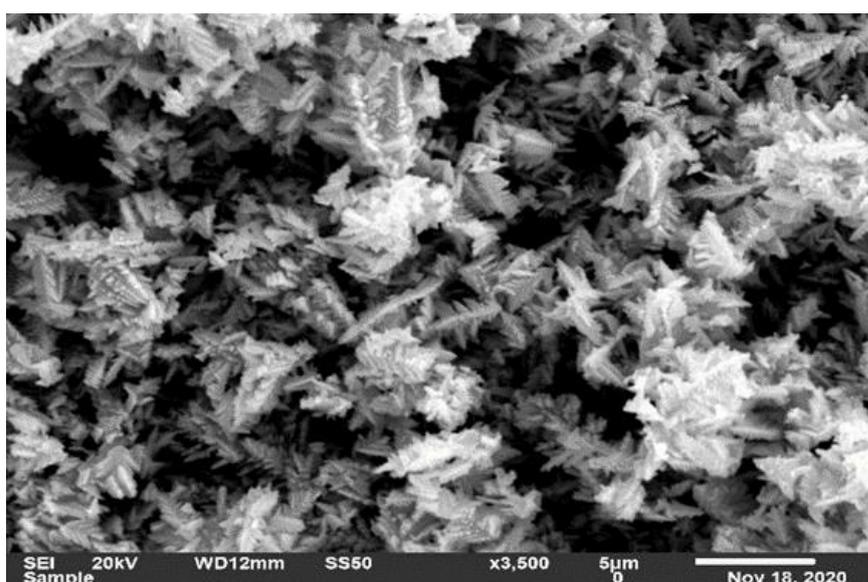
Figure 43: I- SEM image of sample B4
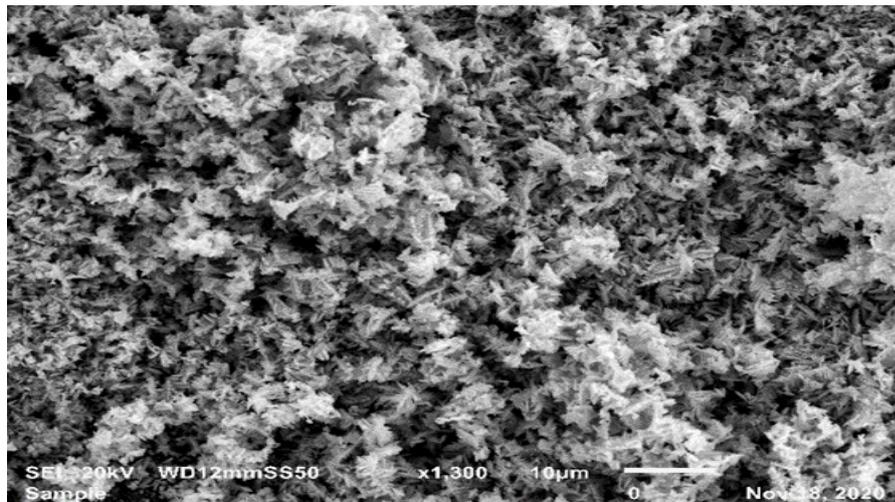
Figure 44: II-SEM image of sample B4

Figure 45 summarises a comparison between Sn electrodepositions using different electrolyte SEM images. Therefore, it can be concluded that the best solution to electrodeposit Sn is the one where it has only tin in it due to the great smooth surface with some cracks. In contrast, when it comes to the mass of tin, adding copper and zinc to the solution resulted in more tin mass electrodeposited such as sample B4. Nevertheless, sample B2 generated acceptable results where tin electrodeposited as well but with a flowery shape with cracks where copper particles roaming around. Finally, sample B4 shows a great mix between the elements but with many gaps in the electrodeposited surface.
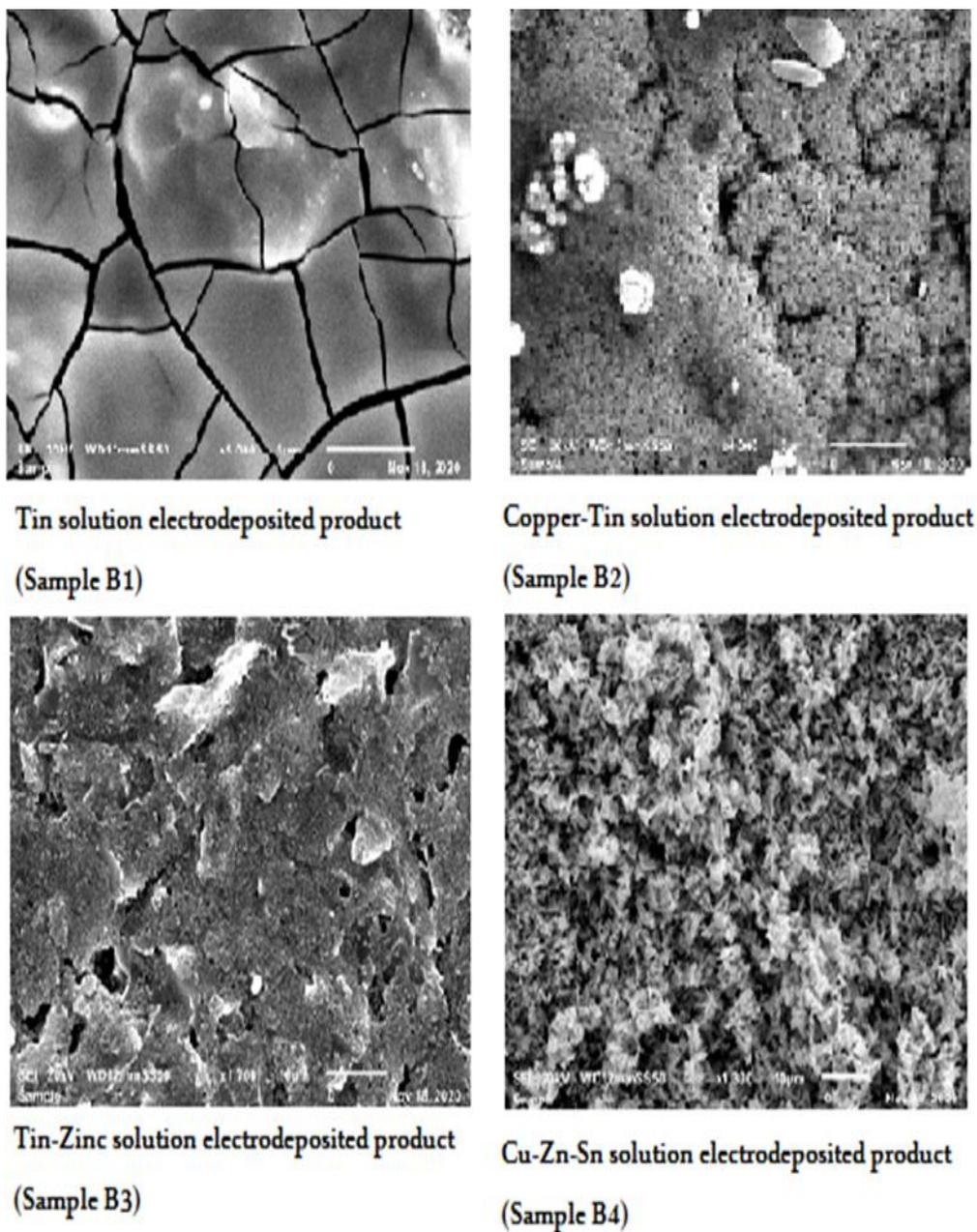
Figure 45: Comparison between Sn electrodepositions using different electrolyte SEM images

It was expected to find Sn and Cu in all electrodeposited carbon substrates because the constant voltage which has been specified, -1.12 V vs. Ag/AgCl, was for Sn region at pH= 3, as shown in Table 7.

Table 7: Sn electrodeposition using different electrolyte composition and mass

Sample Sn	Cu		Zn		Sn	
	Weight %	Atomic %	Weight %	Atomic %	Weight %	Atomic %
B1- plated mass (0.4 mg)	-	-	-	-	66.23	20.91
B2- plated mass (0.6 mg)	47.09	47.92	-	-	46.26	46.26
B3- no plating	-	-	Au	Au	Au	Au
B4- plated mass (1.5 mg)	36.37	44.5	Small traces	Small traces	52.80	34.58

3.2.5 XRD Graphs of Series-B

In case of control sample B1, the perfect electrodeposition of Sn was done as the potential region is specific for the stated metal. The characteristic peaks of Sn are obtained at 2 theta values of 9, 26.5, 28.5, 42.5 and 54.

Considering B2, when along with Sn, Cu metal was also used in the solution to form an alloy and the augmented peak intensities and peak shifts were observed in the XRD graph. There was no peak shift observed for Sn characteristics peak at 2 theta values of 26.5 and 54. While a new characteristic peak at 2 theta values of 19 was observed for Cu-Sn alloy plating. In addition to this, peak shifting was observed from 9 to 9.5. While the peak broadening was observed for the 2-theta value of 28.5 and 42.5. Hence, B2 sample has both Tin and Copper in its composition as shown in EDS spectrum and validated by XRD graph.

Considering B3, when along with Sn, Zn metal was also used in the solution to form an alloy, but XRD graph is showing only Sn peaks of exceptionally low intensity i.e., negligible amount of thin film is formed because Zn is repressing the plating of Sn.

Considering B4, when along with Sn, Cu and Zn metals were also used in the solution to form an alloy but only Cu and Sn peaks are demonstrated in the XRD graph. There was no peak shift observed for Sn characteristics peak at 2 theta values of 26.5 and 54. While a new characteristic peak at 2-theta value of 19 was observed for Cu-Sn alloy. In addition to this, peak shifting was observed from 9 to 9.5. While the peak broadening was observed for the 2 theta values of 28.5 and 42.5.

Hence, B4 sample has both Sn and Cu in its composition as shown in EDS spectrum and validated by XRD graph. There are no additional peaks observed for Zn metal. it was found a trace of copper and tin in B1, B2 and B4 samples which is validated by the SEM results. When it comes to comparing all samples (B1, B2, B3, and B4), it seems that B1 which has a tin solution only is the best when it comes to plate tin under constant -1.12 V. So, the constant voltage of -1.12 V vs. Ag/AgCl is specific to the electrodeposition of Sn and XRD graphs are demonstrating the results comparable results to SEM and EDS analysis, as shown in Figure 46.
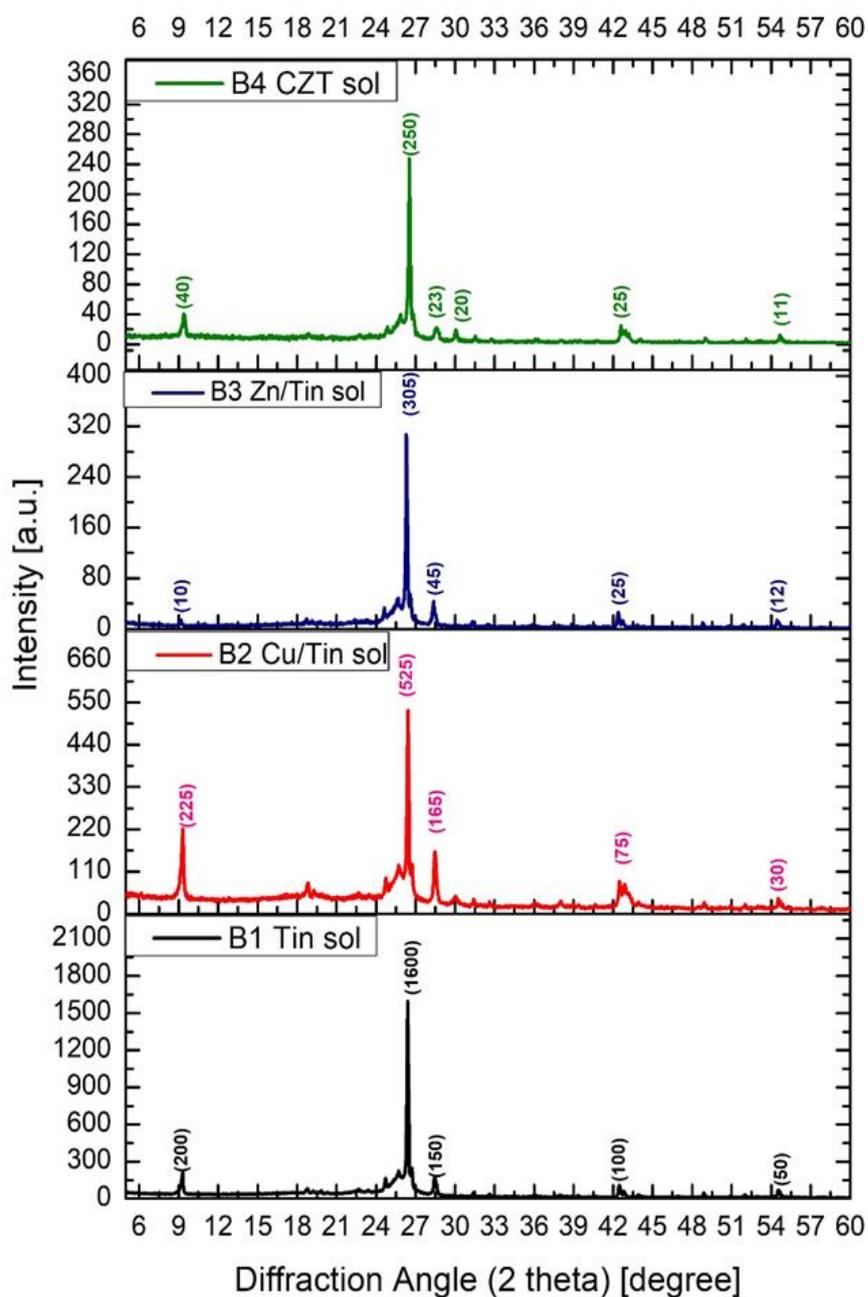
Figure 46: XRD graphs of sample B set

The thin film smooth surface looks better and could be because the energy is distributed to all the thin particles without any disruption from other particles like zinc which will not plate based on the voltage and CV experiments. However, B4 sample had unique structure and surface with majority of the plating was for tin and

good amount of copper. Also, sample B2, had almost half distribution of electrodeposited particles between tin and copper with good overall yield. When it comes to sample B3 which had some zinc and tin, no plating done that could be the result of zinc is repressing the plating of tin. All the results are confirmed by SEM, EDS and XRD. Table 8 shows a summary of the XRD results for sample B.

Table 8: XRD results for sample B set

Peak	$1000 \ast Sin^2\phi$	Reflection	Remarks
9.2°	25	0	0
26.6°	523	1^2+2+2	$1^2+0+0=1$
28.5°	227	1^2+2^2+0	$1^2+2^2+0 =5$
54.4°	661	$2^2+2^2+3^2$	$2^2+2^2+3^2 =17$

At 9.2°, 26.6°, 28.5° and 54.4° the crystallographic directions respectively of 000, 100, 120 and 223 were four distinctive peaks in B samples. In relation to the direction of the characteristic peaks of pure Tin, these peaks were moved towards lower angles, indicating that a certain number of copper atoms had reached the Tin crystal lattice and thereby distorted the unit cell, creating the observed shift of the diffraction peaks. In contrast with the copper and tin, the peaks were moved further when the zinc atoms wrapped the unit cell more in copper bars. The alloy XRD Cu-Tin-Zn reveals there are minor traces of copper of Tin and Zin, since the high point is above the copper peak, so its disturbances are moved.

3.3 Series-C Samples: Zn Electrodeposition using Different Electrolytes

In this experiment, it has been expected to find Zn with potential presence of Cu and Sn in the electrodeposited carbon substrates, because the constant specified voltage as -1.56 V vs. Ag/AgCl, was for Zn region. Also, the time of electrodeposition for all samples was 25 minutes.

3.3.1 Sample-C1: EDS and SEM Analysis

Sample C1 consists of 0.03 M $ZnSO_4$ and 0.125 M $C_6H_5O_7Na_3$; its pH= 3 and the plated mass was 0.7 mg.

It was found from the EDS analysis in Figure 48 that around 86.55% of the mass of this sample was zinc and about 13.45% was oxygen where 61.17 % Zn atoms and 38.83% oxygen, as shown in Figure 47.
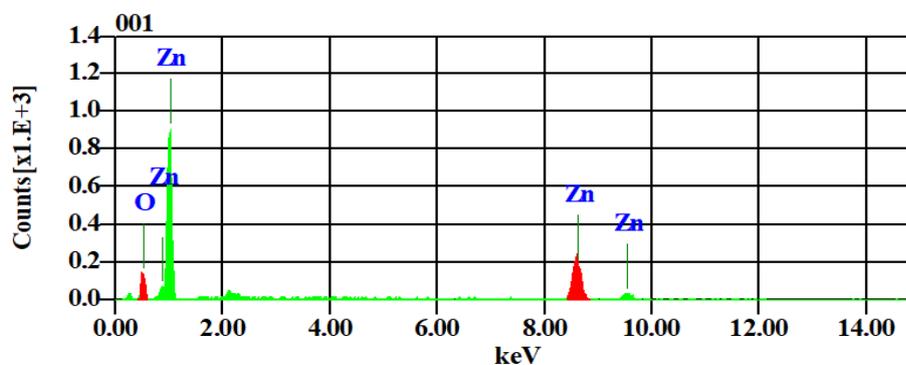
Figure 47: EDS results of sample C1

The SEM image reveals granular textures, and the distribution of the laminate structure is lesser homogeneous. The dimension of the particle is greater than that of the raw materials. It looks that Zn particles where plated in good big grains over carbon substrate with micro level cracks showing in between. Also, the outside

surface looks uniform in the macro level where zinc silver colour was visible over the carbon substrate with 0.7 mg mass, as shown in Figure 48.
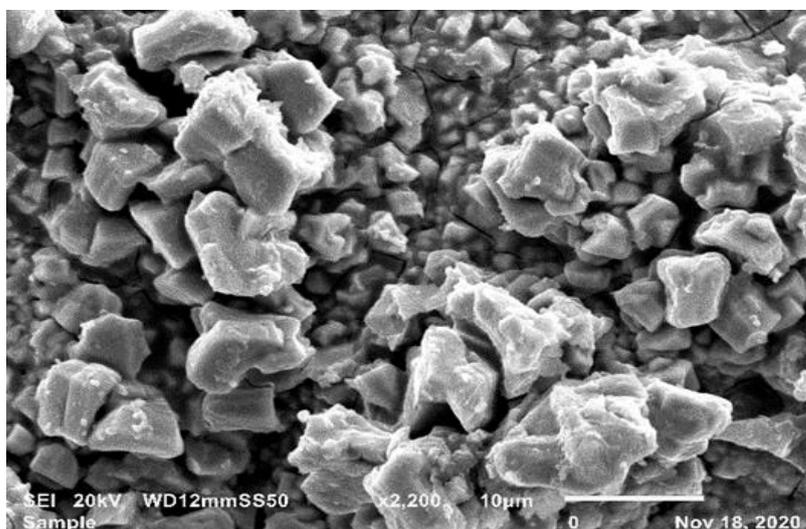
Figure 48: SEM image of sample C1

3.3.2 Sample-C2: EDS and SEM Analysis

Sample C2 consists of 0.03 M $CuSO_4$, 0.03 M $ZnSO_4$, and 0.125 M $C_6H_5O_7Na_3$; its pH= 3 and the plated mass was 0.7 mg.

The EDS analysis revealed that 15.78% of the sample mass was Zn, 4.6% oxygen, and 79.62% Cu. Also, the atomic percentages found to be 13.54% zinc, 16.14% oxygen, and 70.32% Cu, as shown in Figure 49.
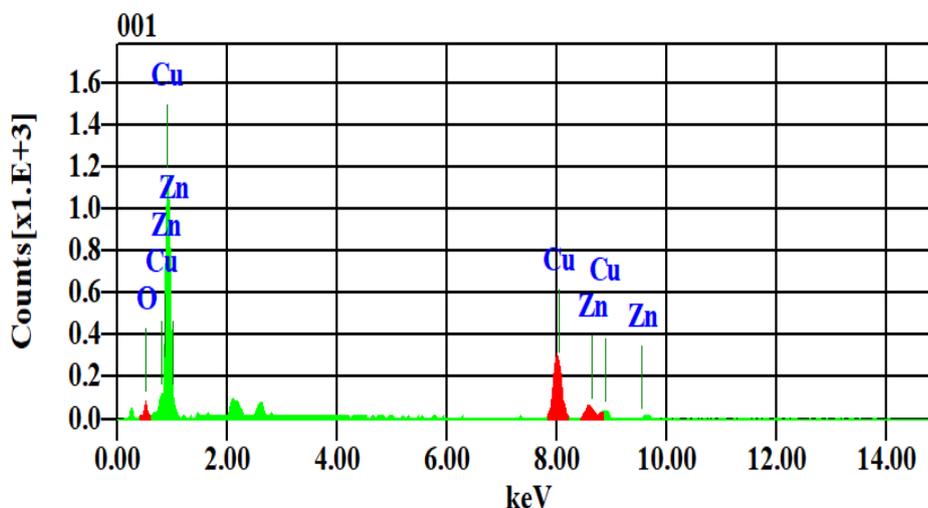
Figure 49: EDS results of sample C2

It looks that all electrodeposited particles were plated in spiral cauliflower shape covering good amount of the carbon substrate surface with limited micro-level spacing and cracks showing in between. Also, the outside surface looks very uniform in the macro level where dark silver colour was visible over the carbon substrate with 0.7 mg mass. Furthermore, SEM image shows a SEM representation of the synthesized Cu-Zn alloy used in this analysis. Individual copper particles clump together and with of Zinc in the SEM picture, as shown in Figure 50.

Figure 50: I-SEM images of sample C2

Particles show agglomerated in Figure 50 with several individual crystals visible. The zinc particle is agglomerated with copper due to the constant voltage, which was specified, -1.56 V, was for zinc region based on the CV experiments with Ag/AgCl reference, as shown in Figure 51.
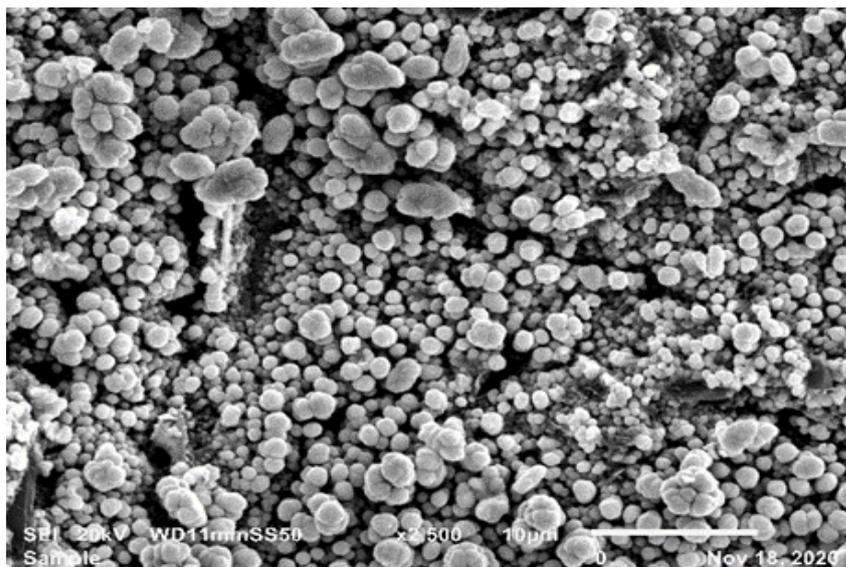
Figure 51: II-SEM images of sample C2

3.3.3 Sample-C3: EDS and SEM Analysis

Sample C3 consists of 0.03 M ZnSO4, 0.03 M SnSO4, and 0.125 M $C_6H_5O_7Na_3$; its pH= 3 and the plated mass was 1.5mg.

It was found from the EDS analysis revealed that 80.95% of the sample mass was Zn, 8.48% oxygen, and 10.57% Sn. Also, the atomic percentages were 66.67% Zn, 28.54% oxygen, and 4.79% Sn, as shown in Figure 52.
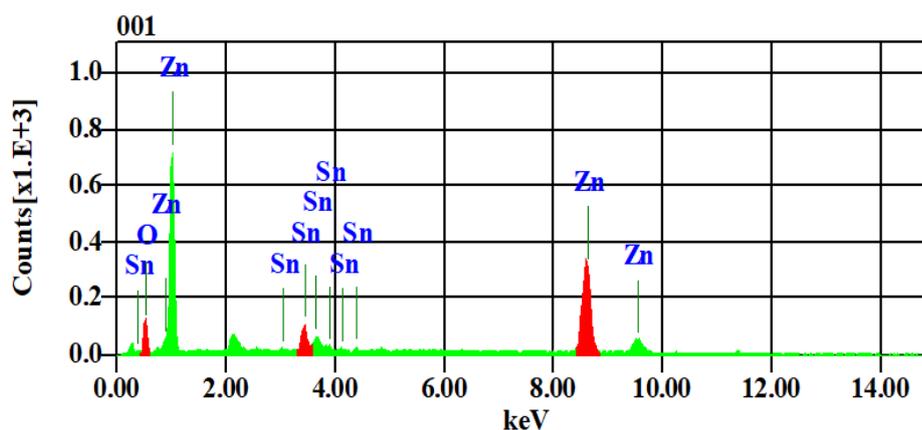
Figure 52: EDS results of sample C3

It looks that all electrodeposited particles where plated in tree branched shape covering good amount of the carbon substrate surface with very limited micro level spacing and cracks showing in between. Also, the outside surface looks very uniform in the macro level where silver colour was visible over the carbon substrate with 1.5 mg mass. Also, Zn particles consumed most of the energy and got plated comparing to the less particles of tin which got plated which in align with the previous result of B3 had mix of tin and zinc in the solution and zinc repress the tin from plating; it means that in such solution, might need larger voltage to achieve the desire plating firstly Zn other than Sn.

The SEM images also shows the surface morphology of the Zn-Sn alloy. The constant voltage which has been specified, -1.56 V, was for zinc region makes most of the zinc unreacted with tin and form tiny crystal like struct of the Cu-Sn alloy. The amount of unreacted zinc dust decreases by decreasing the size of the particles, which not only reduces the amount of zinc dust, but might also improves the efficiency of the reaction, as shown in Figure 53.
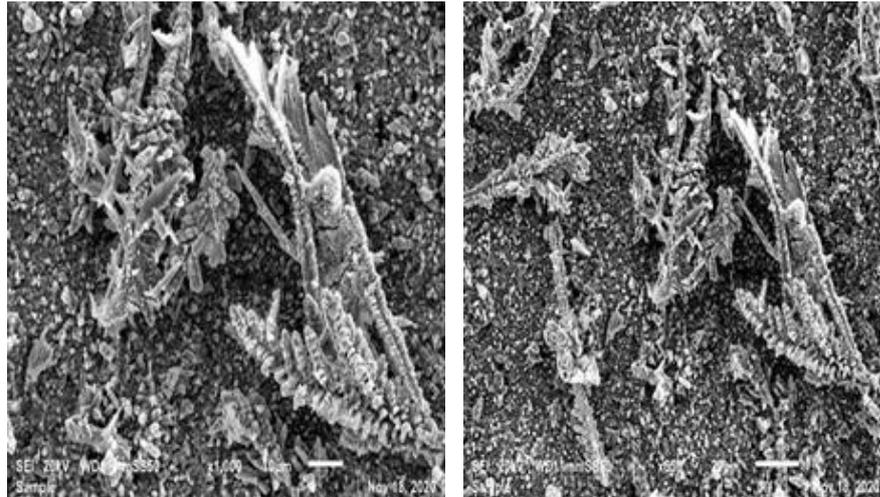
Figure 53: SEM images of sample C3

3.3.4 Sample-C4/D1: EDS and SEM Analysis

Sample C4/D1 consists of 0.03 M $CuSO_4$, 0.03 M $ZcSO_4$, 0.03 M $SnSO_4$, and 0.125 M $C_6H_5O_7Na_3$; its pH= 3 and the plated mass was 0.9 mg. Note: *to compare all there CZTS systems later, C4 sample will be consider as D1 too*.

The EDS analysis revealed that 24.99% of the sample mass was Zn, 7.20% oxygen, Cu 25.06%, and 42.75% Sn. Also, the atom percentages were 24.09% Zn, 28.37% oxygen, 24.85% Cu and 22.69% Sn, as shown in Figure 54,
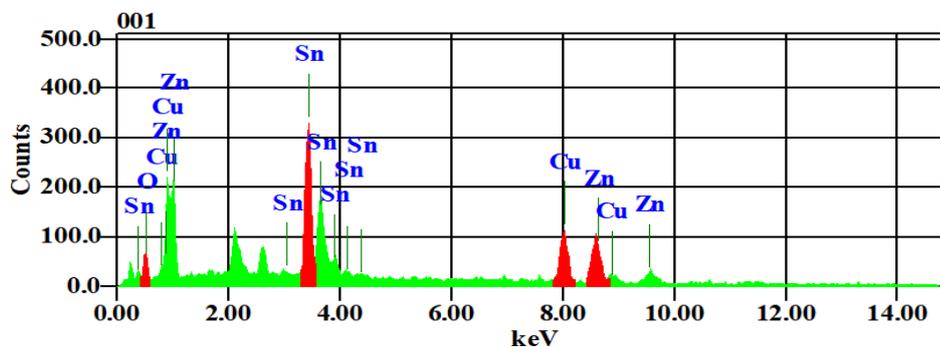
Figure 54: EDS results for C4

It looks that all electrodeposited particles where plated in tree branched non-uniform shape covering good amount of the carbon substrate surface with limited micro level spacing showing in between. Also, the outside surface looks very uniform in the macro level where dark black colour was visible over the carbon substrate with 0.9 mg mass. Strangely, the tin amount was double comparing to copper and zinc. Also, Cu and Zn had same percentage on the plated carbon electrode. Furthermore, the surface morphology of (Cu-Zn-Sn) deposited Zn region (-1.56 V).

The deposit is regular and becomes denser due to refining actions of the agent. Sn cation is easier to obtain electrons provided by reducing agent in depositing of Cu-Zn-Sn. However, the deposition Zn with the same complexing agent is low, which is only 24.99%. The presence of Zn in smaller amount in the deposited alloy with respect to amount of Zn in the electrolyte might be due to the thermodynamic instability of alloy system, as shown in Figure 55.
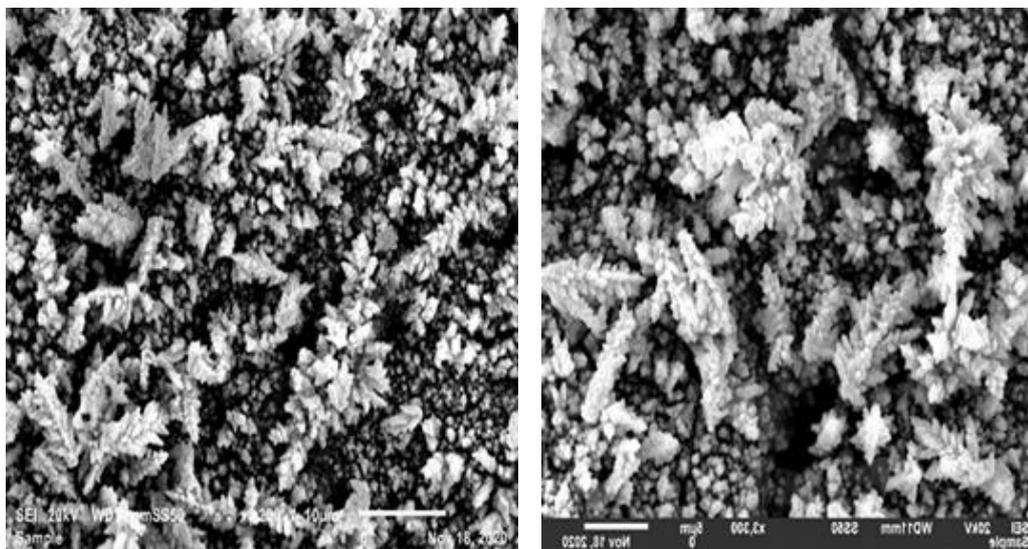
Figure 55: SEM images of sample C4/D1

It was expected to find Zn with trace of Cu and Sn to be present in the electrodeposited carbon substrates because the constant voltage, which was set, -1.56 V vs. Ag/AgCl, and pH3 for Zn region, as reported in Table 9.

Table 9: Zinc electrodeposition using different electrolyte composition and mass

Zinc Mass	Copper		Zinc		Tin	
	Weight %	Atomic %	Weight %	Atomic %	Weight %	Atomic %
C1 plated mass (0.7 mg)	-	-	86.55	61.17	-	-
C2 plated mass (0.7 mg)	79.62	70.32	15.78	13.54	-	-
C3 plated mass (1.5 mg)	-	-	80.95	66.67	10.57	4.79
C4 plated mass (0.9 mg)	25.06	24.85	24.99	24.09	42.75	22.69

The SEM images concluding that the best solution to electrodeposit zinc in terms of electrodeposited mass is C3 which has tin. It appears that zinc was the dominate in the sample with overall good mass of about 1.5 mg. Nevertheless, sample C3 gave a tree shape formation. When it comes to quality, sample C1 has a bigger size grain of pure zinc where sample C2 seems to form spherical shapes where both elements well mixed but with way less zinc amount. Finally, sample C4/D1 got amazing finding where copper and zinc had the about same amount with tin electrodeposited domination. Also, it got some tree nucleation shape with some small gaps, as shown in Figure 56.
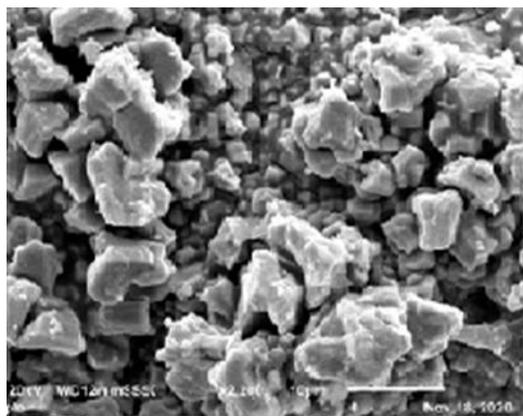
Zn solution electrodeposited product
(Sample C1)
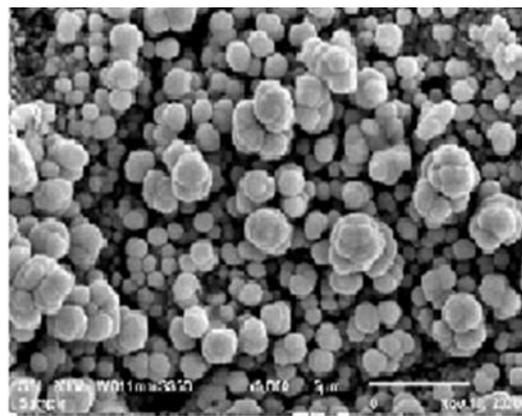
Cu-Zn solution electrodeposited product
(Sample C2)

Zn-Sn solution electrodeposited product
(Sample C3)
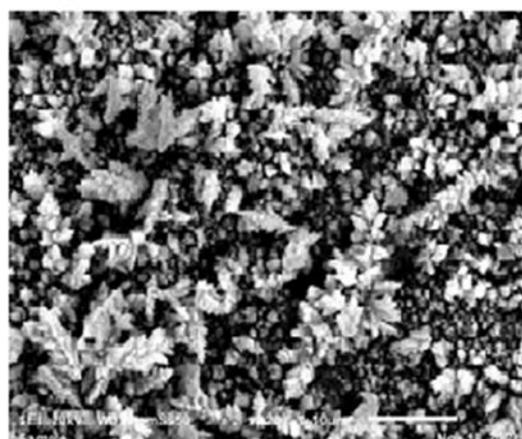
Cu-Zn-Sn solution electrodeposited product
(Sample C4/D1)

Figure 56: Zinc electrodeposition using different electrolyte SEM comparison

3.3.5 XRD Graphs of Sample C Series

The constant voltage of -1.56 V vs. Ag/AgCl is specific to the electrodeposition of Zn and XRD graphs are demonstrating comparable results to the ones found with SEM and EDS.

In case of control sample C1, the perfect electrodeposition of Zn was done as the potential region is specific for the stated metal. The characteristic peaks of Zn are obtained at 2 theta values of 9.2, 26, 28.5, 36, 39, 42.5, 43 and 54.5.

Considering C2, when along with Zn, Cu metal was also used in the solution to form an alloy and the decreased peak intensities and peaks disappearance were observed in the XRD graph. There was no peak shift observed for Zn characteristics peak at 2 theta values of 9.2, 26, 28.5 and 49, 54.5. While different peaks at 2-theta value of 36, 39 and 42.5 was observed for Zn-Cu alloy plating. In addition to this, decrease in peak intensity was observed for 2-theta value at 43. Hence, C2 sample has both plating of both Zinc and Copper in its composition as shown in EDS spectrum and validated by XRD graph.

Considering C3, when along with Zn, Sn metal was also used in the solution to form an alloy plating and XRD graph is showing more heightened peaks and intensity decrement is observed at 2-theta value of 39 and 43.

Considering C4, when along with Sn, Cu and Zn metals were also used in the solution to form an alloy plating and XRD graph is demonstrating the presence of all the three metals.

Hence, the presence of zinc was observed in the XRD graph of C1, C2, C3, and C4 samples. C2 is demonstrating the presence of copper traces. Figure 57 shows XRD graph C sample series. Thus, all graphs are also validating results obtained by the SEM and EDS results.
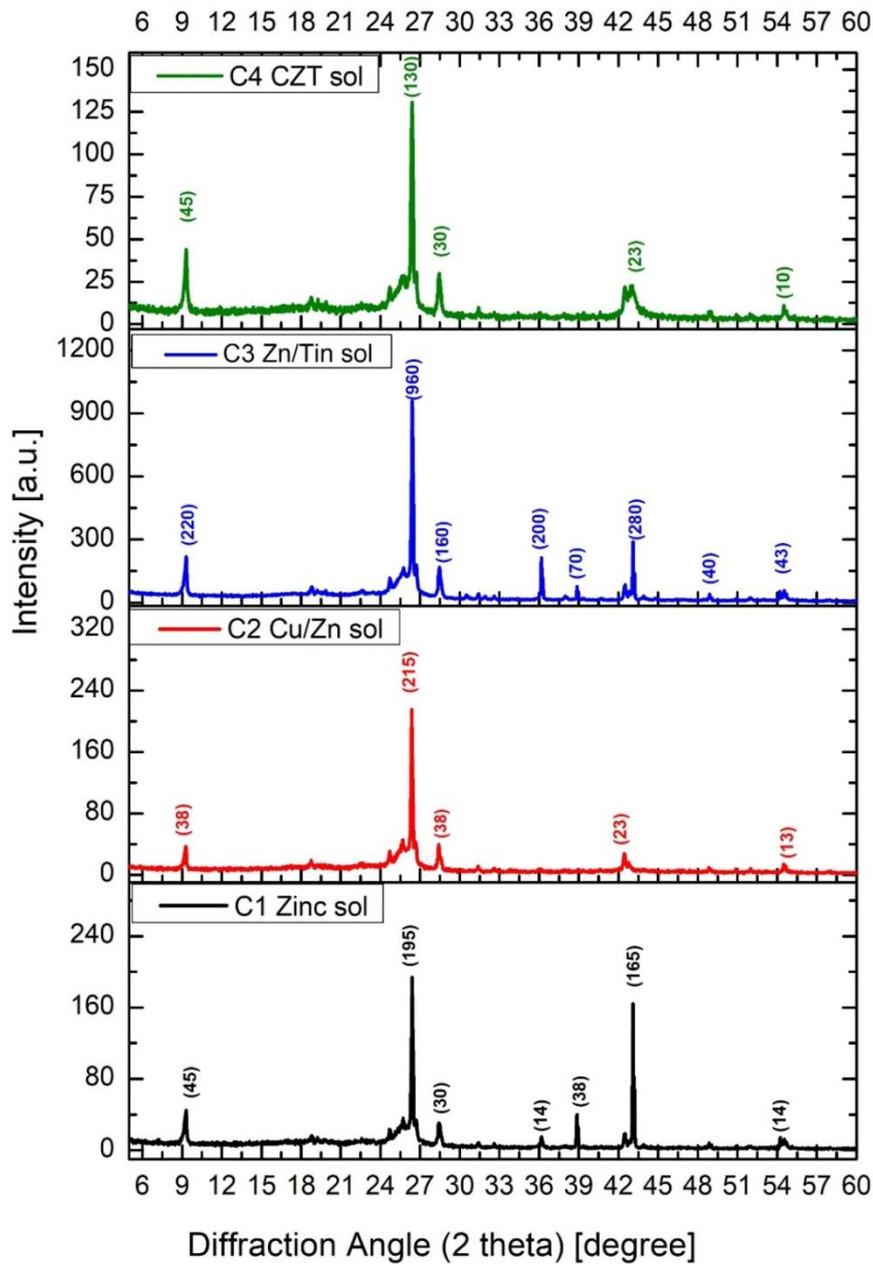
Figure 57: XRD results graphs of the C samples set

Four distinctive peaks at 9.2°, 26.6°, 39° and 43° respectively were the crystallographic paths of 000, 100, 120 and 223, Table 10 has summary of XRD results. Regarding the orientation of the signature peaks of pure zinc these peaks were shifted to lower angles suggesting that the Tin crystal grid was hit by a certain number of copper atoms and hence a unit cell was distorted, and the diffraction peaks

were detected. In comparison to copper and tin, as zinc atoms wrapped further in copper bars of the cell, peaks were pushed further. The alloy XRD Cu-Zn-Sn reveals that the trace of Tin is thin, with the zinc atoms in copper since the main top is close to the copper peak but the diffractive angle is slightly changed.

Table 10: XRD results for C sample set

Peak	$1000*Sin^2\phi$	Reflection	Remarks
9.2°	25	0	0
26.6°	523	1^2+2+2	$1^2+0+0=1$
39°	111	$1^2+1^2+1^2$	$1^2+1^2+1^2=3$
3.6°	138	$1^2+1^2+1^2$	$1^2+1^2+1^2=3$

3.4 Series-D Samples: CZT Electrodeposition using Different Electrolyte

Analysis of series D solutions indicated the presence of Zn, trace of Cu and in the electrodeposited over carbon substrates under the constant voltage that specified at -1.56 V vs. Ag/AgCl (i.e., optimized from the series of experiments by A, B and C samples). Also, the time of electrodeposition for all samples was 25 minutes where the pH was varied as 4.4, 3, 2.

3.4.1 Sample-D2: EDS and SEM Analysis

Sample C4/D2 consists of 0.03 M $CuSO_4$, 0.03 M $ZcSO_4$, 0.03 M $SnSO_4$, and 0.125 M $C_6H_5O_7Na_3$; its pH= 4.4 and the plated mass was 1.0 mg.

The EDS analysis revealed that 33.44% of the sample mass was Zn, 36.34%Cu, and 30.21% Sn. Also, the atom percentages were 38.23% Zn, 42.74% Cu, and 19.02% Sn, as shown in Figure 58.
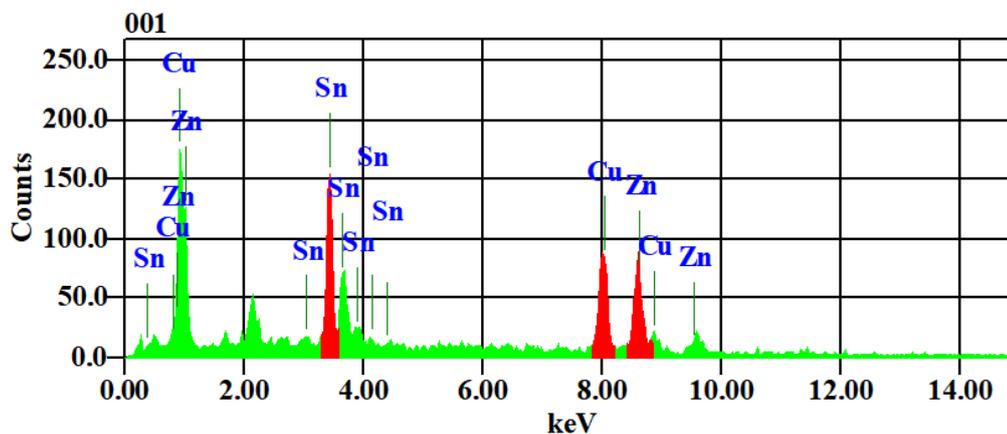
Figure 58: EDS results of sample D2

It looks that all electrodeposited particles where plated in tree branched cauliflower shape covering good amount of the carbon substrate surface with limited micro level spacing showing in between.   Also, the outside surface looks very uniform in the macro level where dark black colour was visible over the carbon substrate with 1 mg mass. Also, all elements electrodeposited with around the same amount. Furthermore, the generated surface images display 1 mm thick of the electrodeposited Cu-Zn-Sn precursors. Films are made up of 0.5-1 mm pillar-shaped grains as the constant voltage defined by us -1.56 V, was used for the Zn-area based on the Ag/AgCl reference CV experiments, as shown in Figure 59.
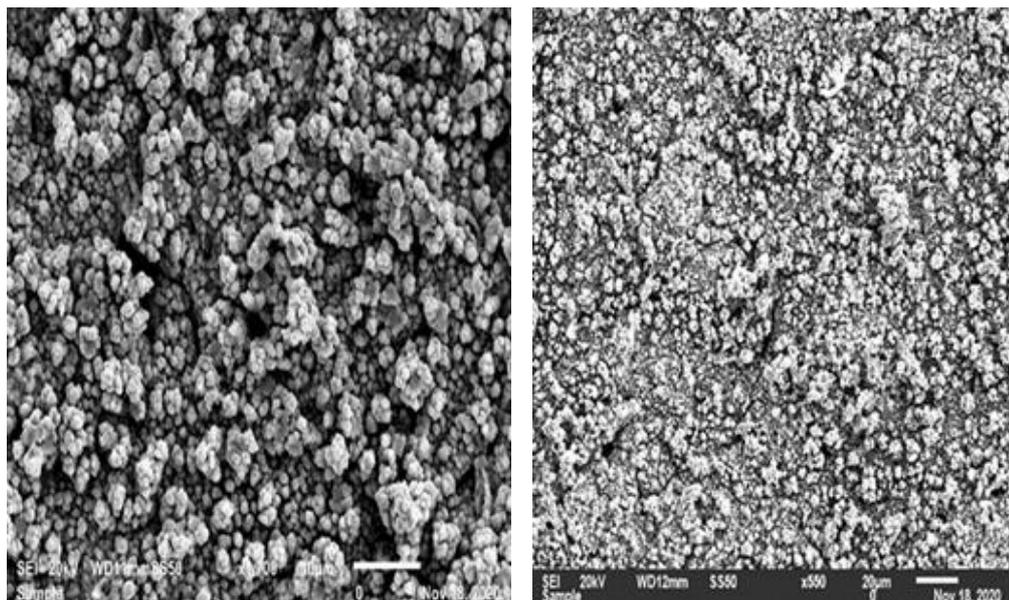
Figure 59: SEM images of sample D2

3.4.2 Sample-D3: EDS and SEM Analysis

Sample C4/D2 consists of 0.03 M $CuSO_4$, 0.03 M $ZcSO_4$, 0.03 M $SnSO_4$, and 0.125 M $C_6H_5O_7Na_3$; its pH dropped to 2 and the plated mass was 1.2 mg.

The EDS analysis showed that 9.46% of the sample mass was Zn, 36.34% Cu, and 30.21% Sn. Also, the atom percentages were 8.17% Zn, 29.48% Cu, 40.57% oxygen, and 21.79% Sn, as shown in Figure 60.
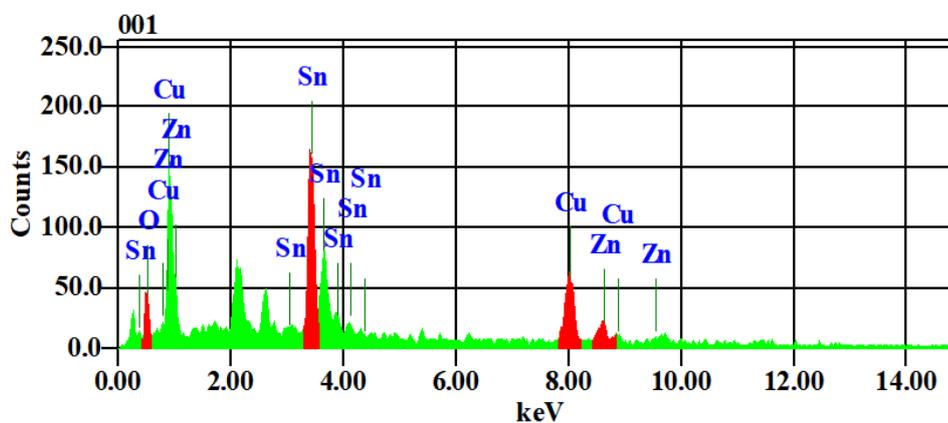
Figure 60: EDS results of D3

It looks that all electrodeposited particles where plated in cauliflower film shape covering good amount of the carbon substrate surface with some micro level spacing and cracks showing in between. Also, the outside surface looks very uniform in the macro level where dark stacked black colour layer was visible over the carbon substrate with 1.2 mg mass. Yet, the surface picture of Cu-Zn-Sn electrodeposited metals was 1 mm thick. Films are made up of 0.5-1 mm pillar-shaped grains with agglomerated together with the constant voltage defined by us -1.56 V, was used for the zinc-area based on the Ag/AgCl reference CV experiments, as shown in Figure 61.
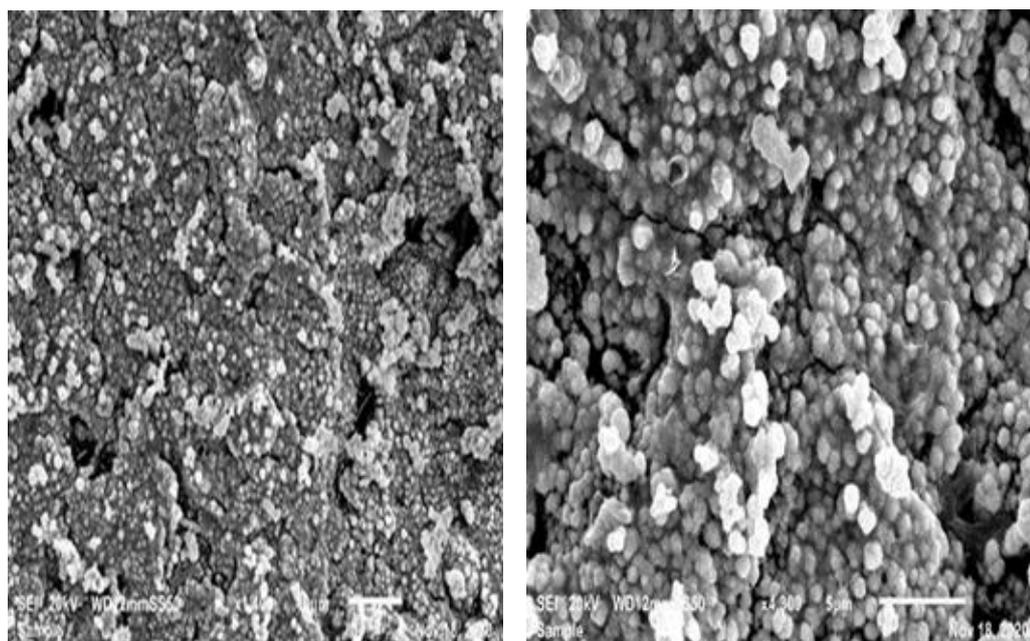
Figure 61: SEM images of sample D3

Analysis of D3 solutions reported the presence of Zn and trace of Cu and Sn in the electrodeposited carbon substrates under constant voltage that specified -1.56 V vs. Ag/AgCl for Zn region as pH was found to be changed for comparison 4.4, 3, and 2. Table 11 summaries the generated results of Sn tin electrodeposition.

Table 11: Tin electrodeposition using different electrolyte composition and mass

Cu-Zn-Sn Sample	Copper		Zinc		Tin	
	Weight %	Atomic %	Weight %	Atomic %	Weight %	Atomic %
D1 (pH = 3) plated mass (0.9 mg)	25.06	24.85	24.99	24.09	42.75	22.69
D2 (pH= 4.4) plated mass (1 mg)	36.37	42.74	33.44	38.23	30.21	19.02
D3 (pH= 2) plated pass (0.9 mg)	36.34	29.48	9.46	8.17	30.21	21.79

The generated SEM images of the D3 sample with pH of 2 had the best surface morphology between all other CZT electrodeposited samples where all samples had about the same mass. Nevertheless, in sample D3, the amount of zinc was significantly lower than the other samples. Sample D1 has the most tin percentage between all other samples. On another hand, it was found that sample D2 had the same amount percentages between all elements where copper then zinc take the most which behaviour has been seen before in other electrodeposited samples such as sample C2. Finally, dropping the pH plays a key role in the plated elements, thus it is advised to design the alloy and the solution based on this before starting the electrodeposition process. Furthermore, lowering the pH showed a disproportional effect with the zinc amount in the CZT solutions, as shown in Figure 62.

Cu-Zn-Sn solution electrodeposited product (Sample C4/D1) pH 3

Cu-Zn-Sn solution electrodeposited product (Sample D2) pH 4.4

Cu-Zn-Sn solution electrodeposited product (Sample D3) pH 2
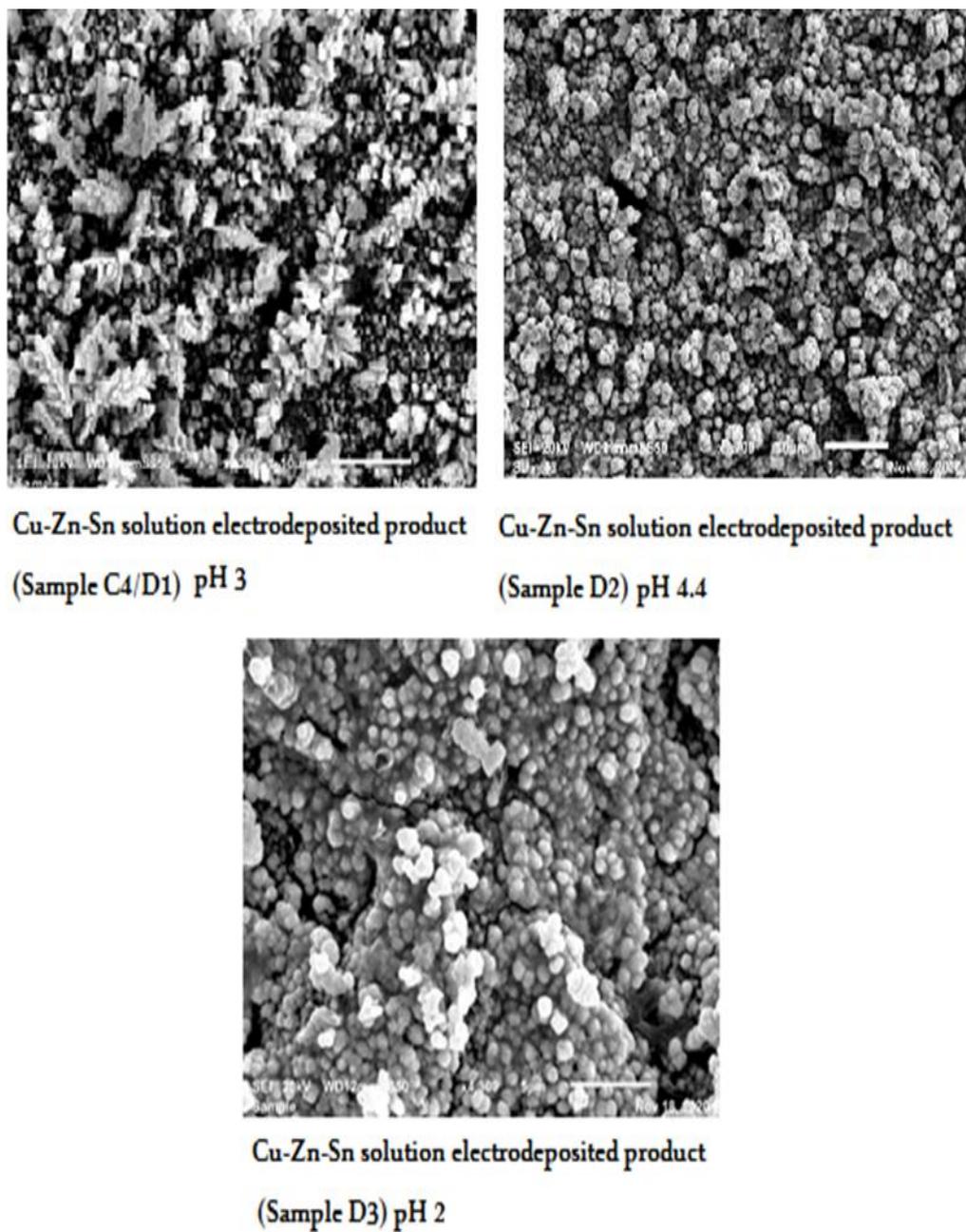
Figure 62: CZT electrodeposition using different electrolyte SEM comparison

3.4.3 XRD Graphs of Sample D Series

Sample D series are showing the comparison of CZT samples based on differences in pH during the plating reaction. The pH range in this study is 2-4.4. By increasing pH up to 4.4 value, the perfect CZTS alloy is plated on the substrate. D2 sample is showing the maximum peak intensities and has close resemblance with JCPDS card

number is 26-0575 for CZTS with has values in Figure 64 from (101), (112), (200), (220), and (312) planes indicating that the films have kieserite CZTS structure. The plating behaviour at various specific potentials of different metals was studied. The main findings of the experiment were:

At -0.4 V vs. Ag/AgCl, only Cu metal gets plated with no disruptions even in the presence of Sn and Zn metal.

At -1.12 V vs. Ag/AgCl, it was found that Zn metal suppresses the plating of Sn. Thus, no plating occurs in sample B3. In fact, the same behaviour was seen in the (Zn-Sn) solution when the voltage increased to -1.56 V, sample C3, where the mass percentage of the electrodeposited zinc was 80.95% while tin was only 10.57%.

Also, using -1.12 V the plated thin film of (Cu-Zn-Sn) solution had composition of only Cu and Sn because Zn needed more voltage to electrodeposit in such a solution which validates the CV experiments. At -1.56 V vs. Ag/AgCl, all the three metals (Zn, Sn and Cu) get electrodeposited on the carbon substrate.

Thus, the optimized potential for plating was found to be equal to -1.56 V. Besides that, pH condition is optimized after potential optimization. The optimized pH value was found to be 4.4 based on experimental results. XRD Figure 63 that has comparison between D set samples.
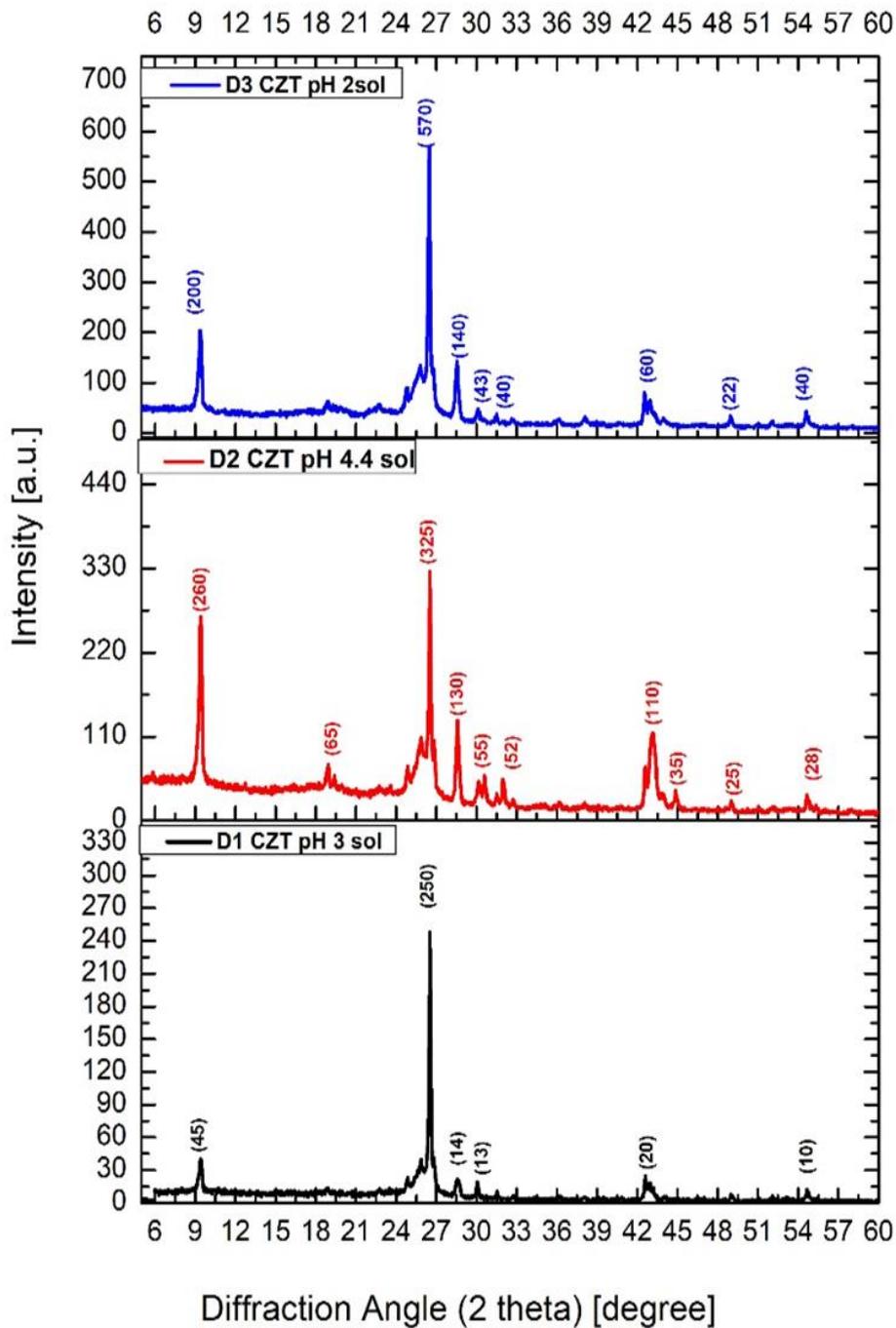
Figure 63: XRD results graphs for the D samples set

The crystallographic pathways from 000, 100, 120 and 223 were four peaks at 9.2°, 26.6°, 39° and 43° respectively, Table 12. With respect to the orientation of pure zinc

signature peaks, these peaks were pushed down to lower angles, indicating that a certain number of copper atoms influenced the Tin crystal grid and thus a unit cell was bent, and peak diffraction was observed. As zinc atoms were wrapped in the copper bars of the cell, peaks were squeezed deeper compared with copper and tin. The pH changes are found the bases of peak intensities. The CZT alloy in solution changes get rise in 9.2° angle peak of pH 3 solution. This peak intensity is 260 at pH 4.4, 45 at pH 3 and 200 at pH 200. The CZT alloy in solution also get rise in 26.6° angle peak of pH 3 solution. This peak intensity is 325 at pH 4.4, 570 at pH 3 and 200 at pH 200.

Table 12: XRD results for D samples set

Peak	$1000*Sin^2\text{ø}$	Reflection	Remarks
9.2°	25	0	000
26.6°	523	1^2+2+2	$1^2+0+0=1$
39°	111	$1^2+1^2+1^2$	$1^2+1^2+1^2=3$
43.6°	138	$1^2+1^2+1^2$	$1^2+1^2+1^2=3$

SEM image for sample A2 have constant voltage which was specified, -0.4 V, was for Cu region and SEM image C2 have zinc region with potential of Cu and Sn to be present in the electrodeposited carbon substrates because the constant voltage, which was specified, -1.56 V. The picture from SEM for sample A1 has shown that the Cu particles synthesized are spherical and less than 3um in scale. The synthesized Cu-Zn alloy used in this study is shown in SEM image C2 sample. Individual copper particles are clumped into the SEM image together with zinc. Particles in SEM C2 image include several single glasses visible particles. The spectrum 1 and 2 have same pH with different masses like 0.2 mg and 0.7 mg. Various areas were

stimulated during EDS measurements, and the associated peaks are shown in EDS A2 and C2 samples images. The differences in weight percent and atomic percentages among the three spectra, as shown in the Table 13.

Table 13: Comparison between samples of A2 and C2

Cu-Zn	Copper		Zinc		Oxygen	
	Weight %	Atomic %	Weight %	Atomic %	Weight %	Atomic %
Spectrum 1/A2 plated mass (0.2 mg)	94.58	13.29	Small Trace	Small trace	5.42	6.48
Spectrum 2/C2 plated mass (0.7 mg)	79.62	70.32	15.78	13.54	4.6	16.14

The voltage which specified was constant, -0.4 V vs. Ag/AgCl for copper region in A3 image and it was expected tin and Cu for all electrodeposited carbon substrates in the B2 image sample, because the constant voltage was specify, -1.12 V vs. Ag/AgCl for tin region. SEM image of sample A3 shows a Cu-Sn alloy, which has been synthesized for this analysis. As seen in the image above, individual copper particles containing small traces of tin agglomerated together. SEM images for B2 sample displays of (Cu-Sn) compound. The film has a porous structure and an enormous surface that helps to render the sensitive. Both spectra 1 and 2 have same pH with different masses like 0.2 mg and 0.7 mg. Various areas were stimulated during the differences in weight percent and atomic percentages among the three spectra, as shown in the Table 14.

Table 14: Comparison between samples of A3 and B2

Cu-Sn	Copper		Sn	
	Weight %	Atomic %	Weight %	Atomic %
Spectrum 1/A3 plated mass (0.2 mg)	91.04	71.96	Small Trace	Small trace
Spectrum 2/B2 plated mass (0.6 mg)	47.09	47.42	46.26	46.26

The SEM image of B3 sample was done in a constant voltage of -1.12 V vs. Ag/AgCl Image C3 of SEM has a zinc region with the copper and tin potential to be present in the electroplates because of the continuous tension defined by us -1.56 V vs. Ag/AgCl. SEM Figure for B3 sample indicates the gold plate surface morphology because the electrodeposition of tin in the solution is suppressed with zinc. The SEM has been placed in gold on a substratum, so the plate is not complete, and gold is a mere part of running the SEM. Moreover, SEM images of C3 samples demonstrates the zinc-tin alloy surface morphology.

The constant voltage of -1.56 V for the zinc region is unreacted by tin and shape small crystal-like structure of the Cu-Sn alloy. The amount of non-reacted zinc pollution decreases by reducing the particle size, not only reducing zinc dust but might improve the reaction's effectiveness. The spectrum1 and 2 have same pH with different masses like 0.2 mg and 1.5 mg. The spectrum 1 and 2 have the same pH of 0.2 mg and 1.5 mg. The weight and atomic percentage disparities of the three spectra, as shown in Table 15.

Table 15: Comparison between SEM of samples C3 and B3

Sn- Tn	Zinc		Tin	
	Weight %	Atomic %	Weight %	Atomic %
Spectrum 1/C3 plated mass (0.2 mg)	Au	Au	Au	Au
Spectrum 2/B3 plated mass (1.5 mg)	80.95	66.67	10.57	4.79

The films consist of 0.5-1 mm column-shaped grains as the constant voltage specified by us-1.56 V, which was used for the zinc-area based on the Ag/AgCl reference CV experiments. However, the deposition of Zn with the same complexing agent is comparatively limited. In the settled alloy the appearance of Zn in the electrolyte in smaller quantity. The occurrence of porosity was also observed for each sample. This might be done due to the release of hydrogen gas at the working electrode during the electrodeposition process. Constant stirring might result to a less homogeneous and less robust surface finish to the D set samples.

To confirm the formation of Cu-Zn-Sn alloy, the SEM-EDS analysis was performed with Zin potential of -1.56 based on the CV experiments with Ag/AgCl reference. During EDS measurements, various areas were stimulated, and the related peaks are shown in the EDS Figures for samples D. Details of three different spectra with different pH 3, 4.4 and 2 are shown with respect to different electrodeposited mass of the spectra 1, 2 and 3 like 0.9 mg, 1 mg and 0.9 mg, respectively, as shown in Table 16.

Table 16: Comparison between samples of D1, D2 and D3

Cu-Zn-Sn	Copper		Zinc		Tin	
	Weight %	Atomic %	Weight %	Atomic %	Weight %	Atomic %
Spectrum 1/D1 plated mass (0.9 mg)	25.06	24.85	24.99	24.09	42.75	22.69
Spectrum 2/D2 plated mass (1 mg)	36.37	42.74	33.44	38.23	30.21	19.02
Spectrum 3/D3 plated mass (0.9 mg)	36.34	29.48	9.46	8.17	30.21	21.79

Another way to compare the electrodeposited samples is by analysing the same solutions where the product was different due to the different voltages used in the electrodeposition process. For example, samples A2 and C2 had the same chemical contents. Nevertheless, sample A2 had only -0.4 V applied which resulted to electrodeposit a sample with 94% of copper. Where sample C2 had -1.56 V applied to the solution which resulted in 79% of copper and 15.78% of zinc in the electrodeposited product. Table 17 presents the differences between the two samples.

Table 17: Comparison between samples A2 and C2 were the voltages different

Cu-Zn solutions	Copper		Zinc	
	Weight %	Atomic%	Weight%	Atomic%
Sample A2 -0.4V pH=3 plated mass (0.2 mg)	94.58	13.29	Small Trace	Small trace
Sample C2 -1.56V pH=3 plated mass (0.7 mg)	79.62	70.32	15.78	13.54

Similarly, Table 18 shows the differences between samples A3 and B2 where both samples had the same chemical contents and conditions, but voltages applied were

different. In the case of sample A3, the voltage was -0.4 V where for sample B2
-1.12. Sample A3 had 91% of copper in the content of the electrodeposited product
with an overall 0.2 mg weight. Sample B2 had 47% of copper and 46.26% in the
content of the electrodeposited product with an overall 0.6 mg weight.

Table 18: Comparison between samples A3and B2 were voltages different

Cu-Sn solutions	Copper		Tin	
	Weight %	Atomic %	Weight %	Atomic %
Sample A3 -0.4V pH=3 Plated Mass (0.2 mg)	91.04	71.96	Small Trace	Small trace
Sample B2 -1.12V pH=3 Plated Mass (0.6 mg)	47.09	47.42	46.26	46.26

Finally, electrodeposited metals alone compared in Table 19. It shows great
electrodeposited layers over the carbon substrate where the whole surface covered by
copper or zinc with good mass.

Table 19: Comparison between all single metals electrodeposited over carbon

Metal Sulphates	Metal	
	Weight %	Atomic %
Sample A1 ($CuSo_4$) -0.4 V pH=3 plated mass (0.8 mg)	96.40	87.08
Sample B1 ($TinSo_4$) -1.12 V pH=3 plated mass (0.4 mg)	66.23	20.91
Sample C1 ($ZnSo_4$) -1.56 V pH=3 plated mass (0.7 mg)	86.55	61.17

Chapter 4: Conclusions, Challenges, and Future Work

4.1 Conclusion

The electrodeposition of Cu-Zn-Sn alloys was examined in this study with the use of Sodium Citrate as a complexing agent. Successfully, all desired deposited elements were as expected. Nevertheless, varying the metal in the solution and the pH would result in different surface and mixture electrodeposited.

To electroplate Cu, Zn, Sn, or Cu-Zn-Sn, a CV study needs to be done to determine the right voltage to be used in each case based on the specified condition and concertation. It would help to know the needed voltage for the deposition to occur because supplying less than the required voltage means no electrodeposition will be done. In the case of this study, copper plated with a voltage of -0.4 and tin with -1.12 V and zinc with -1.56 V with Ag/AgCl reference electrode. Also, preparing the right stable solution was one of the biggest challenges. Having a non-stable solution means a big flaw in the overall study. It was managed to get very stable solutions with 0.03 M for all elements with Sodium Citrate as a complexing agent with pH ranges from 4.4 to about 2 at room temperature. Also, it was found that with decreasing the pH the electroconductivity for the solutions does increase. However, it does not mean better surface or more quantity.

To get the best surface and the desired quantity, a study needed to be done at first on different stable solutions varying the pH to see the compositions till getting the most fitted alloy for the application. In this study, CZT was managed to be electrodeposited successfully where sample D2 with a pH of 4.4 gave us the best surface and an equal amount of all elements. In the case of sample D3 where the pH

was 2, it was got the more quantity with tin higher than Cu or Zn but the surface, not the best comparing to the other samples. In the case of sample D1, it got a much higher tin quantity than Zn or Cu, but it seems that the zinc is higher. In other words, it seems the more the pH dropped, the Zn percentage gets lees in the electrodeposited materials.

In the case of plating copper, tin, or zinc in the sample sets A, B, and C, it seems that it is better to plate a solution where only contains that element to have better energy distribution, which will result in a better surface. Nevertheless, in the case of alloys where a mix of two elements or more needed, carefully picking the mixture and the voltage required will result in better yield. For example, the same solution has been used for tin and zinc, but only managed to plate them after increasing the voltage to the Zn voltage range based on the CV experiment readings. Thus, Zn repressed the tin from plating and even after increasing the voltage Zn was plated more than Sn.

There are many applications for red metals alloys. Staring with just simply Cu like the first set of A samples, Cu has good electrical, thermal conductivity, and strength which has excellent resistance to corrosion. Thus, Cu can be found in wires and electrical motors, parts, and pans. Most importantly, a thin-film layer of Cu over carbon substrate has a property of a small battery that can withhold energy and discharge it. It has the advantage of being light and cost-effective when it is successfully electrodeposited as in the example of the A samples which yielded good mass with good surface morphology.

Bronze has Cu and Sn such as the B2 sample can be used in bearings due to low metal to metal friction, sculptures due to its nice colour and corrosion resistance, and making bronze wool for woodworking applications to avoid some problems

associated with broken filaments like the ones from steel wool. Furthermore, brass which is Cu and Zn, such as sample C2 can be used to replace gold in many decorative applications due to its similar nice appearance. Thus, brass is used in the making of many musical instruments which also last longer due to brass's high density. The more content of Zn in brass the less ductile is especially when it is above 39%. In the plated brass sample C2, the Cu percentage was 79.62% and the Zn was 15.78% which means that it is less strength but higher ductility than a brass sample with a Zn content of more than 39%.

In the case of the targeted system, samples D1, D2 and D3, it was found that electrodeposition of all Cu, Zn, and Sn can be done all at a single step under room temperature without any stirrer. Also, it is possible to make all solutions stable as presented in Chapter 2 without dropping their pH or increasing the temperature. Nevertheless, decreasing the pH might have its own benefits based on the content of the desired product. The CZT alloy with the addition of sulphur which can be done in the annealing or vapour deposition process would yield to active part in the solar cell.

The beauty of such elements not only can be found abound with optimum solar energy property; it also can be integrated into substrates like glass or flexible polymers. Such a feature could open the use of solar cells more than the typical stander uses and applications at the main time. Humans would be able to supply many devices with energy were achieving the same efficiency with way less mass than today's typical silicon-type PV solar cells.

4.2 Challenges

There were many challenges in this study. One major challenge was to make sure that the solutions are stable even after days and weeks. Such requirements hindered the speed of the progress of the study. Nevertheless, it gave us valuable information about the interaction of the elements and more understanding of its behaviour in a mixed solution. It was set from the beginning of this study to try as much as possible to make a stable solution without the need of increasing the temperature, decreasing the pH, and without rotating while plating which will result in a more cost-effective product. Nevertheless, for future study, it is believed that rotating the mixture could result in better-coated elements and yield. Also, trying other complexing agents or even a complex of multiple complexing agents might help to stabilize the solution or even would yield a better surface or more mass.

Besides the solution problem, the noises while plating or during the CV runs had a major effect on the results. In this study and after many trials, it has been decided to try to plate while covering the wires and the glass beaker with some foil to try to lessen the effect of the noises. Also, the plated surface had some edges in its shape which has some effect on the destitution of the voltage, but it was opted to neglect such effect and focus on the presence of the elements, quantity, and the surface.

4.3 Future Work

It is recommended to generate a reaction rate based on the findings which describe the reaction behaviour and would result in better control of the yielded products. With such, prediction of the thickness, band gap, and mass percentage of each element should be easier. Also, engineers would be able to calculate and design the alloy upfront before starting the electrodeposition process.

References

[1] Harsimran, S., Santosh, K., & Rakesh, K. (2021). Overview of corrosion and its control: A critical review. *Proceedings on Engineering*, *3*(1), 13-24.

[2] Helmenstine, M. A. (2020). *Here's why brass doesn't have an element symbol*. Available at: https://www.thoughtco.com/element-symbol-for-brass-604004 (accessed on 13/03/2021).

[3] Sanat, N. H., Nmaya, M. M., Yabagi, J. A., Isah, M., & Kimpa, M. A. A. (2016). Study of thin film copper electrodeposition on carbon substrate for thin film battery electrode application. *Journal of Science and Technology*, *8*(1), 13-16.

[4] Kheraj, V., Patel, K. K., Patel, S. J., & Shah, D. V. (2013). Synthesis and characterisation of Copper Zinc Tin Sulphide (CZTS) compound for absorber material in solar-cells. *Journal of Crystal Growth*, *362*, 174-177.

[5] Liu, F., Sun, K., Li, W., Yan, C., Cui, H., Jiang, L., ..., & Green, M. A. (2014). Enhancing the Cu_2ZnSnS_4 solar cell efficiency by back contact modification: Inserting a thin TiB_2 intermediate layer at Cu_2ZnSnS_4/Mo interface. *Applied Physics Letters*, *104*(5), 051105.

[6] Mitzi, D. B., Gunawan, O., Todorov, T. K., Wang, K., & Guha, S. (2011). The path towards a high-performance solution-processed Kesterite solar cell. *Solar Energy Materials and Solar Cells*, *95*(6), 1421-1436.

[7] Katagiri, H., Jimbo, K., Maw, W. S., Oishi, K., Yamazaki, M., Araki, H., & Takeuchi, A. (2009). Development of CZTS-based thin film solar cells. *Thin Solid Films*, *517*(7), 2455-2460.

[8] Gunawan, O., Gokmen, T., Warren, C. W., Cohen, J. D., Todorov, T. K., Barkhouse, D. A. R., ..., & Mitzi, D. B. (2012). Electronic properties of the $Cu_2ZnSn(Se,S)_4$ absorber layer in solar cells as revealed by admittance spectroscopy and related methods. *Applied Physics Letters*, *100*(25), 253905.

[9] Lu, Y. C., Gallant, B. M., Kwabi, D. G., Harding, J. R., Mitchell, R. R., Whittingham, M. S., & Shao-Horn, Y. (2013). Lithium–oxygen batteries: bridging mechanistic understanding and battery performance. *Energy & Environmental Science*, *6*(3), 750-768.

[10] Scrosati, B., Marsh, R. A., & Scanlon Jr, L. G. (1997). *Thin film lithium polymer battery* [patent]. U.S. Patent No. 5,645,960. Washington, DC: U.S. Patent and Trademark Office.

[11] Wang, Z., Malti, A., Ouyang, L., Tu, D., Tian, W., Wågberg, L., & Hamedi, M. M. (2018). Copper-plated paper for high-performance lithium-ion batteries. *Small*, *14*(48), 1803313.

[12] Kulova, T., Mironenko, A., Rudy, A., & Skundin, A. (2021). *All Solid State Thin-Film Lithium-Ion Batteries: Materials, Technology, and Diagnostics* (pp. 29-73). London: CRC Press.

[13] Carter, R. A. (2018). New techniques for tackling corrosion. *Engineering and Mining Journal*, *219*(10), 40-43.

[14] Leygraf, C., Chang, T., Herting, G., & Wallinder, I. O. (2019). The origin and evolution of copper patina colour. *Corrosion Science*, *157*, 337-346.

[15] Fateh, A., Aliofkhazraei, M., & Rezvanian, A. R. (2020). Review of corrosive environments for copper and its corrosion inhibitors. *Arabian Journal of Chemistry*, *13*(1), 481-544.

[16] Raza, M. W., Amin, R. U., Malik, A. S., Kasi, M., Kasi, B., & Muhammad, F. (2017). Analysis of The Impact of Environmental Factors on Efficiency of Different Types of Solar Cells. *Journal of Applied and Emerging Sciences*, *7*(1), pp76-90.

[17] Khalate, S. A., Kate, R. S., & Deokate, R. J. (2018). A review on energy economics and the recent research and development in energy and the Cu_2ZnSnS_4 (CZTS) solar cells: A focus towards efficiency. *Solar Energy*, *169*, 616-633.

[18] Jackson, P., Hariskos, D., Lotter, E., Paetel, S., Wuerz, R., Menner, R., ..., & Powalla, M. (2011). New world record efficiency for Cu (In, Ga) Se_2 thin-film solar cells beyond 20%. *Progress in Photovoltaics*, *19*(7), 894-897.

[19] Araki, H., Kubo, Y., Jimbo, K., Maw, W. S., Katagiri, H., Yamazaki, M., ..., & Takeuchi, A. (2009). Preparation of Cu_2ZnSnS_4 thin films by sulfurization of co-electroplated Cu-Zn-Sn precursors. *Physica Status Solidi C*, *6*(5), 1266-1268.

[20] Benami, A. (2019). Effect of CZTS parameters on photovoltaic solar cell from numerical simulation. *Journal of Energy and Power Engineering*, *13*(1). 32-36.

[21] Ennaoui, A., Lux-Steiner, M., Weber, A., Abou-Ras, D., Kötschau, I., Schock, H. W., ..., & Kirbs, A. (2009). Cu_2ZnSnS_4 thin film solar cells from electroplated precursors: Novel low-cost perspective. *Thin Solid Films*, *517*(7), 2511-2514.

[22] Liu, Y., Kong, D. Y., You, H., Chen, C. L., Lin, X. H., & Brugger, J. (2013). Structural and optical properties of the $Cu_2ZnSnSe_4$ thin films grown by nano-ink coating and selenization. *Journal of Materials Science: Materials in Electronics*, *24*(2), 529-535.

[23] Dong, Y., Wojtas, L., Martin, J., & Nolas, G. S. (2015). Synthesis, crystal structure, and transport properties of quaternary tetrahedral chalcogenides. *Journal of Materials Chemistry C*, *3*(40), 10436-10441.

[24] Song, X., Ji, X., Li, M., Lin, W., Luo, X., & Zhang, H. (2014). A review on development prospect of CZTS based thin film solar cells. *International Journal of Photoenergy*, https://doi.org/10.1155/2014/613173.

[25] Parasyuk, O. V., Piskach, L. V., Romanyuk, Y. E., Olekseyuk, I. D., Zaremba, V. I., & Pekhnyo, V. I. (2005). Phase relations in the quasi-binary Cu_2GeS_3–ZnS and quasi-ternary Cu_2S–Zn (Cd) S–GeS_2 systems and crystal structure of Cu_2ZnGeS_4. *Journal of Alloys and Compounds*, *397*(1-2), 85-94.

[26] Chen, S., Walsh, A., Luo, Y., Yang, J. H., Gong, X. G., & Wei, S. H. (2010). Wurtzite-derived polytypes of Kesterite and stannite quaternary chalcogenide semiconductors. *Physical Review B*, *82*(19), 195203.

[27] Walsh, A., Chen, S., Wei, S. H., & Gong, X. G. (2012). Kesterite thin-film solar cells: Advances in materials modelling of Cu_2ZnSnS_4. *Advanced Energy Materials*, *2*(4), 400-409.

[28] Redinger, A., Berg, D. M., Dale, P. J., & Siebentritt, S. (2011). The consequences of Kesterite equilibria for efficient solar cells. *Journal of the American Chemical Society*, *133*(10), 3320-3323.

[29] Ribeaucourt, L., Savidand, G., Lincot, D., & Chassaing, E. (2011). Electrochemical study of one-step electrodeposition of copper–indium–gallium

alloys in acidic conditions as precursor layers for Cu (In, Ga) Se$_2$ thin film solar cells. *Electrochimica Acta*, *56*(19), 6628-6637.

[30] Lincot, D. (2005). Electrodeposition of semiconductors. *Thin Solid Films*, *487*(1-2), 40-48.

[31] Scragg, J. J., Dale, P. J., & Peter, L. M. (2008). Towards sustainable materials for solar energy conversion: Preparation and photoelectrochemical characterization of Cu$_2$ZnSnS$_4$. *Electrochemistry Communications*, *10*(4), 639-642.

[32] Cuevas, A. C., Becerril, E. B., Martínez, M. S., & Ruiz, J. L. (2018). Fabrication processes for metal matrix composites. In *Metal Matrix Composites* (pp. 83-114). New York: Springer.

[33] Shin, S., Park, C., Kim, C., Kim, Y., Park, S., & Lee, J. H. (2016). Cyclic voltammetry studies of Copper, Tin and Zinc electrodeposition in a citrate complex system for CZTS solar cell application. *Current Applied Physics*, *16*(2), 207-210.

[34] Ran, F., & Chen, S. (2019). *Advanced Nanomaterials for Electrochemical-Based Energy Conversion and Storage* (pp. 35-67). Amsterdam: Elsevier.

[35] Choudhary, Y. S., Jothi, L., & Nageswaran, G. (2017). Electrochemical characterization. In Thomas, S., Thomas, R., Zachariah, A. K., & Kumar, R. (Eds.): *Microscopy Methods in Nanomaterials Characterization* (pp. 19-54). Amsterdam: Elsevier.

[36] Scragg, J. J. (2010). *Studies of Cu$_2$ZnSnS$_4$ Films Prepared by Sulfurization of Electrodeposited Precursors*-(Doctoral dissertation), University of Bath, UK.

[37] Kurihara, M., Berg, D., Fischer, J., Siebentritt, S., & Dale, P. J. (2009). Kesterite absorber layer uniformity from electrodeposited pre-cursors. *Physica Status Solidi C*, *6*(5), 1241-1244.

[38] Sani, R., Manivannan, R., & Victoria, S. N. (2018). One step electrodeposition of copper zinc tin sulphide using sodium thiocyanate as complexing agent. *Journal of Electrochemical Science and Technology*, *9*(4), 308-319.

[39] Sani, R., Manivannan, R., & Victoria, S. N. (2017). One step electrochemical deposition of CZTS for solar cell applications. *Chalcogenide Letters*, *14*(5), 165-170.

[40] Gür, E., Sarıtaş, S., Demir, E., Demir, K. Ç., & Coşkun, C. (2019). CZTS growth for solar cell application by electrochemical deposition: pH effect. In *2019 IEEE Regional Symposium on Micro and Nanoelectronics* (pp. 123-125), 21-23 Aug. 2019. Pahang, Malaysia. DOI: 10.1109/RSM46715.2019.8943539.

[41] Pawar, S. M., Pawar, B. S., Moholkar, A. V., Choi, D. S., Yun, J. H., Moon, J. H., ..., & Kim, J. H. (2010). Single step electrosynthesis of Cu_2ZnSnS_4 (CZTS) thin films for solar cell application. *Electrochimica Acta*, *55*(12), 4057-4061.

[42] Mkawi, E. M., Ibrahim, K., Ali, M. K. M., Farrukh, M. A., & Salhin Mohamed, A. (2013). Synthesized and characterization of Cu_2ZnSnS_4 (CZTS) thin films deposited by electrodeposition method. *Applied Mechanics and Materials*, 343, 85–89.

[43] Tang, A., Liu, J., Ji, J., Dou, M., Li, Z., & Wang, F. (2016). One-step electrodeposition for targeted off-stoichiometry Cu_2ZnSnS_4 thin films. *Applied Surface Science*, *383*, 253-260.

[44] Sarswat, P. K., Snure, M., Free, M. L., & Tiwari, A. (2012). CZTS thin films on transparent conducting electrodes by electrochemical technique. *Thin Solid Films*, *520*(6), 1694-1697.

[45] Tanaka, K., Fukui, Y., Moritake, N., & Uchiki, H. (2011). Chemical composition dependence of morphological and optical properties of Cu_2ZnSnS_4 thin films deposited by sol–gel sulfurization and Cu_2ZnSnS_4 thin film solar cell efficiency. *Solar Energy Materials and Solar Cells*, *95*(3), 838-842.

[46] Shin, S., Park, C., Kim, C., Kim, Y., Park, S., & Lee, J. H. (2016). Cyclic voltammetry studies of Copper, Tin and Zinc electrodeposition in a citrate complex system for CZTS solar cell application. *Current Applied Physics*, *16*(2), 207-210.

[47] Moriya, K., Tanaka, K., & Uchiki, H. (2008). Cu2ZnSnS4 thin films annealed in H2S atmosphere for solar cell absorber prepared by pulsed laser deposition. *Japanese Journal of Applied Physics*, *47*(1S), 602-604.

[48] Weber, A., Mainz, R., Unold, T., Schorr, S., & Schock, H. W. (2009). In-situ XRD on formation reactions of Cu_2ZnSnS_4 thin films. *Physica Status Solidi C*, *6*(5), 1245-1248.

[49] Tanaka, T., Kawasaki, D., Nishio, M., Guo, Q., & Ogawa, H. (2006). Fabrication of Cu_2ZnSnS_4 thin films by co-evaporation. *Physica Status Solidi C*, *3*(8), 2844-2847.

[50] Araki, H., Mikaduki, A., Kubo, Y., Sato, T., Jimbo, K., Maw, W. S., ..., & Takeuchi, A. (2008). Preparation of Cu_2ZnSnS_4 thin films by sulfurization of stacked metallic layers. *Thin Solid Films*, *517*(4), 1457-1460.

[51] Mkawi, E. M., Ibrahim, K., Ali, M. K. M., Farrukh, M. A., & Mohamed, A. S. (2013). Synthesized and characterization of Cu_2ZnSnS_4 (CZTS) thin films deposited by electrodeposition method. *Applied Mechanics and Materials*, *343*, 85-89.

[52] Shinde, N. M., Deokate, R. J., & Lokhande, C. D. (2013). Properties of spray deposited Cu_2ZnSnS_4 (CZTS) thin films. *Journal of Analytical and Applied Pyrolysis*, *100*, 12-16.

[53] Pine Research Instrumentation. (2021). Applications and tools. Available at: https://pineresearch.com/shop/kb/knowledge-category/applications/ (Accessed on 20/03/2021).

[54] S. AlZahmi, "Electrodeposition of CIGS/CZTS Components from Aqueous Electrolytes", Ph.D, Northeastern University Boston, Massachusetts, 2015.